Applied Soft Computing Journal 95 (2020) 106526

Contents lists available at ScienceDirect

Applied Soft Computing Journal

journal homepage: www.elsevier.com/locate/asoc

An adaptive Harris hawks optimization technique for two dimensional grey gradient based multilevel image thresholding

Aneesh Wunnava [a], Manoj Kumar Naik [a,*], Rutuparna Panda [b], Bibekananda Jena [c], Ajith Abraham [d]

[a] Faculty of Engineering and Technology, Siksha O Anusandhan, Bhubaneswar, Odisha 751030, India
[b] Dept. of Electronics and Telecommunication Engineering, Veer Surendra Sai University of Technology, Burla, Odisha 768018, India
[c] Dept. of Electronics and Communication Engineering, Anil Neerukonda Institute of Technology & Science, Sangivalasa, Visakhapatnam, Andhra Pradesh 531162, India
[d] Machine Intelligence Research Labs, Scientific Network for Innovation and Research Excellence, WA 98071-2259, USA

ARTICLE INFO

Article history:
Received 15 January 2020
Received in revised form 15 April 2020
Accepted 3 July 2020
Available online 6 July 2020

Keywords:
Computational intelligence
Soft computing
Optimal multilevel image thresholding

ABSTRACT

A metaheuristic algorithm called Harris hawks optimization (HHO) is gaining its popularity among its clan and useful for optimization. In this algorithm, the prey gets completely exhausted when the escape energy is equal to zero, therefore it fails to explore further. The random operator chosen in the existing method is a wastage of search agents (Harris hawk). To overcome this issue, we propose an adaptive Harris Hawks optimization (AHHO) technique. In this work, the mutation is employed to restrict the escape energy within the range $[0, 2]$, except for the mutation interval. Our method adaptively decides the chance of the Harris hawk would do perch along with the other family members or move to a random tall tree with the help of average fitness. The proposed AHHO algorithm is benchmarked with 23 classical test functions and 30 modern test function from CEC 2014 test suite consisting of unimodal, multimodal, hybrid and composite functions. The qualitative and quantitative analysis, which include metrics such as statistical results, convergence curves, p-value from Wilcoxon rank-sum test and Friedman mean rank. It reveals that AHHO provides good results when compared with other well-known nature-inspired algorithms. It can be used for multilevel thresholding which is an optimization problem. Recently, 2D histogram based multilevel image thresholding techniques are becoming more popular for different image processing applications. The local averaging scheme used for the construction of a 2D histogram in existing methods fails to preserve the edge information. The choice of the diagonal pixels only results in the loss of information making the earlier multilevel thresholding methods inefficient to retain the spatial correlation information. Although the computation of 2D histogram based on grey gradient information is a better way to threshold an image, it faces problems due to the presence of the edge magnitude peaks. These problems are solved by investigating an improved 2D grey gradient (I2DGG) method, a new technique is suggested in this paper to suppress high edge magnitudes. The I2DGG is a maximization problem, which requires an exhaustive search process. Therefore, AHHO is used to obtain the optimal threshold values. The result of our proposed AHHO based multilevel thresholding using the I2DGG method is obtained using all the 500 images from the Berkeley Segmentation Data set (BSDS 500). When we compare the proposed method I2DGG with 2D Tsallis entropy and 1D Tsallis entropy based multilevel thresholding, the I2DGG outperforms other methods. The experimental results are also compared with the state-of-art optimization-based multilevel thresholding methods, which shows our proposed method is beneficial to the segmentation field of image processing.

1. Introduction

Image segmentation is an important process of image processing, where a given image is segmented into a set of meaningful homogeneous sub-regions [28]. Most of the image segmentation techniques use the similarity approach based on pixel intensity values. It exploits the similarity among the image objects with

* Corresponding author.
E-mail addresses: aneeshwunnava@gmail.com (A. Wunnava), naik.manoj.kumar@gmail.com (M.K. Naik), r_ppanda@yahoo.co.in (R. Panda), bibekananda.jena@gmail.com (B. Jena), ajith.abraham@ieee.org (A. Abraham).

https://doi.org/10.1016/j.asoc.2020.106526

Table 1
Brief literature review on nature-inspired algorithms applied to corresponding image thresholding methods.

Nature-inspired algorithms	Thresholding methods
Ant colony optimization (ACO)	Otsu's method [1]
Artificial bee colony (ABC)	Kapur's entropy [2], Tsallis entropy [3]
Coral Reef optimization (CRO)	Diagonal class entropy [4]
Crow search algorithm (CSA)	Otsu's method [5], Kapur's entropy [6]
Cuckoo search (CS)	Tsallis entropy [7], Kapur's entropy [8]
Differential evolution (DE)	Tsallis entropy [9]
Firefly algorithm (FA)	Otsu's method [10], Minimum cross-entropy [11]
Genetic algorithm (GA)	Wavelet transform [12]
Grey wolf optimizer (GWO)	Otsu's method [13], Kapur's entropy [13]
Honey bee mating optimization (HBMO)	Minimum cross-entropy [14]
Krill herd optimization (KHO)	Otsu's method [15], Kapur's entropy [15]
Moth-flame optimization (MFO)	Otsu's method [16]
Particle swarm optimization (PSO)	Otsu's method [17], Minimum cross-entropy [18]
Symbiotic Organisms Search (SOS)	Kapur's entropy [19]
Whale optimization algorithm (WOA)	Otsu's method [16]
Wind driven optimization (WDO)	Kapur's entropy [8]

Table 2
Brief literature review on modified/hybrid nature-inspired algorithms applied to corresponding image thresholding methods.

Modified/hybrid algorithm	Short description of the algorithm	Thresholding methods
Adaptive Swallow swarm optimization (ASSO)	The control parameters of SSO are made adaptive with fitness value.	Grey gradient [20]
Nelder–Mead simplex search method and particle swarm optimization (NM-PSO)	Hybridization of Nelder–Mead simplex local search mechanism and particle swarm optimization global search mechanism.	Otsu's method [21,22]
Modified bacterial foraging optimization (MBFO)	The best bacteria among all the chemotactic steps are passed to the subsequent generations to improve the global search efficiency.	Otsu's method and Kapur's entropy [23]
Hybrid differential evolution (HDE)	The hybridization of differential evolution with reset strategy of Cuckoo search (CS)	Otsu's method [24]
Improved bat algorithm (IBA)	The adaption of crossover and mutation of differential evolution to speed up the convergence in bat algorithm (BA)	Otsu's method and Kapur's entropy [25]
Modified firefly algorithm (MFA)	The chaotic tent map is used in the initialization process to improve the diversity of the firefly.	Otsu's method, Kapur's entropy and minimum cross-entropy [26]
gravitational search algorithm with genetic algorithm (GSA-GA)	The roulette selection and discrete mutation operators of GA are introduced in GSA to differentiate the population and get away from premature convergence.	Otsu's method and Kapur's entropy [27]

a pre-defined criterion for partitioning. Some popular similarity approaches are thresholding, region growing, region splitting and merging. The thresholding approach rules among all other segmentation methods in terms of accuracy, ease, and robustness, which is based on image histogram. Thresholding partitions the image into different regions using a set of grey level threshold values. If there is only one grey level threshold value, then the image is partitioned into two regions, it refers to bi-level thresholding. Multilevel thresholding is an expansion of bi-level thresholding, where more than one grey level threshold values are used to partition the image into different sub-regions. Various global thresholding methods are presented in the literature to segment the images which extract the patterns of interest [29–36], out of which the histogram-based approach is most commonly used to determine the threshold value in an image. Some of the most common one-dimensional thresholding cited in the literature using the histogram of an image ware based on Otsu's method [37], Kapur's entropy [38], Tsallis entropy [39–42], Rényi entropy [30,43] and Masi entropy [44]. The performance of these methods is encouraging, a few anxieties remain. The major drawback in one-dimensional thresholding based on the 1D histogram is that the spatial correlation among the pixels are not taken into consideration. The thresholding based on two-dimensional entropy is proposed in [45,46] by using a 2D histogram, which is a combination of a 1D histogram and a local average of the neighbourhood pixels. The two-dimensional entropic method based on Otsu is proposed in [47], Tsallis–Havrda–Charvát entropy in [48] and Renyi's entropy in [49], which has shown improved performance over its one-dimensional methods.

Nowadays, multilevel thresholding is strongly recommended over the bi-level thresholding for real-life images, because bi-level thresholding does not give appropriate performance [50]. However, when we extend the bi-level thresholding to multi-level thresholding, the complexity of the problem increases, so practically it cannot be extended to multilevel thresholding. Some researchers have tried to enhance the efficiency in terms of time complexity of multilevel thresholding using recursive algorithms [51–53] to determine the optimal threshold values with the help of lookup tables. However, by increasing the number of threshold values, the computational time increases [54].

The multilevel image thresholding problem can be considered as a precise optimization problem, in which the nature-inspired computing is wise to utilize to find the optimal threshold. A brief literature review on original nature-inspired algorithms-based thresholding methods for selecting optimal threshold values are presented in Table 1. However, any original nature-inspired algorithm is flawed and has its constraint. Hence, one needs to change the search strategies by modifying the original algorithm [55] or hybridize the algorithm with other [56–58]. Several modified and hybrid nature-inspired algorithms are applied to image thresholding to improve the performance and reduce the complexity that is briefly presented in Table 2.

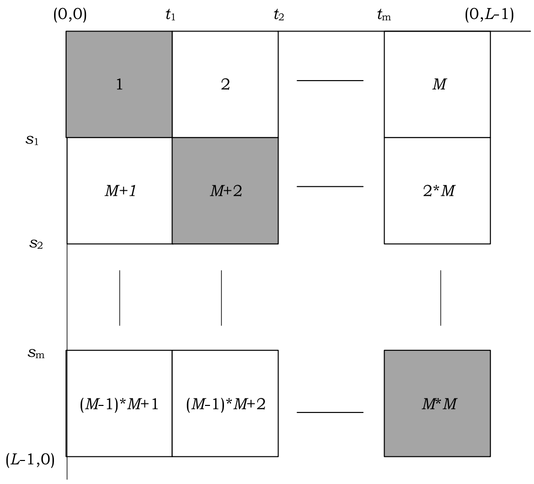

Fig. 1. 2D histogram for multilevel thresholding.

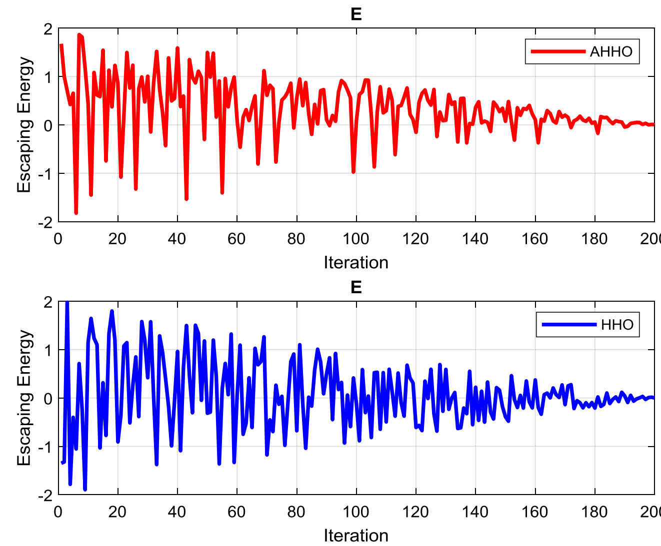

Fig. 2. Behaviour of E during 200 iterations of AHHO and HHO.

Recently, Heidari et al. [59] proposed a new metaheuristic algorithm called Harris Hawks Optimization (HHO) taking inspiration from the cooperative perching strategy of Harris' hawk. The HHO gives a quite impressive results when compared with some well-known optimization algorithms. This has motivated us to analyse the HHO algorithm, where we found that the transition from explorations to exploitations or vice-versa, has depends on a random value. This warrants us to modify the perching strategy control parameter of the exploration and exploitation are made adaptive fitness value of Harris' hawk. The Harris's hawk chasing strategy mostly depends on the rabbit (prey) energy, which is in the range of -2 to 2. The rabbit energy less than 0 means the rabbit has no energy to flagging, that motivates us to do some modification to rabbit energy in the proposed work. The modification of rabbit energy and introducing the adaptive fitness-based control parameter, the proposed algorithm is coined as adaptive Harris hawks optimization (AHHO). The performance of the AHHO is evaluated using the 23 well known classical benchmark test functions [55,60] and modern CEC 2014 test functions [61]. A comparison of AHHO with state-of-art algorithm such as Harris hawks optimization (HHO) [59], crow search algorithm (CSA) [62, 63], Cuckoo search (CS) [64,65], differential evolution (DE) [66–68], firefly algorithm (FA) [69,70], particle swarm optimization (PSO) [71], grey wolf optimizer (GWO) [72], wind driven optimization (WDO) [73], whale optimization algorithm (WOA) [74] and successful history-based adaptive DE with linear population size reduction (L-SHADE) [75,76]. As a result, AHHO shows better convergence along with superior results when compare statistical with Wilcoxon's test and Friedman test.

The image thresholding broadly used a grey level image dataset and colour image dataset. Where the grey level image is the fundamental image consists of one plane, whereas the colour image is a combination of three planes. Though the complexity is less in a grey level image than the colour image, in our belief, if a thresholding method performs well in the grey level image, it has a greater chance to perform well in the colour image. So., we motivated to employ AHHO to find the optimal threshold value in grey level image thresholding. Recently, grey gradient-based multilevel thresholding [20] is proposed based on the gradient information from the 2D histogram of an image. The method exhibits the non-uniformity of edge magnitude, which leads to the valley like structure in 2D histogram. These lead to a formation of improved 2D grey gradient (I2DGG) based multilevel thresholding method by normalize the grey gradient information. As the AHHO performance is superior in test functions, the same can be used to grey-level thresholding to obtain the threshold value. The paper uses the maximization objective function such as I2DGG along with 1D Tsallis entropy and 2D Tsallis entropy to obtain the optimal threshold value. For the compression of AHHO based multilevel thresholding, the state-of-art algorithm based multilevel thresholding such as CSA [6], CS [7,8], DE [9], FA [10], GWO [13], PSO [17], WDO [8], WOA [16] are used along with HHO [59] and L-SHADE [75,76]. The performance evaluation, experiments are performed using the Berkeley Segmentation Data Set (BSDS 500) [77] with the help of statistical measure and Wilcoxon's test.

The main contribution of this suggested work is as follows:

1. An adaptive Harris hawks optimization (AHHO) is suggested by modifying the escaping energy and perching strategy control parameter in HHO. The AHHO shows a better convergence with superior results when compared with the state-of-art algorithm with the help of a well-known 23 classical benchmark test function and modern 30 test functions form the CEC 2014 test suite.
2. An improved 2D grey gradient (I2DGG) multilevel threshold is proposed by normalizing the grey gradient information to overcome the non-uniformity in edge information.
3. The AHHO based multilevel thresholding is validated using the BSDS 500 and shows the superior result when compared with the state-of-art algorithm HHO, CSA, CS, DE, PSO, GWO, WDO, WOA and L-SHADE based multilevel thresholding.

A more detailed discussion on the work are presented in the following sections. The rest of the paper is structured as follows. A brief review of the 1D Tsallis entropy, 2D Tsallis entropy, and HHO algorithm are presented in Section 2. In Section 3, we propose a novel adaptive Harris hawks optimization (AHHO) algorithm and a comparative performance over the HHO. Section 4 describes the problem formulation based on an improved 2D grey gradient (I2DGG). The result and discussions are presented in Section 5. Concluding remarks are drawn in Section 6.

2. Preliminaries

2.1. Multilevel thresholding

Let assume grey image of size $M \times N$ with L grey level values $\{0, 1, \cdots, L-1\}$. The n_i represents the number of pixels with

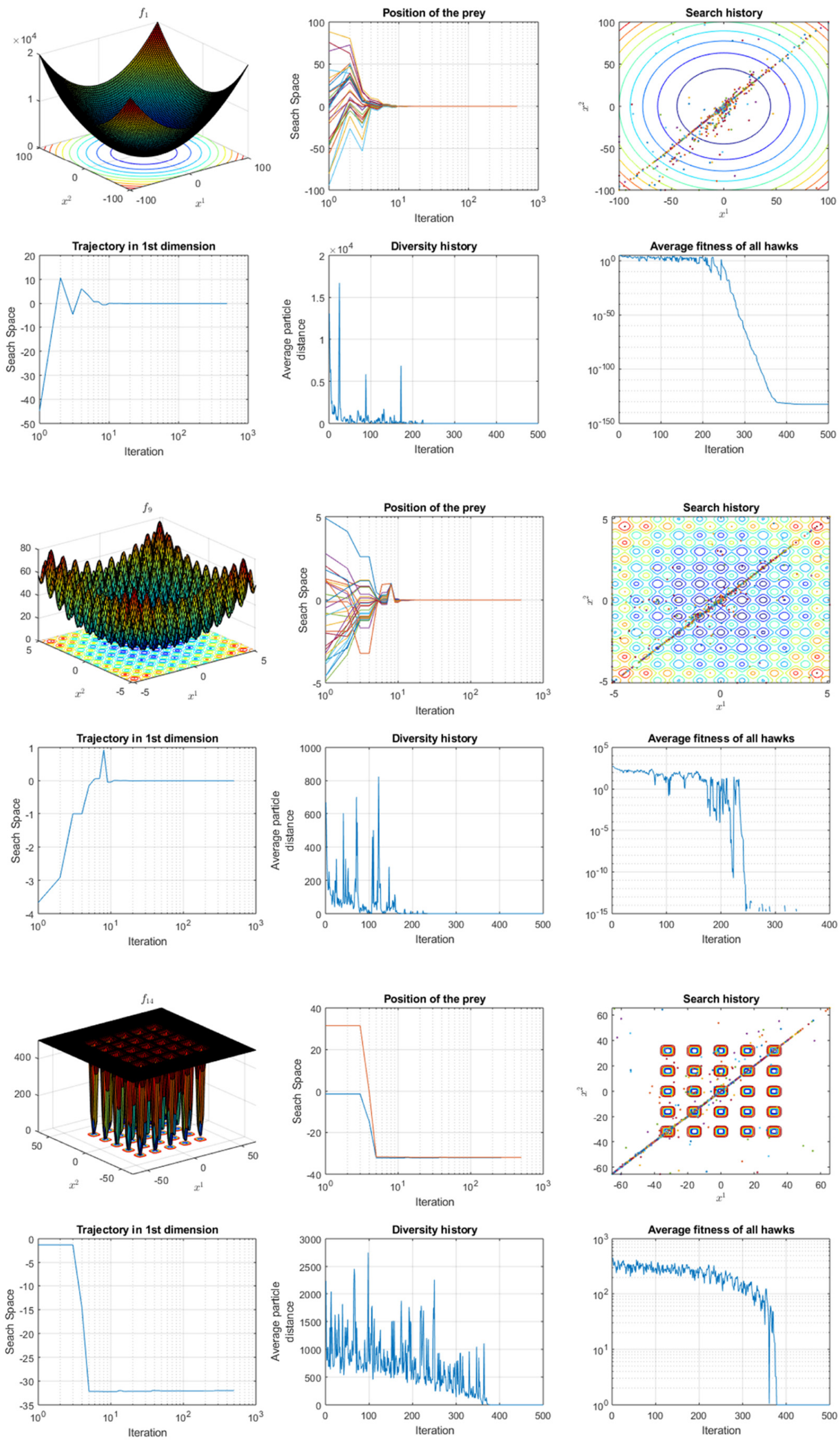

Fig. 3. Qualitative result of classical test functions f_1, f_9 and f_{14}.

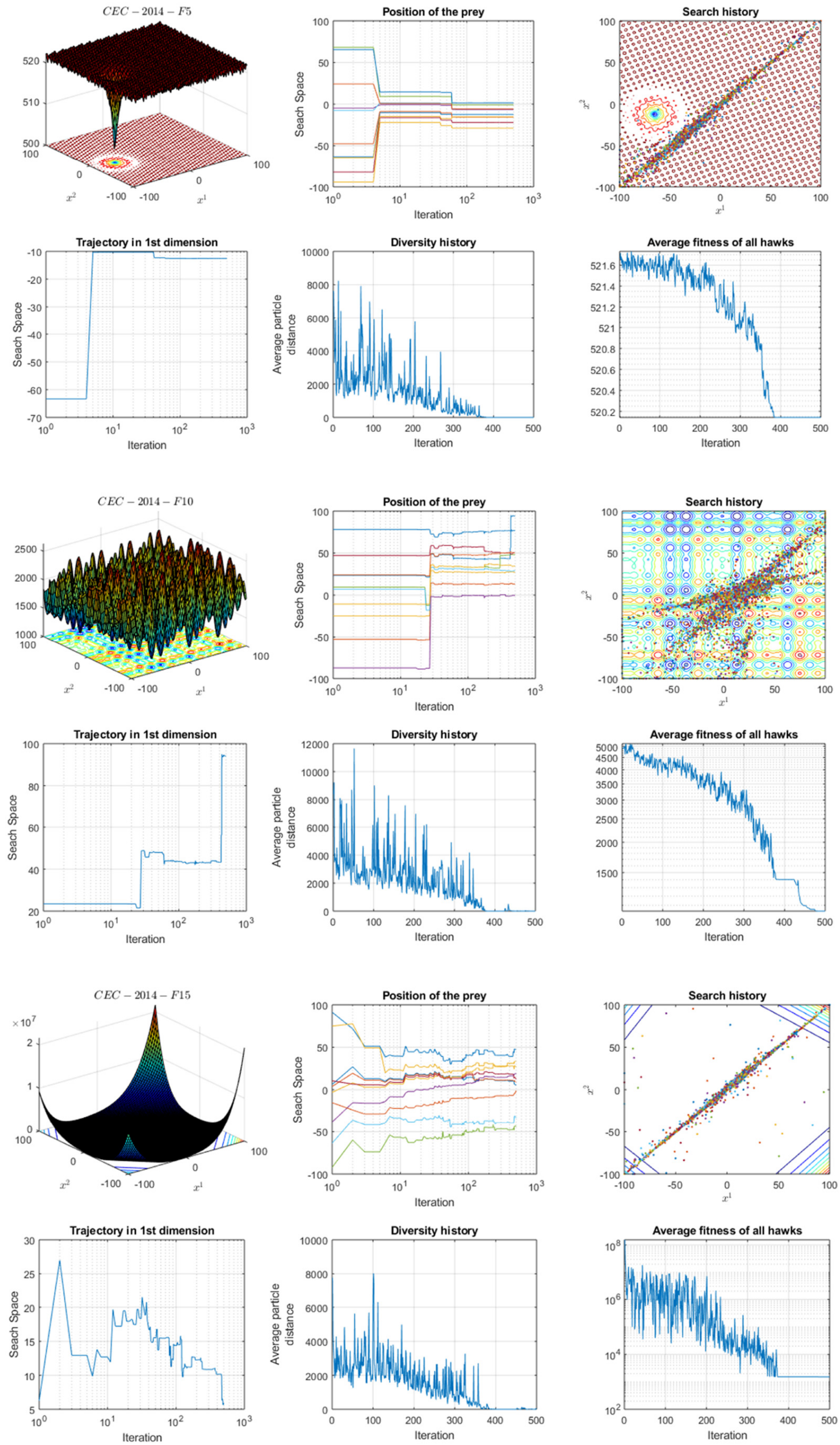

Fig. 4. Qualitative result of modern test functions F5, F10 and F15 from CEC 2014 test suite.

Table 3
Parameter setting of various optimization algorithm.

Algorithm	Parameters
AHHO	$p_{m\_max} = 0.3$ and $p_{m\_min} = 0.1$
CSA	Flight length $fl = 1$, and awareness probability $AP = 0.1$
CS	Abandon probability $p_a = 0.25$, step size $\alpha = 1$, and $\lambda = 1.5$
DE	Scaling factor $F = 0.5$, and crossover probability $C_r = 0.9$
FA	$\alpha = 0.5$, $\beta = 0.2$, and $\gamma = 1$
GWO	$a = [2\ 0]$
PSO	Inertia factor $= 0.3$, $c_1 = 2$, and $c_2 = 2$
WDO	RT coefficient $= 5$, gravitational constant $= 0.2$, constant in the update equation $= 0.5$, Coriolis effect $= 0.4$ and maximum allowed speed $= 0.3$
WOA	$a = [0, 2]$, $b = 1$, and $l = [-1, 1]$
L-SHADE	$H = 6$, $p = 0.11$ and Arc rate $= 2.6$.

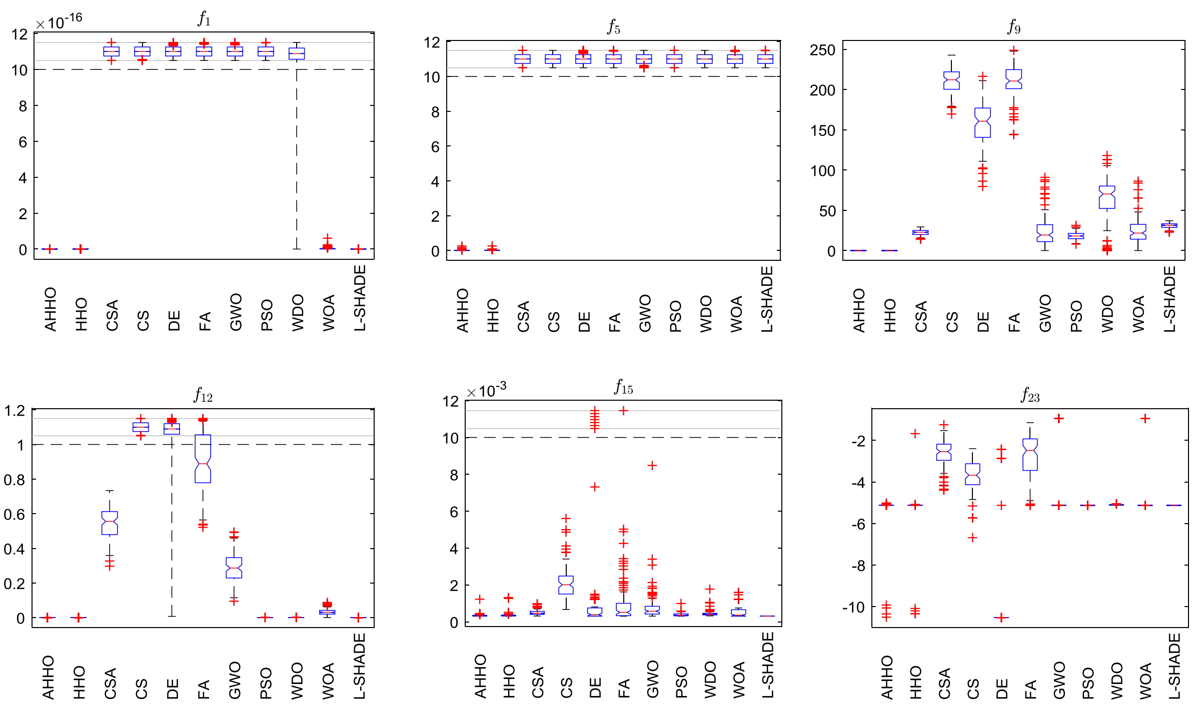

Fig. 5. Boxplot of the six classical test functions.

grey level values i, then the probability distribution of the ith $(i = 0, 1, \ldots, L-1)$ grey levels is

$$p_i = \frac{n_i}{M \times N}, \tag{1}$$

and

$$\sum_{i=0}^{L-1} p_i = 1. \tag{2}$$

For a M classes problem [23,78,79] with m thresholds $[t_1, t_2, \ldots, t_m]$, should follow $0 < t_1 < t_2 \cdots < t_m < L-1$. Then the M classes are defined as:

$$\begin{array}{r} [0, t_1] \in C_1 \\ [t_1+1,\ t_2] \in C_2 \\ \vdots \\ [t_m+1, L-1] \in C_M \end{array} \tag{3}$$

2.1.1. 1D Tsallis entropy

Tsallis proposed a generalized Tsallis entropy [40], which can be applied to a non-extensive system and can be used for thresholding an image with the help of a pseudo-additive entropic rule [42].

The Tsallis entropy for a multilevel thresholding of M classes problem [23,78,79] with m thresholds $[t_1, t_2, \ldots, t_m]$ is a maximization problem is formulated as

$$\begin{aligned} &[t_1, t_2, \ldots, t_m]_{opt} \\ &= \operatorname{argmax}[S_q^1(t) + S_q^2(t) + \cdots + S_q^k(t) + \cdots + S_q^M(t) \\ &\quad + (1-q) \times S_q^1(t) \times S_q^2(t) \times \cdots \times S_q^k(t) \times \cdots \times SqMt], \end{aligned} \tag{4}$$

where the Tsallis entropy of each class S_q^k can be

$$S_q^1(t) = \frac{1 - \sum_{i=0}^{t_1} \left(\frac{p_i}{p1}\right)^q}{q-1}$$

$$S_q^2(t) = \frac{1 - \sum_{i=t_1+1}^{t_2} \left(\frac{p_i}{p2}\right)^q}{q-1}$$

$$S_q^k(t) = \frac{1 - \sum_{i=t_{k-1}+1}^{t_k} \left(\frac{p_i}{pk}\right)^q}{q-1}$$

$$S_q^M(t) = \frac{1 - \sum_{i=t_m+1}^{L-1} \left(\frac{p_i}{pM}\right)^q}{q-1}, M = m+1$$

Table 4
Statistical result of scalable benchmark functions f_{1-13} with $d = 30$ for $N = 10$ of AHHO, HHO, CSA, CS, DE, FA, GWO, PSO, WDO, and WOA. The N of L-SHADE decrease from 18×30 to 4.

Benchmark	Metric	AHHO	HHO	CSA	CS	DE	FA	GWO	PSO	WDO	WOA	L-SHADE
f_1	Best	**4.565E−115**	5.091E−112	1.526E−01	5.651E+00	4.503E+03	1.299E+00	6.904E−11	6.343E−02	9.894E−24	3.024E−15	1.644E−26
	Worst	**4.814E−85**	1.005E−81	3.342E−01	9.389E+00	2.694E+04	8.770E+00	1.566E−06	1.951E−01	2.877E−01	3.830E−12	5.521E−24
	Average	**4.818E−87**	2.094E−83	2.377E−01	7.505E+00	1.213E+04	5.332E+00	9.901E−08	1.302E−01	9.473E−02	2.649E−13	1.019E−24
	Std. Dev.	4.814E−86	1.203E−82	4.214E−02	8.524E−01	4.430E+03	1.907E+00	2.628E−07	2.952E−02	1.024E−01	5.414E−13	1.349E−24
f_2	Best	1.100E−61	**2.232E−64**	1.308E+00	1.026E+01	1.555E+01	5.652E+00	2.291E−06	1.198E+00	7.463E−12	2.408E−09	1.705E−13
	Worst	**3.986E−44**	7.968E−41	2.492E+00	1.399E+01	7.622E+01	1.461E+01	3.663E−04	2.602E+00	2.545E+00	1.485E−07	8.288E−12
	Average	**9.794E−46**	9.608E−43	2.045E+00	1.223E+01	3.751E+01	1.050E+01	4.702E−05	1.709E+00	8.778E−01	3.317E−08	1.156E−12
	Std. Dev.	5.314E−45	8.101E−42	2.215E−01	8.345E−01	1.002E+01	2.235E+00	5.932E−05	2.650E−01	8.713E−01	2.763E−08	1.193E−12
f_3	Best	**2.012E−99**	2.675E−87	1.546E−01	3.903E+01	5.042E+03	4.728E+00	2.929E−04	4.707E−01	4.570E−04	3.811E−05	1.651E−12
	Worst	**2.199E−50**	5.250E−46	7.538E−01	6.147E+02	4.007E+04	4.065E+01	2.133E+00	1.913E+00	7.275E−01	5.564E−01	1.248E−08
	Average	**2.204E−52**	5.714E−48	4.650E−01	1.959E+02	1.744E+04	1.528E+01	3.245E−01	1.018E+00	3.160E−01	2.236E−02	7.728E−10
	Std. Dev.	2.199E−51	5.263E−47	1.300E−01	1.254E+02	7.725E+03	6.284E+00	4.129E−01	2.751E−01	1.897E−01	6.666E−02	1.562E−09
f_4	Best	**2.245E−63**	5.753E−57	1.318E−01	7.499E−01	3.189E+01	5.267E−01	1.127E−02	1.541E−01	6.372E−13	1.482E−04	4.383E−06
	Worst	**1.142E−43**	4.577E−41	2.291E−01	9.564E−01	9.334E+01	9.255E−01	6.063E−01	4.448E−01	2.347E−01	2.598E−02	5.790E−04
	Average	**1.556E−45**	6.830E−43	1.832E−01	8.774E−01	5.133E+01	8.258E−01	1.341E−01	2.430E−01	5.309E−02	3.935E−03	1.479E−04
	Std. Dev.	1.550E−44	4.895E−42	1.977E−02	4.443E−02	9.841E+00	7.022E−02	1.173E−01	5.062E−02	8.078E−02	4.602E−03	1.269E−04
f_5	Best	**4.046E−08**	1.086E−06	4.009E+01	2.812E+02	1.606E+06	1.785E+02	2.749E+01	3.312E+01	2.871E+01	2.601E+01	1.490E+01
	Worst	1.168E+00	**9.950E−01**	6.327E+01	5.036E+02	8.540E+07	1.395E+03	2.895E+01	5.405E+01	5.455E+01	2.938E+01	1.792E+01
	Average	**7.900E−02**	9.300E−02	5.186E+01	3.883E+02	1.690E+07	7.403E+02	2.870E+01	4.139E+01	3.908E+01	2.777E+01	1.613E+01
	Std. Dev.	1.670E−01	1.700E−01	4.898E+00	5.037E+01	1.251E+07	2.605E+02	3.216E−01	3.917E+00	1.029E+01	8.247E−01	6.659E−01
f_6	Best	2.381E−07	3.086E−08	3.942E+00	1.733E+01	4.952E+03	6.293E+00	2.365E+00	7.529E−02	1.038E−03	7.422E−01	**2.871E−26**
	Worst	3.100E−02	2.000E−02	6.321E+00	3.139E+01	2.508E+04	1.575E+01	5.235E+00	2.449E−01	4.481E−01	2.949E+00	**3.337E−23**
	Average	3.000E−03	1.000E−03	5.174E+00	2.647E+01	1.214E+04	1.087E+01	3.895E+00	1.386E−01	2.336E−01	1.816E+00	**2.157E−24**
	Std. Dev.	5.001E−03	2.012E−03	4.710E−01	2.299E+00	4.161E+03	2.017E+00	5.992E−01	3.453E−02	1.216E−01	5.187E−01	5.207E−24
f_7	Best	**5.020E−07**	7.179E−06	4.126E−02	6.475E+00	5.143E−01	2.310E+00	2.729E−03	6.097E−02	1.471E−02	2.555E−03	5.177E−04
	Worst	**2.012E−03**	4.000E−03	2.361E−01	6.542E+01	3.484E+01	7.312E+01	9.737E−02	6.491E−01	2.954E−01	6.582E−02	2.497E−03
	Average	**4.592E−04**	5.620E−04	1.320E−01	3.081E+01	6.998E+00	3.555E+01	1.538E−02	2.630E−01	1.397E−01	1.998E−02	1.335E−03
	Std. Dev.	4.585E−04	6.693E−04	4.323E−02	1.178E+01	6.257E+00	1.873E+01	1.186E−02	9.189E−02	6.562E−02	1.364E−02	4.260E−04
f_8	Best	**−1.256E+04**	**−1.256E+04**	−1.010E+01	−4.758E+03	−8.685E+03	−7.676E+00	−6.270E+01	−3.592E+02	−9.017E+01	−8.461E+03	−1.247E+04
	Worst	**−1.250E+04**	−1.189E+04	−5.089E+00	−2.893E+03	−5.233E+03	−1.199E+00	−1.983E+01	−1.183E+02	−8.903E+01	−5.728E+03	−1.140E+04
	Average	**−1.256E+04**	−1.255E+04	−6.662E+00	−3.767E+03	−7.246E+03	−4.282E+00	−3.563E+01	−1.880E+02	−8.950E+01	−7.274E+03	−1.194E+04
	Std. Dev.	8.014E+00	6.712E+01	8.275E−01	3.724E+02	6.862E+02	1.364E+00	8.001E+00	4.472E+01	2.631E−01	5.750E+02	2.144E+02
f_9	Best	**0.000E+00**	**0.000E+00**	2.579E+01	1.344E+02	6.659E+01	1.738E+02	3.931E−06	1.578E+01	0.000E+00	1.296E−08	2.281E+01
	Worst	**0.000E+00**	**0.000E+00**	6.573E+01	2.576E+02	1.874E+02	2.906E+02	8.529E+01	5.176E+01	1.110E+02	1.048E+02	3.699E+01
	Average	**0.000E+00**	**0.000E+00**	4.534E+01	2.267E+02	1.155E+02	2.282E+02	2.039E+01	3.199E+01	6.048E+01	3.586E+01	3.096E+01
	Std. Dev.	0.000E+00	0.000E+00	8.198E+00	1.877E+01	2.278E+01	2.315E+01	1.660E+01	7.497E+00	3.433E+01	2.386E+01	3.136E+00
f_{10}	Best	**8.881E−16**	**8.881E−16**	4.720E−01	3.240E+00	1.234E+01	2.143E+00	2.985E−06	2.851E−01	1.539E−12	4.270E−09	4.352E−14
	Worst	**8.881E−16**	**8.881E−16**	9.074E−01	3.794E+00	1.996E+01	3.764E+00	3.399E−04	1.560E+00	9.287E−01	1.203E−06	1.095E−12
	Average	**8.881E−16**	**8.881E−16**	7.213E−01	3.564E+00	1.557E+01	3.323E+00	5.715E−05	6.772E−01	2.841E−01	2.056E−07	3.035E−13
	Std. Dev.	0.000E+00	0.000E+00	8.601E−02	1.318E−01	1.443E+00	3.431E−01	6.247E−05	2.807E−01	3.049E−01	1.853E−07	2.080E−13
f_{11}	Best	**0.000E+00**	**0.000E+00**	4.907E−03	2.176E−01	3.886E+01	6.848E−02	2.244E−12	4.205E−03	0.000E+00	4.441E−16	**0.000E+00**
	Worst	**0.000E+00**	**0.000E+00**	1.787E−02	4.512E−01	2.517E+02	3.803E−01	3.088E−07	1.540E−02	1.459E−02	1.300E−12	**0.000E+00**
	Average	**0.000E+00**	**0.000E+00**	1.121E−02	3.287E−01	1.143E+02	2.648E−01	7.224E−09	8.411E−03	4.957E−03	6.440E−14	**0.000E+00**
	Std. Dev.	0.000E+00	0.000E+00	2.498E−03	4.778E−02	4.070E+01	7.384E−02	3.236E−08	2.397E−03	5.368E−03	2.035E−13	0.000E+00
f_{12}	Best	2.947E−08	6.001E−08	3.273E−01	1.564E+00	3.007E+05	4.925E−01	1.168E−01	1.057E−03	4.124E−05	2.915E−02	**5.610E−28**
	Worst	1.012E−03	6.313E−04	8.639E−01	4.053E+00	2.562E+08	1.793E+00	8.545E−01	4.856E−03	2.066E−03	2.135E−01	**1.919E−23**
	Average	1.746E−04	7.394E−05	6.568E−01	3.065E+00	1.599E+07	1.088E+00	3.806E−01	2.469E−03	5.074E−04	9.553E−02	**3.110E−25**
	Std. Dev.	2.602E−04	1.169E−04	1.044E−01	5.093E−01	2.823E+07	2.397E−01	1.269E−01	7.410E−04	3.448E−04	4.175E−02	1.929E−24
f_{13}	Best	2.021E−10	1.427E−08	2.245E+00	6.757E−01	1.349E+06	2.974E+00	1.588E+00	1.559E−02	9.301E−05	5.945E−01	**1.382E−26**
	Worst	6.034E−03	7.216E−03	3.490E+00	1.369E+00	3.476E+08	4.939E+00	2.828E+00	9.257E−02	7.277E−02	2.049E+00	**3.580E−23**
	Average	7.039E−04	8.141E−04	3.093E+00	1.125E+00	5.769E+07	3.990E+00	2.244E+00	5.208E−02	8.325E−03	1.291E+00	**2.456E−24**
	Std. Dev.	1.001E−03	1.006E−03	2.328E−01	1.261E−01	6.071E+07	4.429E−01	2.744E−01	1.688E−02	8.387E−03	2.851E−01	5.013E−24
Friedman average rank		1.54	2.00	7.85	9.31	10.23	9.62	5.77	6.54	5.85	4.77	2.54
Rank		1	2	8	9	11	10	5	7	6	4	3

Table 5
Statistical result of scalable benchmark functions f_{1-13} with $d = 30$ for $N = 30$ of AHHO, HHO, CSA, CS, DE, FA, GWO, PSO, WDO, and WOA. The N of L-SHADE decrease from 18×30 to 4.

Benchmark	Metric	AHHO	HHO	CSA	CS	DE	FA	GWO	PSO	WDO	WOA	L-SHADE
f_1	Best	**2.024E−138**	4.687E−120	6.538E−02	4.243E+00	5.848E−05	2.013E−01	4.941E−11	2.912E−02	2.310E−23	3.577E−21	1.644E−26
	Worst	**6.014E−109**	1.964E−94	1.600E−01	8.005E+00	4.885E+02	7.732E+00	5.408E−07	9.791E−02	2.839E−01	6.056E−17	5.521E−24
	Average	**6.080E−111**	4.390E−96	1.138E−01	6.676E+00	9.068E+00	1.794E+00	3.044E−08	5.426E−02	8.897E−02	3.435E−18	1.019E−24
	Std. Dev.	6.013E−110	2.179E−95	1.912E−02	7.138E−01	4.970E+01	1.684E+00	8.108E−08	1.462E−02	1.042E−01	7.060E−18	1.349E−24
f_2	Best	**5.493E−63**	5.134E−60	1.199E+00	8.763E+00	1.184E−04	2.563E+00	2.747E−06	7.505E−01	1.075E−11	4.470E−12	1.705E−13
	Worst	**3.526E−49**	1.111E−47	1.763E+00	1.327E+01	4.067E−01	1.079E+01	5.374E−04	1.440E+00	2.494E+00	3.374E−10	8.288E−12
	Average	**4.296E−51**	1.195E−49	1.456E+00	1.156E+01	2.829E−02	4.971E+00	3.144E−05	1.059E+00	6.159E−01	3.881E−11	1.156E−12
	Std. Dev.	3.539E−50	1.111E−48	1.351E−01	7.827E−01	7.128E−02	1.910E+00	5.618E−05	1.447E−01	7.539E−01	4.058E−11	1.193E−12
f_3	Best	**1.129E−106**	2.455E−104	9.420E−02	2.131E+01	1.093E+02	2.475E+00	6.911E−03	2.758E−01	7.431E−05	5.664E−09	1.651E−12
	Worst	**5.496E−76**	7.537E−64	3.074E−01	3.018E+02	2.199E+03	2.032E+01	1.227E+00	7.760E−01	6.581E−01	1.646E−03	1.248E−08
	Average	**7.320E−78**	7.848E−66	2.041E−01	1.147E+02	6.563E+02	9.251E+00	2.877E−01	5.161E−01	3.089E−01	4.435E−05	7.728E−10
	Std. Dev.	5.603E−77	7.540E−65	3.889E−02	6.176E+01	4.482E+02	3.800E+00	2.780E−01	1.185E−01	1.697E−01	1.807E−04	1.562E−09
f_4	Best	**5.717E−62**	2.885E−57	8.780E−02	7.511E−01	1.229E+01	3.036E−01	4.527E−04	9.158E−02	5.451E−13	2.463E−06	4.383E−06
	Worst	**1.867E−49**	5.927E−46	1.501E−01	9.324E−01	4.879E+01	8.883E−01	4.351E−01	2.230E−01	2.146E−01	2.361E−03	5.790E−04
	Average	**3.108E−51**	9.419E−48	1.246E−01	8.564E−01	2.355E+01	6.606E−01	1.198E−01	1.451E−01	5.469E−02	1.206E−04	1.479E−04
	Std. Dev.	2.012E−50	6.198E−47	1.154E−02	3.941E−02	6.435E+00	1.653E−01	8.698E−02	2.410E−02	8.450E−02	2.625E−04	1.269E−04
f_5	Best	**3.269E−08**	5.770E−05	3.494E+01	2.742E+02	2.845E+01	5.238E+01	2.716E+01	2.964E+01	2.873E+01	2.522E+01	1.490E+01
	Worst	**2.591E−01**	2.604E−01	4.437E+01	4.367E+02	5.038E+05	9.888E+02	2.894E+01	3.772E+01	5.746E+01	2.906E+01	1.792E+01
	Average	**1.706E−02**	1.908E−02	3.949E+01	3.630E+02	1.238E+04	3.068E+02	2.872E+01	3.329E+01	3.598E+01	2.654E+01	1.613E+01
	Std. Dev.	3.600E−02	3.201E−02	1.786E+00	3.827E+01	5.379E+04	2.764E+02	3.234E−01	1.567E+00	9.325E+00	9.144E−01	6.659E−01
f_6	Best	8.977E−10	2.226E−09	3.214E+00	2.046E+01	1.540E−04	4.065E+00	1.911E+00	2.446E−02	7.838E−03	2.129E−01	**2.871E−26**
	Worst	5.012E−02	9.090E−04	5.709E+00	2.844E+01	6.823E+02	1.249E+01	4.730E+00	9.411E−02	4.294E−01	2.002E+00	**3.337E−23**
	Average	3.172E−04	1.405E−04	4.875E+00	2.472E+01	1.775E+01	8.331E+00	3.478E+00	5.736E−02	2.116E−01	7.923E−01	**2.157E−24**
	Std. Dev.	6.565E−04	1.766E−04	4.017E−01	1.868E+00	7.282E+01	1.919E+00	5.948E−01	1.432E−02	1.261E−01	3.538E−01	5.207E−24
f_7	Best	2.671E−06	**2.062E−06**	1.743E−02	1.767E+01	3.410E−02	3.914E−01	9.853E−04	5.973E−02	3.821E−02	7.143E−04	5.177E−04
	Worst	1.015E−02	1.023E−02	7.043E−02	5.900E+01	1.386E−01	5.641E+01	1.759E−02	2.532E−01	3.291E−01	3.031E−02	**2.497E−03**
	Average	1.395E−04	1.544E−04	4.297E−02	3.921E+01	6.591E−02	1.113E+01	5.647E−03	1.306E−01	1.593E−01	7.631E−03	**1.335E−03**
	Std. Dev.	1.672E−04	2.022E−04	1.170E−02	8.737E+00	1.939E−02	1.532E+01	3.384E−03	3.701E−02	7.061E−02	5.246E−03	4.260E−04
f_8	Best	**−1.256E+04**	**−1.256E+04**	−9.478E+00	−5.098E+03	−1.036E+04	−9.377E+00	−6.114E+01	−2.593E+02	−9.521E+01	−9.720E+03	−1.247E+04
	Worst	**−1.192E+04**	−1.166E+04	−5.756E+00	−3.458E+03	−4.899E+03	−2.764E+00	−2.336E+01	−1.183E+02	−9.043E+01	−6.570E+03	−1.140E+04
	Average	**−1.256E+04**	−1.255E+04	−7.375E+00	−4.005E+03	−7.458E+03	−5.327E+00	−3.901E+01	−1.576E+02	−9.285E+01	−7.946E+03	−1.194E+04
	Std. Dev.	68.187	93.069	7.901E−01	3.196E+02	1.200E+03	1.155E+00	7.525E+00	3.153E+01	1.072E+00	5.561E+02	2.144E+02
f_9	Best	**0.000E+00**	**0.000E+00**	1.416E+01	1.695E+02	7.957E+01	1.439E+02	1.224E−07	8.009E+00	0.000E+00	6.253E−13	2.281E+01
	Worst	**0.000E+00**	**0.000E+00**	2.935E+01	2.426E+02	2.163E+02	2.486E+02	9.088E+01	3.126E+01	1.181E+02	8.618E+01	3.699E+01
	Average	**0.000E+00**	**0.000E+00**	2.237E+01	2.106E+02	1.579E+02	2.099E+02	2.508E+01	1.813E+01	6.089E+01	2.463E+01	3.096E+01
	Std. Dev.	0.000E+00	0.000E+00	3.615E+00	1.535E+01	2.825E+01	2.096E+01	2.114E+01	4.582E+00	3.336E+01	1.607E+01	3.136E+00
f_{10}	Best	**8.881E−16**	**8.881E−16**	2.843E−01	3.033E+00	2.946E−03	6.413E−01	4.313E−06	1.763E−01	1.482E−12	4.694E−11	4.352E−14
	Worst	**8.881E−16**	**8.881E−16**	5.730E−01	3.632E+00	3.836E+00	3.535E+00	7.751E−04	1.274E+00	8.055E−01	2.521E−09	1.095E−12
	Average	**8.881E−16**	**8.881E−16**	4.262E−01	3.423E+00	1.723E+00	2.421E+00	8.098E−05	3.108E−01	2.053E−01	5.535E−10	3.035E−13
	Std. Dev.	0.000E+00	0.000E+00	5.267E−02	1.242E−01	8.781E−01	8.978E−01	1.057E−04	1.768E−01	2.594E−01	4.595E−10	2.080E−13
f_{11}	Best	**0.000E+00**	**0.000E+00**	2.313E−03	1.657E−01	2.621E−04	1.079E−02	5.001E−12	1.659E−03	0.000E+00	0.000E+00	**0.000E+00**
	Worst	**0.000E+00**	**0.000E+00**	8.702E−03	3.597E−01	1.695E+00	3.539E−01	8.514E−08	5.798E−03	1.587E−02	3.331E−16	**0.000E+00**
	Average	**0.000E+00**	**0.000E+00**	5.252E−03	2.757E−01	1.825E−01	1.203E−01	3.049E−09	3.338E−03	3.233E−03	1.998E−17	**0.000E+00**
	Std. Dev.	0.000E+00	0.000E+00	1.077E−03	3.684E−02	2.566E−01	9.874E−02	1.046E−08	8.833E−04	5.037E−03	5.323E−17	0.000E+00
f_{12}	Best	2.613E−10	2.358E−08	2.970E−01	1.656E+00	7.204E−03	5.219E−01	9.500E−02	2.788E−04	9.391E−06	4.479E−04	**5.610E−28**
	Worst	1.186E−04	6.653E−05	7.341E−01	3.787E+00	1.591E+05	1.482E+00	4.945E−01	1.340E−03	1.649E−03	8.809E−02	**1.919E−23**
	Average	1.685E−05	8.956E−06	5.461E−01	2.653E+00	5.106E+03	8.995E−01	2.873E−01	7.846E−04	3.974E−04	3.370E−02	**3.110E−25**
	Std. Dev.	3.060E−05	1.204E−05	9.350E−02	4.062E−01	2.082E+04	1.868E−01	8.662E−02	1.964E−04	2.649E−04	1.789E−02	1.929E−24
f_{13}	Best	3.181E−10	5.946E−08	2.401E+00	5.647E−01	2.942E−01	2.344E+00	1.480E+00	4.844E−03	8.102E−04	2.879E−03	**1.382E−26**
	Worst	2.008E−02	3.100E−02	3.484E+00	1.243E+00	1.356E+06	4.453E+00	2.559E+00	3.626E−02	1.610E−02	1.320E+00	**3.580E−23**
	Average	1.222E−04	1.221E−04	2.978E+00	9.987E−01	7.276E+04	3.545E+00	2.106E+00	1.851E−02	7.497E−03	7.066E−01	**2.456E−24**
	Std. Dev.	2.863E−04	2.816E−04	2.273E−01	1.167E−01	2.208E+05	4.352E−01	2.544E−01	7.317E−03	4.511E−03	2.592E−01	5.013E−24
Friedman average rank		1.62	1.92	7.54	9.92	9.38	9.54	6.00	6.31	6.38	4.54	2.85
Rank		1	2	8	11	9	10	5	6	7	4	3

Table 6
Statistical result of scalable benchmark functions f_{1-13} with $d = 100$ for $N = 10$ of AHHO, HHO, CSA, CS, DE, FA, GWO, PSO, WDO, and WOA. The N of L-SHADE decrease from 18×100 to 4.

Benchmark	Metric	AHHO	HHO	CSA	CS	DE	FA	GWO	PSO	WDO	WOA	L-SHADE
f_1	Best	**3.818E−118**	1.714E−110	7.640E−01	2.456E+01	5.093E+04	2.260E+01	1.633E−05	1.763E+00	1.124E−23	2.143E−07	7.311E−12
	Worst	**1.219E−84**	1.223E−82	1.407E+00	3.226E+01	1.237E+05	3.158E+01	1.474E−02	4.050E+00	1.941E+00	2.104E−05	3.211E−11
	Average	**1.511E−86**	1.974E−84	1.077E+00	2.848E+01	8.072E+04	2.749E+01	1.833E−03	2.991E+00	1.560E−01	2.953E−06	1.808E−11
	Std. Dev.	1.228E−85	1.406E−83	1.379E−01	1.727E+00	1.662E+04	1.669E+00	2.550E−03	3.987E−01	4.410E−01	3.059E−06	9.678E−12
f_2	Best	**4.835E−59**	1.032E−54	6.666E+00	4.115E+01	1.503E+02	4.096E+01	8.812E−04	1.272E+01	2.320E−11	1.654E−04	1.782E−06
	Worst	**1.465E−42**	8.588E−42	9.628E+00	5.073E+01	2.956E+02	4.775E+01	3.815E−02	1.868E+01	1.084E+01	1.659E−03	1.288E−05
	Average	**1.900E−44**	2.082E−43	8.375E+00	4.551E+01	2.215E+02	4.474E+01	7.147E−03	1.525E+01	1.757E+00	6.502E−04	4.407E−06
	Std. Dev.	1.483E−43	1.146E−42	5.738E−01	1.665E+00	2.821E+01	1.473E+00	5.771E−03	1.283E+00	3.150E+00	3.309E−04	3.449E−06
f_3	Best	**3.846E−90**	1.261E−80	2.867E+00	2.167E+03	7.133E+04	4.439E+01	7.755E+00	1.032E+01	1.543E−01	1.610E+00	3.140E−04
	Worst	**1.899E−33**	6.190E−28	8.554E+00	2.318E+04	3.584E+05	4.836E+02	5.700E+01	3.653E+01	1.004E+01	3.549E+01	8.701E−04
	Average	**1.899E−35**	6.936E−30	5.163E+00	8.502E+03	1.649E+05	1.713E+02	2.506E+01	2.213E+01	4.701E+00	1.482E+01	4.579E−04
	Std. Dev.	1.899E−34	6.223E−29	1.329E+00	4.535E+03	6.594E+04	8.601E+01	1.120E+01	5.645E+00	1.689E+00	7.698E+00	1.573E−04
f_4	Best	**6.565E−59**	2.383E−56	2.078E−01	8.810E−01	9.461E+01	8.852E−01	4.683E−01	5.041E−01	1.009E−13	4.640E−01	3.200E−03
	Worst	**2.363E−44**	8.365E−41	3.058E−01	9.871E−01	9.896E+01	9.625E−01	9.099E−01	8.829E−01	3.142E−01	9.206E−01	5.829E−03
	Average	**7.264E−46**	1.652E−42	2.502E−01	9.613E−01	9.716E+01	9.295E−01	6.893E−01	6.372E−01	3.476E−02	7.123E−01	4.535E−03
	Std. Dev.	3.270E−45	1.003E−41	1.844E−02	1.957E−02	1.080E+00	1.581E−02	8.047E−02	6.838E−02	9.077E−02	1.023E−01	8.421E−04
f_5	Best	**9.015E−09**	7.436E−06	1.675E+02	1.134E+03	5.882E+07	3.231E+03	9.887E+01	3.515E+02	9.805E+01	9.691E+01	9.143E+01
	Worst	2.709E+00	**2.280E+00**	2.441E+02	1.912E+03	3.469E+08	4.920E+03	3.214E+02	6.176E+02	2.886E+02	9.911E+01	9.345E+01
	Average	**2.151E−01**	2.980E−01	2.068E+02	1.544E+03	1.447E+08	4.129E+03	1.168E+02	4.538E+02	1.312E+02	9.829E+01	9.222E+01
	Std. Dev.	3.980E−01	4.851E−01	1.538E+01	1.716E+02	5.415E+07	3.314E+02	3.630E+01	5.061E+01	6.044E+01	4.428E−01	5.715E−01
f_6	Best	6.207E−07	6.832E−07	1.983E+01	8.203E+01	4.573E+04	3.907E+01	1.626E+01	2.985E+00	1.306E−02	1.183E+01	**6.856E−10**
	Worst	1.411E−01	3.903E−02	2.417E+01	1.054E+02	1.173E+05	5.448E+01	2.073E+01	5.475E+00	3.916E+00	1.681E+01	**1.691E−09**
	Average	1.318E−02	4.002E−03	2.246E+01	9.819E+01	7.864E+04	4.712E+01	1.881E+01	3.907E+00	9.816E−01	1.473E+01	**1.063E−09**
	Std. Dev.	2.101E−02	7.016E−03	7.473E−01	3.822E+00	1.551E+04	3.351E+00	9.643E−01	4.587E−01	9.227E−01	9.429E−01	3.226E−10
f_7	Best	7.439E−06	**4.619E−06**	7.800E−01	2.742E+02	5.331E+01	4.964E+02	3.408E−02	8.391E+00	6.040E−03	3.247E−02	1.652E−03
	Worst	**0.003**	0.005	2.930E+00	9.291E+02	5.151E+02	8.364E+02	4.592E+00	3.673E+01	4.895E+00	2.957E−01	3.147E−03
	Average	**4.752E−04**	5.403E−04	1.713E+00	6.408E+02	2.215E+02	7.085E+02	3.759E−01	1.695E+01	5.032E−01	1.334E−01	2.444E−03
	Std. Dev.	5.982E−04	6.883E−04	4.314E−01	1.083E+02	8.996E+01	6.855E+01	5.905E−01	5.714E+00	1.097E+00	6.370E−02	4.252E−04
f_8	Best	**−4.189E+04**	**-4189E+04**	−1.711E+01	−9.222E+03	−2.129E+04	−1.338E+01	−1.131E+02	−1.535E+03	−2.189E+02	−1.921E+04	−7.505E+03
	Worst	−3.261E+04	**−4.144E+04**	−8.627E+00	−5.810E+03	−1.353E+04	−2.390E+00	−4.687E+01	−5.849E+02	−1.752E+02	−1.490E+04	−5.640E+03
	Average	−4.178E+04	**−4.187E+04**	−1.243E+01	−6.938E+03	−1.664E+04	−7.629E+00	−7.349E+01	−8.462E+02	−1.943E+02	−1.704E+04	−6.382E+03
	Std. Dev.	927.324	53.453	1.440E+00	6.878E+02	1.506E+03	2.469E+00	1.225E+01	1.726E+02	8.688E+00	9.271E+02	5.345E+02
f_9	Best	**0.000E+00**	**0.000E+00**	1.276E+02	7.680E+02	5.878E+02	7.797E+02	5.063E+00	2.920E+02	0.000E+00	3.385E+00	2.475E+02
	Worst	**0.000E+00**	**0.000E+00**	2.595E+02	9.554E+02	9.209E+02	9.873E+02	3.352E+02	4.511E+02	6.005E+02	5.636E+02	2.859E+02
	Average	**0.000E+00**	**0.000E+00**	1.891E+02	8.892E+02	7.196E+02	8.873E+02	9.507E+01	3.834E+02	1.098E+02	1.817E+02	2.703E+02
	Std. Dev.	0.000E+00	0.000E+00	2.482E+01	3.774E+01	6.824E+01	4.064E+01	6.682E+01	2.981E+01	2.059E+02	1.374E+02	1.082E+01
f_{10}	Best	**8.881E−16**	**8.881E−16**	6.231E−01	3.591E+00	1.655E+01	3.429E+00	4.272E−04	1.627E+00	9.992E−13	5.103E−05	8.988E−07
	Worst	**8.881E−16**	**8.881E−16**	1.065E+00	3.883E+00	1.997E+01	3.869E+00	3.087E−02	2.308E+00	1.202E+00	8.527E−04	2.917E−06
	Average	**8.881E−16**	**8.881E−16**	8.636E−01	3.736E+00	1.814E+01	3.665E+00	5.350E−03	1.940E+00	1.038E−01	3.327E−04	1.720E−06
	Std. Dev.	0.000E+00	0.000E+00	9.271E−02	6.564E−02	6.366E−01	7.797E−02	4.272E−03	1.430E−01	2.507E−01	1.502E−04	6.690E−07
f_{11}	Best	**0.000E+00**	**0.000E+00**	1.254E−02	3.498E−01	3.941E+02	3.572E−01	9.630E−08	4.157E−02	0.000E+00	2.761E−09	1.427E−13
	Worst	**0.000E+00**	**0.000E+00**	3.245E−02	5.187E−01	1.148E+03	5.412E−01	1.495E−04	8.766E−02	3.484E−02	2.406E−07	1.494E−12
	Average	**0.000E+00**	**0.000E+00**	2.072E−02	4.548E−01	6.792E+02	4.439E−01	1.684E−05	6.744E−02	6.167E−03	5.154E−08	7.067E−13
	Std. Dev.	0.000E+00	0.000E+00	3.582E−03	3.509E−02	1.360E+02	3.894E−02	2.320E−05	9.388E−03	1.104E−02	5.124E−08	4.112E−13
f_{12}	Best	4.458E−08	**1.010E−08**	8.507E−01	2.798E+00	1.497E+07	9.036E−01	4.788E−01	2.277E−02	8.598E−06	2.300E−01	2.397E−08
	Worst	4.854E−04	3.333E−04	1.083E+00	4.149E+00	6.386E+08	1.503E+00	8.232E−01	1.758E−01	7.503E−03	5.959E−01	**4.107E−08**
	Average	6.986E−05	4.600E−05	9.729E−01	3.579E+00	2.062E+08	1.281E+00	6.544E−01	7.431E−02	1.041E−03	3.929E−01	**3.105E−08**
	Std. Dev.	9.984E−05	6.405E−05	5.225E−02	2.591E−01	1.173E+08	1.358E−01	6.871E−02	3.026E−02	1.696E−03	7.081E−02	6.302E−09
f_{13}	Best	**1.924E−08**	2.637E−07	1.201E+01	3.553E+00	1.529E+08	1.343E+01	8.673E+00	1.492E+00	3.956E−03	6.241E+00	1.099E−02
	Worst	1.901E−02	1.923E−02	1.372E+01	4.806E+00	9.747E+08	1.836E+01	1.222E+01	7.094E+00	5.517E−01	9.011E+00	**1.099E−02**
	Average	**1.078E−03**	1.189E−03	1.314E+01	4.300E+00	4.536E+08	1.610E+01	1.005E+01	3.299E+00	5.099E−02	7.814E+00	1.099E−02
	Std. Dev.	2.001E−03	3.001E−03	3.267E−01	2.417E−01	1.900E+08	9.374E−01	6.465E−01	1.158E+00	9.735E−02	5.425E−01	1.939E−07
Friedman average rank		1.50	1.81	7.15	9.31	10.15	9.54	6.08	7.00	5.23	5.00	3.23
Rank		1	2	8	9	11	10	6	7	5	4	3

Table 7
Statistical result of scalable benchmark functions f_{1-13} with $d = 100$ for $N = 30$ of AHHO, HHO, CSA, CS, DE, FA, GWO, PSO, WDO, and WOA. The N of L-SHADE decrease from 18×100 to 4.

Benchmark	Metric	AHHO	HHO	CSA	CS	DE	FA	GWO	PSO	WDO	WOA	L-SHADE
f_1	Best	**1.026E−118**	8.536E−118	4.188E−01	2.372E+01	2.780E+03	2.517E+01	8.165E−05	1.101E+00	4.450E−23	1.334E−09	7.311E−12
	Worst	**1.005E−96**	3.032E−92	6.349E−01	2.757E+01	8.772E+03	2.801E+01	9.267E−03	1.735E+00	2.143E−02	2.723E−08	3.211E−11
	Average	**2.804E−98**	3.066E−94	5.226E−01	2.639E+01	4.636E+03	2.647E+01	1.977E−03	1.310E+00	2.425E−03	8.283E−09	1.808E−11
	Std. Dev.	1.369E−97	3.032E−93	7.813E−02	1.141E+00	1.626E+03	1.110E+00	3.036E−03	1.831E−01	6.735E−03	7.754E−09	9.678E−12
f_2	Best	**1.217E−60**	6.450E−61	4.946E+00	4.180E+01	1.899E+01	4.165E+01	2.209E−03	9.417E+00	3.732E−11	9.175E−06	1.782E−06
	Worst	**4.526E−49**	6.475E−48	6.080E+00	4.664E+01	3.754E+01	4.567E+01	2.028E−02	1.302E+01	6.474E+00	4.243E−05	1.288E−05
	Average	**7.373E−51**	2.872E−49	5.780E+00	4.434E+01	2.839E+01	4.368E+01	8.269E−03	1.063E+01	1.607E+00	2.371E−05	4.407E−06
	Std. Dev.	4.697E−50	1.021E−48	3.378E−01	1.425E+00	6.089E+00	1.182E+00	5.604E−03	1.089E+00	2.417E+00	9.912E−06	3.449E−06
f_3	Best	7.294E−103	1.529E−97	1.434E+00	1.703E+03	4.086E+04	7.225E+01	1.112E+01	9.519E+00	5.834E−03	6.197E−01	3.140E−04
	Worst	**3.329E−57**	1.803E−41	2.390E+00	9.337E+03	9.432E+04	1.644E+02	5.428E+01	2.002E+01	8.506E+00	1.048E+01	8.701E−04
	Average	**3.329E−59**	1.803E−43	1.892E+00	4.541E+03	6.916E+04	1.110E+02	2.819E+01	1.489E+01	4.595E+00	5.170E+00	4.579E−04
	Std. Dev.	3.329E−58	1.803E−42	3.217E−01	2.348E+03	1.647E+04	3.013E+01	1.170E+01	3.221E+00	2.120E+00	3.521E+00	1.573E−04
f_4	Best	**4.486E−60**	3.097E−58	1.569E−01	9.192E−01	9.368E+01	9.042E−01	6.424E−01	4.518E−01	2.122E−13	1.776E−01	3.200E−03
	Worst	**1.648E−49**	1.316E−45	1.910E−01	9.722E−01	9.810E+01	9.440E−01	8.395E−01	5.550E−01	3.251E−02	4.972E−01	5.829E−03
	Average	**3.498E−51**	1.431E−47	1.768E−01	9.528E−01	9.632E+01	9.216E−01	7.286E−01	5.131E−01	3.251E−03	3.762E−01	4.535E−03
	Std. Dev.	1.919E−50	1.318E−46	1.145E−02	1.716E−02	1.317E+00	1.062E−02	6.747E−02	3.031E−02	1.028E−02	1.102E−01	8.421E−04
f_5	Best	**8.813E−07**	1.657E−04	1.463E+02	1.323E+03	7.808E+05	3.261E+03	9.893E+01	2.093E+02	9.813E+01	9.690E+01	9.143E+01
	Worst	**3.700E−01**	6.690E−01	1.616E+02	1.621E+03	7.651E+06	3.958E+03	1.614E+02	3.222E+02	1.033E+02	9.844E+01	9.345E+01
	Average	5.011E−02	**4.202E−02**	1.526E+02	1.487E+03	3.277E+06	3.694E+03	1.095E+02	2.783E+02	9.952E+01	9.790E+01	9.222E+01
	Std. Dev.	7.412E−02	8.104E−02	5.553E+00	1.089E+02	1.966E+06	2.586E+02	1.908E+01	3.342E+01	1.558E+00	5.781E−01	5.715E−01
f_6	Best	9.532E−07	9.245E−07	2.117E+01	8.914E+01	2.661E+03	4.183E+01	1.724E+01	1.433E+00	9.737E−02	9.147E+00	**6.856E−10**
	Worst	8.104E−03	3.006E−03	2.259E+01	9.844E+01	6.101E+03	4.713E+01	1.921E+01	1.896E+00	2.346E+00	1.295E+01	**1.691E−09**
	Average	1.650E−03	4.610E−04	2.203E+01	9.500E+01	4.273E+03	4.442E+01	1.829E+01	1.631E+00	1.166E+00	1.125E+01	**1.063E−09**
	Std. Dev.	1.751E−03	7.223E−04	4.539E−01	2.593E+00	1.167E+03	1.794E+00	6.547E−01	1.361E−01	8.045E−01	1.014E+00	3.226E−10
f_7	Best	**2.464E−07**	7.435E−07	3.290E−01	6.196E+02	2.032E+00	5.688E+02	2.415E−02	3.525E+00	8.442E−03	2.929E−02	1.652E−03
	Worst	**7.280E−04**	0.001	5.173E−01	7.717E+02	9.517E+00	7.701E+02	1.207E+00	5.946E+00	3.320E+00	5.730E−02	3.147E−03
	Average	**1.324E−04**	1.566E−04	4.308E−01	6.811E+02	4.597E+00	6.821E+02	2.029E−01	4.784E+00	5.778E−01	4.446E−02	2.444E−03
	Std. Dev.	1.296E−04	1.823E−04	6.916E−02	5.188E+01	2.561E+00	5.320E+01	3.596E−01	6.654E−01	1.018E+00	1.069E−02	4.252E−04
f_8	Best	**−4.189E+04**	**-4189E+04**	−1.701E+01	−8.824E+03	−1.932E+04	−1.440E+01	−1.042E+02	−8.768E+02	−2.659E+02	−2.150E+04	−7.505E+03
	Worst	−**3.710E+04**	−3.444E+04	−1.169E+01	−6.717E+03	−8.412E+03	−7.184E+00	−6.313E+01	−4.943E+02	−2.420E+02	−1.987E+04	−5.640E+03
	Average	−**4.184E+04**	−4.179E+04	−1.416E+01	−7.443E+03	−1.359E+04	−9.539E+00	−7.662E+01	−6.876E+02	−2.494E+02	−2.056E+04	−6.382E+03
	Std. Dev.	478.863	776.971	1.456E+00	6.185E+02	3.642E+03	2.310E+00	1.164E+01	1.190E+02	7.616E+00	4.925E+02	5.345E+02
f_9	Best	**0.000E+00**	**0.000E+00**	8.907E+01	8.105E+02	2.100E+02	8.060E+02	7.977E+01	2.226E+02	0.000E+00	1.940E+01	2.475E+02
	Worst	**0.000E+00**	**0.000E+00**	1.098E+02	9.096E+02	8.970E+02	8.893E+02	3.801E+02	2.784E+02	1.739E+01	2.924E+02	2.859E+02
	Average	**0.000E+00**	**0.000E+00**	1.009E+02	8.632E+02	6.354E+02	8.433E+02	1.562E+02	2.424E+02	3.901E+00	1.494E+02	2.703E+02
	Std. Dev.	0.000E+00	0.000E+00	7.943E+00	3.244E+01	2.176E+02	3.046E+01	9.312E+01	1.757E+01	5.507E+00	8.375E+01	1.082E+01
f_{10}	Best	**8.881E−16**	**8.881E−16**	4.738E−01	3.569E+00	8.387E+00	3.545E+00	1.025E−03	1.159E+00	2.751E−12	8.481E−06	8.988E−07
	Worst	**8.881E−16**	**8.881E−16**	6.347E−01	3.746E+00	1.996E+01	3.691E+00	1.425E−02	1.676E+00	1.181E+00	3.150E−05	2.917E−06
	Average	**8.881E−16**	**8.881E−16**	5.581E−01	3.672E+00	1.108E+01	3.642E+00	3.854E−03	1.447E+00	1.437E−01	2.065E−05	1.720E−06
	Std. Dev.	0.000E+00	0.000E+00	4.743E−02	5.842E−02	3.336E+00	4.003E−02	4.425E−03	1.833E−01	3.670E−01	8.291E−06	6.690E−07
f_{11}	Best	**0.000E+00**	**0.000E+00**	7.965E−03	3.464E−01	1.772E+01	3.310E−01	6.268E−08	2.499E−02	0.000E+00	4.835E−11	1.427E−13
	Worst	**0.000E+00**	**0.000E+00**	1.209E−02	4.773E−01	7.835E+01	4.394E−01	7.150E−05	3.990E−02	2.833E−02	5.579E−10	1.494E−12
	Average	**0.000E+00**	**0.000E+00**	9.980E−03	4.221E−01	3.355E+01	4.007E−01	1.625E−05	3.239E−02	4.242E−03	1.661E−10	7.067E−13
	Std. Dev.	0.000E+00	0.000E+00	1.201E−03	3.909E−02	1.878E+01	3.205E−02	2.108E−05	5.088E−03	8.883E−03	1.635E−10	4.112E−13
f_{12}	Best	5.074E−09	**1.422E−09**	7.875E−01	3.229E+00	7.939E+04	8.591E−01	4.999E−01	6.423E−03	1.024E−04	1.627E−01	2.397E−08
	Worst	7.358E−05	2.153E−05	9.861E−01	3.690E+00	8.252E+06	1.427E+00	7.103E−01	1.926E−02	4.735E−04	2.668E−01	**4.107E−08**
	Average	6.792E−06	2.943E−06	9.027E−01	3.452E+00	1.850E+06	1.184E+00	6.046E−01	1.163E−02	3.387E−04	2.242E−01	**3.105E−08**
	Std. Dev.	1.182E−05	3.874E−05	6.984E−02	1.503E−01	2.468E+06	1.525E−01	6.075E−02	3.639E−03	1.391E−04	3.434E−02	6.302E−09
f_{13}	Best	**1.879E−08**	3.889E−08	1.226E+01	3.858E+00	5.021E+05	1.394E+01	9.078E+00	4.259E−01	1.014E−02	5.661E+00	1.099E−02
	Worst	2.003E−03	**9.966E−04**	1.317E+01	4.519E+00	1.186E+07	1.651E+01	1.120E+01	1.015E+00	2.313E−01	7.592E+00	1.099E−02
	Average	1.761E−04	**1.511E−04**	1.283E+01	4.059E+00	5.058E+06	1.528E+01	9.979E+00	7.692E−01	4.053E−02	6.796E+00	1.099E−02
	Std. Dev.	3.481E−04	2.113E−04	3.127E−01	2.151E−01	3.407E+06	7.636E−01	7.918E−01	1.815E−01	6.725E−02	5.867E−01	1.939E−07
Friedman average rank		1.58	1.73	6.85	9.31	9.92	9.69	6.46	7.08	5.15	4.85	3.38
Rank		1	2	7	9	11	10	6	8	5	4	3

Table 8
Statistical result of fixed dimension benchmark functions f_{14-23} for $N = 10$ of AHHO, HHO, CSA, CS, DE, FA, GWO, PSO, WDO, and WOA. The N of L-SHADE decrease from $18 \times d$ to 4.

Benchmark	Metric	AHHO	HHO	CSA	CS	DE	FA	GWO	PSO	WDO	WOA	L-SHADE
f_{14}	Best	**9.980E−01**	**9.980E−01**	1.267E+01	**9.980E−01**	**9.980E−01**	1.267E+01	1.267E+01	1.267E+01	1.267E+01	**9.980E−01**	**9.980E−01**
	Worst	5.928E+00	5.928E+00	1.267E+01	7.911E+00	2.107E+01	1.267E+01	1.267E+01	1.267E+01	1.267E+01	1.076E+01	**9.980E−01**
	Average	1.236E+00	1.295E+00	1.267E+01	2.681E+00	4.847E+00	1.267E+01	1.267E+01	1.267E+01	1.267E+01	2.979E+00	**9.980E−01**
	Std. Dev.	6.610E−01	8.370E−01	3.877E−11	1.402E+00	4.690E+00	1.499E−13	2.384E−10	5.865E−12	1.610E−11	3.394E+00	2.246E−15
f_{15}	Best	3.078E−04	3.080E−04	3.174E−04	6.936E−04	4.661E−04	3.087E−04	3.101E−04	3.107E−04	3.132E−04	3.076E−04	**3.075E−04**
	Worst	0.002	0.002	1.399E−03	1.631E−02	6.841E−02	1.196E−01	1.303E−01	1.784E−03	1.796E−03	7.147E−03	**3.075E−04**
	Average	4.162E−04	4.395E−04	6.686E−04	3.939E−03	7.664E−03	1.101E−02	3.940E−03	4.726E−04	5.077E−04	7.156E−04	**3.075E−04**
	Std. Dev.	2.367E−04	2.941E−04	2.594E−04	2.661E−03	1.101E−02	2.503E−02	1.885E−02	2.496E−04	2.664E−04	7.341E−04	4.290E−19
f_{16}	Best	**−1.031E+00**	**−1.031E+00**	**−1.031E+00**	**−1.031E+00**	**−1.031E+00**	**−1.031E+00**	**−1.031E+00**	**−1.031E+00**	**−1.031E+00**	**−1.031E+00**	**−1.031E+00**
	Worst	**−1.031E+00**	**−1.031E+00**	−1.012E+00	−7.923E−01	−2.154E−01	−8.877E−01	−9.977E−01	**−1.031E+00**	**−1.030E+00**	**−1.031E+00**	**−1.031E+00**
	Average	**−1.031E+00**	**−1.031E+00**	−1.028E+00	−1.002E+00	−1.020E+00	−1.028E+00	−1.027E+00	**−1.031E+00**	**−1.031E+00**	**−1.031E+00**	**−1.031E+00**
	Std. Dev.	4.242E−07	8.547E−06	3.994E−03	3.689E−02	8.471E−02	1.808E−02	1.035E−02	9.486E−06	2.570E−04	2.550E−09	1.539E−15
f_{17}	Best	**3.979E−01**	**3.979E−01**	2.791E+01	3.980E−01	3.979E−01	2.129E+01	**3.979E−01**	3.979E−01	**3.979E−01**	**3.979E−01**	4.058E−01
	Worst	**3.990E−01**	4.020E−01	3.284E+01	5.522E−01	1.477E+00	4.087E+01	1.950E+01	5.040E+00	4.353E−01	5.040E+00	1.854E+00
	Average	**3.988E−01**	**3.988E−01**	2.943E+01	4.264E−01	4.516E−01	2.866E+01	1.462E+00	7.693E−01	**3.988E−01**	1.001E+00	7.288E−01
	Std. Dev.	2.403E−04	5.415E−04	9.122E−01	3.181E−02	1.903E−01	3.633E+00	2.569E+00	1.266E+00	4.113E−03	1.569E+00	2.793E−01
f_{18}	Best	**3.000E+00**	**3.000E+00**	3.010E+00	3.064E+00	**3.000E+00**	**3.000E+00**	**3.000E+00**	**3.000E+00**	**3.000E+00**	**3.000E+00**	**3.000E+00**
	Worst	3.116E+00	3.007E+00	1.935E+01	4.172E+01	8.774E+01	6.632E+01	**3.000E+01**	3.002E+00	**3.000E+01**	**3.000E+00**	**3.000E+00**
	Average	3.001E+00	**3.000E+00**	5.856E+00	8.563E+00	1.015E+01	1.711E+01	5.179E+00	**3.000E+00**	3.285E+00	**3.000E+00**	**3.000E+00**
	Std. Dev.	1.108E−02	7.406E−04	2.622E+00	6.813E+00	2.086E+01	1.479E+01	7.356E+00	3.560E−04	2.699E+00	1.030E−06	1.652E−15
f_{19}	Best	**−3.862E+00**	**−3.862E+00**	−3.858E+00	−3.862E+00	−3.863E+00	−3.863E+00	−3.863E+00	−3.863E+00	−3.862E+00	−3.863E+00	**−3.863E+00**
	Worst	−3.791E+00	−3.801E+00	−3.178E+00	−3.726E+00	−3.026E+00	−9.921E−01	−6.797E−02	−8.722E−01	−3.839E+00	−5.799E−01	**−3.863E+00**
	Average	−3.853E+00	−3.856E+00	−3.731E+00	−3.829E+00	−3.800E+00	−2.919E+00	−3.268E+00	−3.823E+00	−3.855E+00	−3.736E+00	**−3.863E+00**
	Std. Dev.	1.180E−02	9.003E−03	1.363E−01	2.467E−02	1.720E−01	1.257E+00	1.221E+00	3.000E−01	4.160E−03	6.030E−01	6.249E−15
f_{20}	Best	−3.299E+00	−3.274E+00	−3.200E+00	−3.244E+00	−3.322E+00	−3.322E+00	−3.319E+00	−3.312E+00	−3.288E+00	−3.322E+00	**−3.322E+00**
	Worst	−2.155E+00	−2.149E+00	−2.253E+00	−2.421E+00	−9.779E−01	−1.832E+00	−3.066E−02	−1.578E+00	−2.116E+00	−1.182E−01	**−3.203E+00**
	Average	−2.912E+00	−2.911E+00	−2.733E+00	−2.835E+00	−3.060E+00	−3.095E+00	−2.117E+00	−2.973E+00	−3.102E+00	−2.395E+00	**−3.286E+00**
	Std. Dev.	2.100E−01	2.270E−01	2.004E−01	1.737E−01	3.488E−01	2.932E−01	9.776E−01	3.932E−01	1.770E−01	7.946E−01	5.476E−02
f_{21}	Best	**−9.889E+00**	−9.315E+00	−4.287E+00	−4.818E+00	−1.015E+01	−5.055E+00	−5.055E+00	−5.055E+00	−5.055E+00	−5.055E+00	−5.055E+00
	Worst	−4.815E+00	−4.846E+00	−1.008E+00	−1.257E+00	−1.854E+00	**−5.842E−01**	−4.973E−01	−8.810E−01	−5.001E+00	−4.973E−01	−5.055E+00
	Average	**−5.065E+00**	−5.060E+00	−1.896E+00	−2.907E+00	−4.882E+00	−1.646E+00	−3.403E+00	−4.677E+00	−5.040E+00	−3.795E+00	−5.055E+00
	Std. Dev.	4.890E−01	4.320E−01	6.009E−01	7.617E−01	2.881E+00	9.422E−01	2.078E+00	1.200E+00	1.286E−02	1.935E+00	5.649E−07
f_{22}	Best	**−1.039E+01**	−1.009E+01	−4.470E+00	−5.818E+00	−1.040E+01	−5.019E+00	−5.088E+00	−5.087E+00	−5.087E+00	−5.088E+00	−6.784E+00
	Worst	−1.811E+00	−1.832E+00	−9.830E−01	−1.502E+00	−1.432E+00	−6.349E−01	−5.211E−01	−9.081E−01	−5.032E+00	−5.211E−01	**−5.088E+00**
	Average	−5.076E+00	**−5.163E+00**	−2.021E+00	−2.908E+00	−5.402E+00	−1.440E+00	−3.429E+00	−4.918E+00	−5.074E+00	−3.785E+00	−5.109E+00
	Std. Dev.	6.280E−01	9.500E−01	6.815E−01	8.207E−01	3.126E+00	6.590E−01	2.086E+00	8.225E−01	1.118E−02	1.954E+00	1.748E−01
f_{23}	Best	−1.019E+01	−1.049E+01	−3.614E+00	−6.316E+00	**−1.054E+01**	−4.541E+00	−5.128E+00	−5.128E+00	−5.128E+00	−5.128E+00	−5.128E+00
	Worst	−2.361E+00	−1.856E+00	−9.553E−01	−1.404E+00	−8.316E−01	−7.180E−01	−5.542E−01	−9.445E−01	−5.032E+00	−5.545E−01	**−5.128E+00**
	Average	−5.260E+00	−5.152E+00	−1.975E+00	−3.128E+00	**−5.664E+00**	−1.478E+00	−3.616E+00	−5.001E+00	−5.113E+00	−3.653E+00	−5.128E+00
	Std. Dev.	0.758	1.011	5.504E−01	8.991E−01	3.384E+00	6.727E−01	2.037E+00	7.167E−01	1.628E−02	2.022E+00	2.230E−06
Friedman average rank		4.61	4.83	7.35	6.70	5.96	7.43	7.30	5.87	5.48	6.13	4.35
Rank		2	3	10	8	6	11	9	5	4	7	1

Table 9

Statistical result of fixed dimension benchmark functions f_{14-23} for $N = 30$ of AHHO, HHO, CSA, CS, DE, FA, GWO, PSO, WDO, and WOA. The N of L-SHADE decrease from $18 \times d$ to 4.

Benchmark	Metric	AHHO	HHO	CSA	CS	DE	FA	GWO	PSO	WDO	WOA	L-SHADE
f_{14}	Best	**9.980E−01**	**9.980E−01**	1.267E+01	**9.980E−01**	**9.980E−01**	1.267E+01	1.267E+01	1.267E+01	1.267E+01	**9.980E−01**	**9.980E−01**
	Worst	2.982E+00	5.928E+00	1.267E+01	3.311E+00	3.968E+00	1.267E+01	1.267E+01	1.267E+01	1.267E+01	2.982E+00	**9.980E−01**
	Average	1.097E+00	1.482E+00	1.267E+01	1.442E+00	1.048E+00	1.267E+01	1.267E+01	1.267E+01	1.267E+01	1.058E+00	**9.980E−01**
	Std. Dev.	3.310E−01	1.273E+00	1.529E−11	5.464E−01	3.265E−01	1.452E−13	2.226E−13	1.764E−12	1.084E−11	3.402E−01	2.246E−15
f_{15}	Best	**3.075E−04**	3.076E−04	3.152E−04	6.716E−04	**3.075E−04**	**3.075E−04**	3.096E−04	3.085E−04	3.225E−04	**3.075E−04**	**3.075E−04**
	Worst	0.001	0.001	9.863E−04	5.606E−03	2.036E−02	1.160E−01	8.482E−03	9.939E−04	1.774E−03	1.595E−03	**3.075E−04**
	Average	3.471E−04	3.617E−04	4.965E−04	2.106E−03	2.008E−03	2.081E−03	8.355E−04	3.851E−04	4.520E−04	5.453E−04	**3.075E−04**
	Std. Dev.	9.434E−05	1.378E−04	1.336E−04	9.233E−04	5.117E−03	1.155E−02	9.386E−04	9.129E−05	1.867E−04	3.382E−04	4.290E−19
f_{16}	Best	**−1.031E+00**	**−1.031E+00**	**−1.031E+00**	**−1.031E+00**	**−1.031E+00**	**−1.031E+00**	**−1.031E+00**	**−1.031E+00**	**−1.031E+00**	**−1.031E+00**	**−1.031E+00**
	Worst	**−1.031E+00**	**−1.031E+00**	**−1.025E+00**	**−9.754E−01**	**−1.031E+00**	**−1.031E+00**	**−9.972E−01**	**−1.031E+00**	**−1.030E+00**	**−1.031E+00**	**−1.031E+00**
	Average	**−1.031E+00**	**−1.031E+00**	**−1.030E+00**	**−1.022E+00**	**−1.031E+00**	**−1.031E+00**	**−1.028E+00**	**−1.031E+00**	**−1.031E+00**	**−1.031E+00**	**−1.031E+00**
	Std. Dev.	2.939E−09	2.980E−08	1.612E−03	9.477E−03	1.560E−15	1.473E−15	1.045E−02	1.002E−06	2.805E−04	1.947E−10	1.539E−15
f_{17}	Best	**3.979E−01**	**3.979E−01**	2.784E+01	3.981E−01	**3.979E−01**	2.019E+01	**3.979E−01**	**3.979E−01**	**3.979E−01**	**3.979E−01**	4.058E−01
	Worst	**3.979E−01**	**3.979E−01**	3.010E+01	4.295E−01	**3.979E−01**	3.273E+01	5.040E+00	5.040E+00	3.994E−01	5.040E+00	1.854E+00
	Average	**3.979E−01**	**3.979E−01**	2.871E+01	4.053E−01	**3.979E−01**	2.442E+01	6.735E−01	4.907E−01	3.981E−01	4.907E−01	7.288E−01
	Std. Dev.	6.005E−05	5.222E−05	5.452E−01	6.529E−03	1.060E−15	2.789E+00	1.096E+00	6.532E−01	2.463E−04	6.532E−01	2.793E−01
f_{18}	Best	**3.000E+00**	**3.000E+00**	3.057E+00	3.003E+00	**3.000E+00**	**3.000E+00**	**3.000E+00**	**3.000E+00**	**3.000E+00**	**3.000E+00**	**3.000E+00**
	Worst	**3.000E+00**	**3.000E+00**	7.863E+00	9.919E+00	**3.000E+00**	3.000E+01	3.000E+01	**3.000E+00**	3.000E+01	**3.000E+00**	**3.000E+00**
	Average	**3.000E+00**	**3.000E+00**	4.265E+00	4.412E+00	**3.000E+00**	8.973E+00	4.366E+00	**3.000E+00**	3.286E+00	**3.000E+00**	**3.000E+00**
	Std. Dev.	2.506E−06	5.142E−07	1.085E+00	1.391E+00	1.566E−15	1.123E+01	5.910E+00	5.668E−05	2.699E+00	2.303E−08	1.652E−15
f_{19}	Best	−3.862E+00	−3.862E+00	−3.860E+00	−3.862E+00	**−3.863E+00**	**−3.863E+00**	**−3.863E+00**	**−3.863E+00**	**−3.863E+00**	**−3.863E+00**	**−3.863E+00**
	Worst	−3.825E+00	−3.814E+00	−3.553E+00	−3.825E+00	**−3.863E+00**	−1.001E+00	−8.722E−01	−3.854E+00	−3.838E+00	−3.855E+00	**−3.863E+00**
	Average	−3.860E+00	−3.859E+00	−3.791E+00	−3.849E+00	**−3.863E+00**	−3.671E+00	−3.767E+00	−3.857E+00	−3.855E+00	−3.858E+00	**−3.863E+00**
	Std. Dev.	4.002E−03	6.128E−03	5.991E−02	9.088E−03	6.249E−15	4.808E−01	4.967E−01	3.119E−03	4.428E−03	3.845E−03	6.249E−15
f_{20}	Best	−3.293E+00	−3.312E+00	−3.246E+00	−3.219E+00	**−3.322E+00**	−3.322E+00	−3.322E+00	−3.318E+00	−3.307E+00	**−3.322E+00**	**−3.322E+00**
	Worst	−2.816E+00	−2.727E+00	−2.483E+00	−2.727E+00	−3.138E+00	−2.981E+00	−2.079E−01	−2.267E+00	−2.405E+00	−1.172E+00	**−3.203E+00**
	Average	−3.076E+00	−3.119E+00	−2.874E+00	−2.965E+00	−3.236E+00	−3.258E+00	−2.593E+00	−3.084E+00	−3.108E+00	−2.839E+00	**−3.286E+00**
	Std. Dev.	0.108	0.109	1.470E−01	8.534E−02	5.446E−02	8.593E−02	7.403E−01	2.452E−01	1.221E−01	5.546E−01	5.476E−02
f_{21}	Best	−1.006E+01	**−1.013E+01**	−4.853E+00	−6.312E+00	−1.015E+01	−5.055E+00	−5.055E+00	−5.055E+00	−5.054E+00	−5.055E+00	−5.055E+00
	Worst	−5.038E+00	−5.010E+00	−1.209E+00	−1.984E+00	−2.630E+00	−1.081E+00	−8.810E−01	−5.053E+00	−4.970E+00	**−5.055E+00**	**−5.055E+00**
	Average	**−5.292E+00**	−5.245E+00	−2.619E+00	−3.563E+00	−9.122E+00	−2.796E+00	−4.552E+00	−5.055E+00	−5.032E+00	−5.055E+00	−5.055E+00
	Std. Dev.	1.058E+00	9.620E−01	7.455E−01	7.478E−01	2.259E+00	1.151E+00	1.362E+00	3.677E−04	1.841E−02	6.185E−06	5.649E−07
f_{22}	Best	**−1.037E+01**	−1.033E+01	−4.547E+00	−6.769E+00	−1.040E+01	−5.088E+00	−5.088E+00	−5.088E+00	−5.087E+00	−5.088E+00	−6.784E+00
	Worst	−5.015E+00	−3.719E+00	−1.487E+00	−2.109E+00	−2.752E+00	−1.120E+00	−9.081E−01	−5.086E+00	−5.006E+00	−9.081E−01	**−5.088E+00**
	Average	**−5.320E+00**	−5.232E+00	−2.557E+00	−3.660E+00	−9.747E+00	−2.705E+00	−4.626E+00	−5.087E+00	−5.065E+00	−4.962E+00	−5.109E+00
	Std. Dev.	8.630E−01	1.112E+00	7.076E−01	8.686E−01	1.999E+00	1.050E+00	1.313E+00	2.815E−04	1.672E−02	7.162E−01	1.748E−01
f_{23}	Best	**−1.051E+01**	−1.034E+01	−4.400E+00	−6.684E+00	−1.054E+01	−5.128E+00	−5.128E+00	−5.128E+00	−5.128E+00	−5.128E+00	−5.128E+00
	Worst	−5.014E+00	−1.674E+00	−1.247E+00	−2.399E+00	−2.427E+00	−1.144E+00	−9.445E−01	−5.127E+00	−5.049E+00	−9.471E−01	**−5.128E+00**
	Average	**−5.325E+00**	−5.294E+00	−2.631E+00	−3.682E+00	−1.001E+01	−2.769E+00	−4.750E+00	−5.128E+00	−5.106E+00	−5.003E+00	−5.128E+00
	Std. Dev.	1.004E+00	1.073E+00	6.417E−01	7.663E−01	1.946E+00	1.049E+00	1.202E+00	3.641E−04	1.828E−02	7.168E−01	2.230E−06
Friedman average rank		4.96	5.00	7.57	7.09	4.37	7.00	7.22	6.04	6.22	5.87	4.67
Rank		3	4	11	9	1	8	10	6	7	5	2

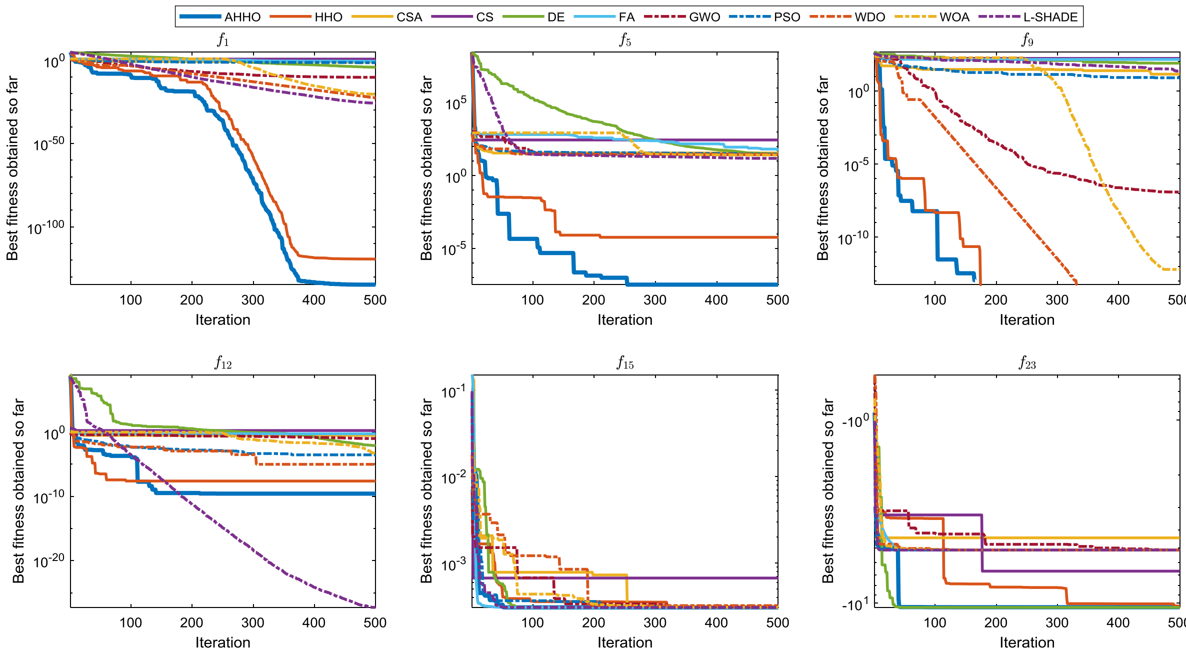

Fig. 6. The convergence curve of the six classical test functions f_1, f_5, f_9, f_{12}, f_{15} and f_{23}.

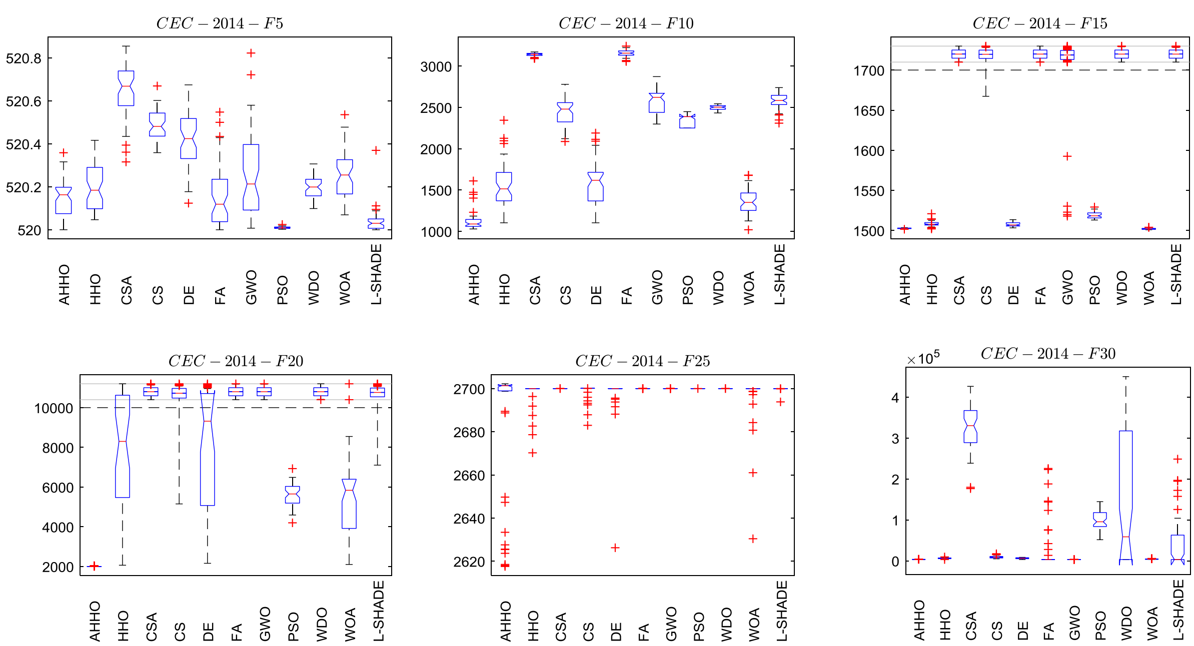

Fig. 7. Boxplot of the six modern CEC 2014 test functions.

and the cumulative probability distribution of class k is

$$P^k = \sum_{i=t_{k-1}}^{t_k} p_i.$$

q is the measure of the degree of non-extensivity of the system called Tsallis parameter or even entropic index. The Eq. (4) serves as a fitness function in a maximization problem for 1D Tsallis based multilevel thresholding. It found to be an exhaustive search process as the number of thresholds m increases, leads to an optimization problem.

2.1.2. 2D Tsallis entropy

Assume a digital image of size $M \times N$, and $[f(x, y)|x \in \{1, 2, \ldots, M\}, y \in \{1, 2, \ldots, N\}]$ represent the pixel intensity (grey level) values for a point (x, y). Let the set of all grey levels $\{0, 1, \ldots, L-1\}$ for an image having the L grey level (for an 8bit image the $L = 256$), then the one-dimensional histogram can be $h(i)$ for $i \in \{0, 1, 2, \ldots, L-1\}$. The global threshold selection uses the grey level histogram of the image by optimizing a suitable objective function as desired.

The 2D histogram depends on the average grey level values at the point (x, y) and its neighbourhood pixels in the adjacent field of $k \times k$ [49,80]. Let us define the $a(x, y)$ be the average grey level

Table 10
p-value of the Wilcoxon rank-sum test with 5% significance of scalable benchmark functions f_{1-13} with $d = 30$ for $N = 10$ of AHHO, HHO, CSA, CS, DE, FA, GWO, PSO, WDO, and WOA. The N of L-SHADE decrease from 18 × 30 to 4. (p-values ≥ 0.05 are shown in boldface). + means that AHHO is statistically significantly better at p-value at 0.05 than another algorithm; ≈ means that AHHO is statistically no significant at p-value at 0.05 than another algorithm; − means that AHHO is statistically significant worse than another algorithm. Counts +/≈ /− is the number of problems the AHHO is statistically better/equal/worse than other algorithms.

	HHO	CSA	CS	DE	FA	GWO	PSO	WDO	WOA	L-SHADE
f_1	1.94E−03	4.16E−23	4.16E−23	4.16E−23	4.16E−23	4.16E−23	4.16E−23	4.16E−23	4.16E−23	4.16E−23
f_2	**3.68E−01**	4.16E−23	4.16E−23	4.16E−23	4.16E−23	4.16E−23	4.16E−23	4.16E−23	4.16E−23	4.16E−23
f_3	1.71E−05	4.16E−23	4.16E−23	4.16E−23	4.16E−23	4.16E−23	4.16E−23	4.16E−23	4.16E−23	4.16E−23
f_4	6.80E−06	4.16E−23	4.16E−23	4.16E−23	4.16E−23	4.16E−23	4.16E−23	4.16E−23	4.16E−23	4.16E−23
f_5	**4.84E−01**	4.16E−23	4.16E−23	4.16E−23	4.16E−23	4.16E−23	4.16E−23	4.16E−23	4.16E−23	4.16E−23
f_6	3.57E−02	4.16E−23	4.16E−23	4.16E−23	4.16E−23	4.16E−23	4.16E−23	1.40E−20	4.16E−23	4.16E−23
f_7	**7.64E−01**	4.16E−23	4.16E−23	4.16E−23	4.16E−23	4.16E−23	4.16E−23	4.16E−23	4.16E−23	5.50E−16
f_8	**9.20E−01**	4.16E−23	4.16E−23	4.16E−23	4.16E−23	4.16E−23	4.16E−23	4.16E−23	4.16E−23	4.16E−23
f_9	**1.00E+00**	4.16E−23	4.16E−23	4.16E−23	4.16E−23	4.16E−23	4.16E−23	4.04E−28	4.16E−23	4.16E−23
f_{10}	**1.00E+00**	4.16E−23	4.16E−23	4.16E−23	4.16E−23	4.16E−23	4.16E−23	4.16E−23	4.16E−23	4.16E−23
f_{11}	**1.00E+00**	4.16E−23	4.16E−23	4.16E−23	4.16E−23	4.16E−23	4.16E−23	2.07E−25	4.16E−23	**1.00E+00**
f_{12}	1.24E−02	4.16E−23	4.16E−23	4.16E−23	4.16E−23	4.16E−23	4.16E−23	2.98E−10	4.16E−23	4.16E−23
f_{13}	**4.84E−01**	4.16E−23	4.16E−23	4.16E−23	4.16E−23	4.16E−23	4.16E−23	1.40E−20	4.16E−23	4.16E−23
Counts +/≈ /−	5/3/5	13/0/0	13/0/0	13/0/0	13/0/0	13/0/0	13/0/0	13/0/0	13/0/0	12/1/0

Table 11
p-value of the Wilcoxon rank-sum test with 5% significance of scalable benchmark functions f_{1-13} with $d = 30$ for $N = 30$ of AHHO, HHO, CSA, CS, DE, FA, GWO, PSO, WDO, and WOA. The N of L-SHADE decrease from 18 × 30 to 4. (p-values ≥ 0.05 are shown in boldface). + means that AHHO is statistically significantly better at p-value at 0.05 than another algorithm; ≈ means that AHHO is statistically no significant at p-value at 0.05 than another algorithm; − means that AHHO is statistically significant worse than another algorithm. Counts +/≈ /− is the number of problems the AHHO is statistically better/equal/worse than other algorithms.

	HHO	CSA	CS	DE	FA	GWO	PSO	WDO	WOA	L-SHADE
f_1	4.16E−23	4.16E−23	4.16E−23	4.16E−23	4.16E−23	4.16E−23	4.16E−23	4.16E−23	4.16E−23	4.16E−23
f_2	**8.91E−02**	4.16E−23	4.16E−23	4.16E−23	4.16E−23	4.16E−23	4.16E−23	4.16E−23	4.16E−23	4.16E−23
f_3	3.57E−02	4.16E−23	4.16E−23	4.16E−23	4.16E−23	4.16E−23	4.16E−23	4.16E−23	4.16E−23	4.16E−23
f_4	6.80E−06	4.16E−23	4.16E−23	4.16E−23	4.16E−23	4.16E−23	4.16E−23	4.16E−23	4.16E−23	4.16E−23
f_5	**1.34E−01**	4.16E−23	4.16E−23	4.16E−23	4.16E−23	4.16E−23	4.16E−23	4.16E−23	4.16E−23	4.16E−23
f_6	**5.74E−02**	4.16E−23	4.16E−23	9.03E−20	4.16E−23	4.16E−23	4.16E−23	4.16E−23	4.16E−23	4.16E−23
f_7	**4.84E−01**	4.16E−23	4.16E−23	4.16E−23	4.16E−23	4.16E−23	4.16E−23	4.16E−23	4.16E−23	4.16E−23
f_8	2.14E−02	4.16E−23	4.16E−23	4.16E−23	4.16E−23	4.16E−23	4.16E−23	4.16E−23	4.16E−23	3.01E−22
f_9	**1.00E+00**	4.16E−23	4.16E−23	4.16E−23	4.16E−23	4.16E−23	4.16E−23	2.52E−29	4.16E−23	4.16E−23
f_{10}	**1.00E+00**	4.16E−23	4.16E−23	4.16E−23	4.16E−23	4.16E−23	4.16E−23	4.16E−23	4.16E−23	4.16E−23
f_{11}	**1.00E+00**	4.16E−23	4.16E−23	4.16E−23	4.16E−23	4.16E−23	4.16E−23	6.62E−24	6.10E−05	**1.00E+00**
f_{12}	**1.00E+00**	4.16E−23	4.16E−23	4.16E−23	4.16E−23	4.16E−23	4.16E−23	3.01E−22	4.16E−23	4.16E−23
f_{13}	**1.94E−01**	4.16E−23	4.16E−23	4.16E−23	4.16E−23	4.16E−23	4.16E−23	4.16E−23	4.16E−23	4.16E−23
Counts +/≈ /−	4/4/5	13/0/0	13/0/0	13/0/0	13/0/0	13/0/0	13/0/0	13/0/0	13/0/0	13/0/0

Table 12
p-value of the Wilcoxon rank-sum test with 5% significance of scalable benchmark functions f_{1-13} with $d = 100$ for $N = 10$ of AHHO, HHO, CSA, CS, DE, FA, GWO, PSO, WDO, and WOA. The N of L-SHADE decrease from 18 × 100 to 4. (p-values ≥ 0.05 are shown in boldface). + means that AHHO is statistically significantly better at p-value at 0.05 than another algorithm; ≈ means that AHHO is statistically no significant at p-value at 0.05 than another algorithm; − means that AHHO is statistically significant worse than another algorithm. Counts +/≈ /− is the number of problems the AHHO is statistically better/equal/worse than other algorithms.

	HHO	CSA	CS	DE	FA	GWO	PSO	WDO	WOA	L-SHADE
f_1	1.24E−02	4.16E−23	4.16E−23	4.16E−23	4.16E−23	4.16E−23	4.16E−23	4.16E−23	4.16E−23	4.16E−23
f_2	9.67E−04	4.16E−23	4.16E−23	4.16E−23	4.16E−23	4.16E−23	4.16E−23	4.16E−23	4.16E−23	4.16E−23
f_3	4.13E−05	4.16E−23	4.16E−23	4.16E−23	4.16E−23	4.16E−23	4.16E−23	4.16E−23	4.16E−23	4.16E−23
f_4	6.80E−06	4.16E−23	4.16E−23	4.16E−23	4.16E−23	4.16E−23	4.16E−23	4.16E−23	4.16E−23	4.16E−23
f_5	**1.94E−01**	4.16E−23	4.16E−23	4.16E−23	4.16E−23	4.16E−23	4.16E−23	4.16E−23	4.16E−23	4.16E−23
f_6	3.73E−03	4.16E−23	4.16E−23	4.16E−23	4.16E−23	4.16E−23	4.16E−23	4.16E−23	4.16E−23	4.16E−23
f_7	**4.84E−01**	4.16E−23	4.16E−23	4.16E−23	4.16E−23	4.16E−23	4.16E−23	4.16E−23	4.16E−23	1.40E−20
f_8	**7.64E−01**	4.16E−23	4.16E−23	4.16E−23	4.16E−23	4.16E−23	4.16E−23	4.16E−23	4.16E−23	4.16E−23
f_9	**1.00E+00**	4.16E−23	4.16E−23	4.16E−23	4.16E−23	4.16E−23	4.16E−23	8.27E−25	4.16E−23	4.16E−23
f_{10}	**1.00E+00**	4.16E−23	4.16E−23	4.16E−23	4.16E−23	4.16E−23	4.16E−23	4.16E−23	4.16E−23	4.16E−23
f_{11}	**1.00E+00**	4.16E−23	4.16E−23	4.16E−23	4.16E−23	4.16E−23	4.16E−23	1.32E−23	4.16E−23	4.16E−23
f_{12}	**1.94E−01**	4.16E−23	4.16E−23	4.16E−23	4.16E−23	4.16E−23	4.16E−23	2.10E−21	4.16E−23	4.16E−23
f_{13}	**1.00E+00**	4.16E−23	4.16E−23	4.16E−23	4.16E−23	4.16E−23	4.16E−23	4.16E−23	4.16E−23	2.10E−21
Counts +/≈ /−	5/4/4	13/0/0	13/0/0	13/0/0	13/0/0	13/0/0	13/0/0	13/0/0	13/0/0	13/0/0

for the point located at (x, y) as:

$$a(x, y) = \left\lfloor \frac{1}{k^2} \sum_{i=-\frac{k-1}{2}}^{\frac{k-1}{2}} \sum_{j=-\frac{k-1}{2}}^{\frac{k-1}{2}} f(x+i, y+j) \right\rfloor \tag{5}$$

where $\lfloor z \rfloor$ represents the integer part of z.

The 2D histogram is constructed using the grey level values $f(x, y)$ and average grey level values $a(x, y)$ as:

$$p(i, j) = \frac{1}{M \bullet N} \left\{ n_{ij} | f(x, y) = i, a(x, y) = j; i, j \in (0, L-1) \right\} \tag{6}$$

where the n_{ij} represents the number of pixels with grey level values with i and average grey level values with j.

The 2D histogram plane for multilevel thresholding as presented in Fig. 1, is subdivided by a set of m thresholds $t = [t_1, t_2, \ldots, t_m]$ of grey-level image and a set of m threshold values $s = [s_1, s_2, \ldots, s_m]$ of average grey level, which resulted in a $M \times M$ quadrants, where $M = m + 1$. Among all possible planes, the diagonal planes can be used for the separation objects, backgrounds, and intermediate class. The other planes consist of mostly edges and noises information, which can be ignored. Let

Table 13
p-value of the Wilcoxon rank-sum test with 5% significance of scalable benchmark functions f_{1-13} with $d = 100$ for $N = 30$ of AHHO, HHO, CSA, CS, DE, FA, GWO, PSO, WDO, and WOA. The N of L-SHADE decrease from 18 × 100 to 4. (p-values ≥ 0.05 are shown in boldface). + means that AHHO is statistically significantly better at p-value at 0.05 than another algorithm; ≈ means that AHHO is statistically no significant at p-value at 0.05 than another algorithm; − means that AHHO is statistically significant worse than another algorithm. Counts +/≈ /− is the number of problems the AHHO is statistically better/equal/worse than other algorithms.

	HHO	CSA	CS	DE	FA	GWO	PSO	WDO	WOA	L-SHADE
f_1	6.80E−06	4.16E−23	4.16E−23	4.16E−23	4.16E−23	4.16E−23	4.16E−23	4.16E−23	4.16E−23	4.16E−23
f_2	6.93E−03	4.16E−23	4.16E−23	4.16E−23	4.16E−23	4.16E−23	4.16E−23	4.16E−23	4.16E−23	4.16E−23
f_3	2.16E−04	4.16E−23	4.16E−23	4.16E−23	4.16E−23	4.16E−23	4.16E−23	4.16E−23	4.16E−23	4.16E−23
f_4	6.80E−06	4.16E−23	4.16E−23	4.16E−23	4.16E−23	4.16E−23	4.16E−23	4.16E−23	4.16E−23	4.16E−23
f_5	**9.20E−01**	4.16E−23	4.16E−23	4.16E−23	4.16E−23	4.16E−23	4.16E−23	4.16E−23	4.16E−23	4.16E−23
f_6	1.24E−02	4.16E−23	4.16E−23	4.16E−23	4.16E−23	4.16E−23	4.16E−23	4.16E−23	4.16E−23	4.16E−23
f_7	**2.71E−01**	4.16E−23	4.16E−23	4.16E−23	4.16E−23	4.16E−23	4.16E−23	4.16E−23	4.16E−23	4.16E−23
f_8	2.14E−02	4.16E−23	4.16E−23	4.16E−23	4.16E−23	4.16E−23	4.16E−23	4.16E−23	4.16E−23	4.16E−23
f_9	**1.00E+00**	4.16E−23	4.16E−23	4.16E−23	4.16E−23	4.16E−23	4.16E−23	1.73E−18	4.16E−23	4.16E−23
f_{10}	**1.00E+00**	4.16E−23	4.16E−23	4.16E−23	4.16E−23	4.16E−23	4.16E−23	4.16E−23	4.16E−23	4.16E−23
f_{11}	**1.00E+00**	4.16E−23	4.16E−23	4.16E−23	4.16E−23	4.16E−23	4.16E−23	1.65E−24	4.16E−23	4.16E−23
f_{12}	**1.34E−01**	4.16E−23	4.16E−23	4.16E−23	4.16E−23	4.16E−23	4.16E−23	4.16E−23	4.16E−23	5.58E−19
f_{13}	**2.71E−01**	4.16E−23	4.16E−23	4.16E−23	4.16E−23	4.16E−23	4.16E−23	4.16E−23	4.16E−23	4.16E−23
Counts +/≈ /−	6/3/4	13/0/0	13/0/0	13/0/0	13/0/0	13/0/0	13/0/0	13/0/0	13/0/0	13/0/0

Table 14
p-value of the Wilcoxon rank-sum test with 5% significance of fixed dimension benchmark functions f_{14-23} for $N = 10$ of AHHO, HHO, CSA, CS, DE, FA, GWO, PSO, WDO, and WOA. The N of L-SHADE decrease from 18 × d to 4. (p-values ≥ 0.05 are shown in boldface). + means that AHHO is statistically significantly better at p-value at 0.05 than another algorithm; ≈ means that AHHO is statistically no significant at p-value at 0.05 than another algorithm; − means that AHHO is statistically significant worse than another algorithm. Counts +/≈ /− is the number of problems the AHHO is statistically better/equal/worse than other algorithms.

	HHO	CSA	CS	DE	FA	GWO	PSO	WDO	WOA	L-SHADE
f_{14}	**1.94E−01**	4.16E−23	1.36E−14	1.16E−07	4.16E−23	4.16E−23	4.16E−23	4.16E−23	3.68E−01	4.16E−23
f_{15}	**1.00E+00**	6.38E−14	4.16E−23	2.10E−21	1.04E−16	1.25E−12	**1.34E−01**	2.60E−06	3.40E−07	4.16E−23
f_{16}	2.16E−04	4.16E−23	4.16E−23	3.64E−09	1.40E−20	1.06E−09	2.98E−10	4.16E−23	2.79E−15	4.16E−23
f_{17}	**3.68E−01**	4.16E−23	3.01E−22	9.58E−07	4.16E−23	2.16E−04	4.13E−05	2.16E−04	3.64E−09	4.16E−23
f_{18}	4.65E−04	4.16E−23	4.16E−23	6.93E−03	1.24E−02	3.32E−18	2.16E−04	2.10E−21	2.79E−15	4.16E−23
f_{19}	1.24E−02	9.03E−20	2.88E−13	**5.74E−02**	**2.71E−01**	6.93E−03	**1.94E−01**	3.57E−02	**3.68E−01**	4.16E−23
f_{20}	**4.84E−01**	3.80E−08	1.94E−03	1.16E−07	3.64E−09	2.16E−04	3.73E−03	3.64E−09	6.93E−03	4.16E−23
f_{21}	**7.64E−01**	4.16E−23	4.16E−23	6.93E−03	3.01E−22	**2.71E−01**	2.08E−11	9.67E−04	2.16E−04	3.01E−22
f_{22}	**9.20E−01**	4.16E−23	2.10E−21	**5.74E−02**	4.16E−23	**4.84E−01**	1.25E−12	3.73E−03	9.67E−04	3.01E−22
f_{23}	4.65E−04	4.16E−23	1.40E−20	**8.91E−02**	4.16E−23	3.57E−02	2.79E−15	4.65E−04	3.73E−03	2.10E−21
Counts +/≈ /−	4/1/5	10/0/0	10/0/0	7/0/3	9/0/1	8/0/2	8/0/2	10/0/0	9/0/1	10/0/0

Table 15
p-value of the Wilcoxon rank-sum test with 5% significance of fixed dimension benchmark functions f_{14-23} for $N = 30$ of AHHO, HHO, CSA, CS, DE, FA, GWO, PSO, WDO, and WOA. The N of L-SHADE decrease from 18 × d to 4. (p-values ≥ 0.05 are shown in boldface). + means that AHHO is statistically significantly better at p-value at 0.05 than another algorithm; ≈ means that AHHO is statistically no significant at p-value at 0.05 than another algorithm; − means that AHHO is statistically significant worse than another algorithm. Counts +/≈ /− is the number of problems the AHHO is statistically better/equal/worse than other algorithms.

	HHO	CSA	CS	DE	FA	GWO	PSO	WDO	WOA	L-SHADE
f_{14}	**4.84E−01**	4.16E−23	3.32E−18	1.40E−20	4.16E−23	4.16E−23	4.16E−23	4.16E−23	3.32E−18	4.16E−23
f_{15}	**1.34E−01**	5.58E−19	4.16E−23	2.14E−02	1.06E−09	1.04E−16	9.67E−04	5.50E−16	**4.84E−01**	4.16E−23
f_{16}	**2.71E−01**	4.16E−23	4.16E−23	4.16E−23	4.16E−23	4.16E−23	3.01E−22	4.16E−23	**2.71E−01**	4.16E−23
f_{17}	3.57E−02	4.16E−23	3.01E−22	4.16E−23	4.16E−23	8.03E−11	1.71E−05	2.79E−15	2.08E−11	4.16E−23
f_{18}	3.80E−08	4.16E−23	4.16E−23	4.16E−23	3.40E−07	4.16E−23	3.64E−09	4.16E−23	2.60E−06	4.16E−23
f_{19}	**7.64E−01**	3.01E−22	1.04E−16	4.16E−23	4.65E−04	5.20E−12	3.80E−08	1.25E−12	**1.34E−01**	4.16E−23
f_{20}	2.14E−02	2.88E−13	2.60E−06	3.32E−18	5.50E−16	1.24E−02	2.71E−01	4.84E−01	**2.71E−01**	1.40E−20
f_{21}	**3.68E−01**	4.16E−23	2.10E−21	5.58E−19	3.01E−22	**7.64E−01**	2.88E−13	2.08E−11	5.58E−19	5.58E−19
f_{22}	**4.84E−01**	4.16E−23	9.03E−20	1.90E−17	9.03E−20	**2.71E−01**	5.50E−16	2.79E−15	5.58E−19	1.40E−20
f_{23}	**1.00E+00**	4.16E−23	9.03E−20	3.32E−18	2.10E−21	4.65E−04	1.25E−12	5.20E−12	3.32E−18	9.03E−20
Counts +/≈ /−	3/1/6	10/0/0	10/0/0	10/0/0	10/0/0	8/0/2	10/0/0	10/0/0	6/0/4	10/0/0

us define the posterior class probability of diagonal regions as:

$$P_{D1}(t,s) = \sum_{i=0}^{t_1}\sum_{j=0}^{s_1} p(i,j),$$

$$P_{D2}(t,s) = \sum_{i=t_1+1}^{t_2}\sum_{j=s_1+1}^{s_2} p(i,j),$$

and

$$P_{Dm}(t,s) = \sum_{i=t_m+1}^{L-1}\sum_{j=s_m+1}^{L-1} p(i,j). \tag{7}$$

The 2D Tsallis entropy for a M classes multilevel thresholding problem [9] with m thresholds $[t_1, t_2, \ldots, t_m]$ for a given image by maximization problem as:

$$[t_1, t_2, \ldots, t_m]_{opt} = \text{argmax}\left[S_q^1(t,s) + S_q^2(t,s) + \cdots + S_q^M(t,s) + (1-q) \times S_q^1(t,s) \times S_q^2(t,s) \times \cdots \times S_q^M(t,s)\right] \tag{8}$$

where

$$S_q^1(t,s) = \frac{1}{q-1}\left[1 - \sum_{i=0}^{t_1}\sum_{j=0}^{s_1}\left(\frac{p(i,j)}{P_{D1}(t,s)}\right)^q\right],$$

$$S_q^2(t,s) = \frac{1}{q-1}\left[1 - \sum_{i=t_1+1}^{t_2}\sum_{j=s_1+1}^{s_2}\left(\frac{p(i,j)}{P_{D2}(t,s)}\right)^q\right],$$

Table 16
Statistical result of CEC-BC-2014 test functions.

Benchmark	Metric	AHHO	HHO	CSA	CS	DE	FA	GWO	PSO	WDO	WOA	L-SHADE
CEC-2014-F1	Best	**1.381E+02**	5.927E+03	4.430E+09	1.303E+07	8.871E+05	4.419E+09	1.683E+07	2.555E+06	3.852E+09	2.616E+04	3.039E+07
	Worst	**6.585E+05**	5.511E+06	4.472E+09	8.131E+07	4.833E+07	4.495E+09	3.938E+09	5.110E+07	3.973E+09	1.010E+07	5.533E+08
	Average	**3.717E+04**	8.944E+05	4.454E+09	4.942E+07	1.429E+07	4.460E+09	4.150E+08	2.452E+07	3.907E+09	1.217E+06	2.180E+08
	Std. Dev.	9.885E+04	1.231E+06	9.859E+06	1.850E+07	1.058E+07	1.640E+07	5.637E+08	1.301E+07	2.616E+07	1.872E+06	1.176E+08
CEC-2014-F2	Best	6.547E+02	**2.000E+02**	1.584E+10	1.631E+09	1.557E+05	1.582E+10	4.341E+09	1.796E+05	1.367E+10	1.837E+04	2.819E+09
	Worst	**7.645E+03**	4.549E+05	1.599E+10	8.778E+09	1.343E+06	1.618E+10	1.035E+10	3.026E+06	1.399E+10	2.185E+05	8.302E+09
	Average	**3.458E+03**	1.046E+04	1.593E+10	5.967E+09	6.211E+05	1.595E+10	7.618E+09	9.006E+05	1.382E+10	7.421E+04	5.286E+09
	Std. Dev.	1.509E+03	6.353E+04	3.494E+07	1.545E+09	2.769E+05	6.929E+07	1.273E+09	4.686E+05	6.772E+07	4.450E+04	1.317E+09
CEC-2014-F3	Best	**3.000E+02**	3.650E+02	2.447E+06	1.005E+04	1.958E+03	1.539E+06	1.292E+04	3.616E+03	1.676E+04	9.042E+02	7.761E+03
	Worst	**3.904E+02**	1.371E+03	2.925E+06	2.175E+04	1.413E+04	4.634E+06	1.853E+04	1.323E+04	1.779E+04	6.082E+03	1.934E+04
	Average	**3.055E+02**	7.548E+02	2.651E+06	1.704E+04	6.510E+03	2.437E+06	1.796E+04	8.348E+03	1.727E+04	1.846E+03	1.653E+04
	Std. Dev.	1.883E+01	2.475E+02	1.204E+05	2.259E+03	2.542E+03	6.392E+05	8.738E+02	2.533E+03	2.324E+02	1.100E+03	2.137E+03
CEC-2014-F4	Best	**4.000E+02**	**4.000E+02**	1.151E+04	5.772E+02	4.003E+02	1.157E+04	1.797E+03	4.009E+02	9.947E+03	4.008E+02	8.725E+02
	Worst	**4.353E+02**	4.675E+02	1.167E+04	1.752E+03	5.808E+02	1.182E+04	8.195E+03	6.536E+02	1.018E+04	5.020E+02	3.565E+03
	Average	**4.206E+02**	4.282E+02	1.162E+04	9.396E+02	4.486E+02	1.166E+04	3.421E+03	4.679E+02	1.008E+04	4.265E+02	2.084E+03
	Std. Dev.	1.579E+01	1.529E+01	3.064E+01	2.291E+02	3.643E+01	4.960E+01	1.581E+03	5.184E+01	5.528E+01	1.786E+01	6.498E+02
CEC-2014-F5	Best	**5.200E+02**	5.201E+02	5.203E+02	5.204E+02	5.201E+02	**5.200E+02**	**5.200E+02**	**5.200E+02**	5.201E+02	**5.200E+02**	**5.200E+02**
	Worst	5.204E+02	5.205E+02	5.209E+02	5.207E+02	5.207E+02	5.205E+02	5.208E+02	**5.200E+02**	5.203E+02	5.204E+02	5.204E+02
	Average	5.202E+02	5.203E+02	5.206E+02	5.205E+02	5.204E+02	5.202E+02	5.203E+02	**5.200E+02**	5.202E+02	5.201E+02	5.200E+02
	Std. Dev.	1.084E−01	1.181E−01	1.271E−01	7.137E−02	1.318E−01	1.398E−01	1.945E−01	4.487E−03	4.882E−02	8.240E−02	5.541E−02
CEC-2014-F6	Best	**6.000E+02**	6.004E+02	6.142E+02	6.081E+02	6.043E+02	6.141E+02	6.105E+02	6.120E+02	6.129E+02	6.048E+02	6.097E+02
	Worst	**6.047E+02**	6.089E+02	6.145E+02	6.116E+02	6.105E+02	6.145E+02	6.139E+02	6.138E+02	6.142E+02	6.103E+02	6.120E+02
	Average	**6.011E+02**	6.035E+02	6.143E+02	6.103E+02	6.077E+02	6.143E+02	6.126E+02	6.131E+02	6.136E+02	6.081E+02	6.111E+02
	Std. Dev.	1.296E+00	1.634E+00	5.760E−02	6.804E−01	1.452E+00	9.465E−02	8.472E−01	3.095E−01	3.784E−01	1.385E+00	6.280E−01
CEC-2014-F7	Best	**7.000E+02**	7.002E+02	1.109E+03	7.433E+02	7.004E+02	1.108E+03	8.579E+02	7.008E+02	1.070E+03	7.004E+02	7.677E+02
	Worst	**7.002E+02**	7.009E+02	1.112E+03	8.483E+02	7.016E+02	1.114E+03	9.889E+02	7.117E+02	1.074E+03	7.018E+02	9.291E+02
	Average	**7.000E+02**	7.005E+02	1.111E+03	7.944E+02	7.010E+02	1.111E+03	9.165E+02	7.044E+02	1.072E+03	7.010E+02	8.588E+02
	Std. Dev.	3.928E−02	1.480E−01	6.871E−01	2.449E+01	2.233E−01	1.095E+00	2.878E+01	2.689E+00	1.069E+00	2.144E−01	3.728E+01
CEC-2014-F8	Best	**8.020E+02**	8.031E+02	9.691E+02	8.548E+02	8.047E+02	9.649E+02	8.880E+02	8.428E+02	9.017E+02	8.104E+02	8.661E+02
	Worst	**8.288E+02**	8.358E+02	9.723E+02	9.015E+02	8.461E+02	9.764E+02	9.450E+02	8.637E+02	9.116E+02	8.516E+02	8.969E+02
	Average	8.156E+02	**8.138E+02**	9.708E+02	8.816E+02	8.295E+02	9.720E+02	9.165E+02	8.540E+02	9.058E+02	8.356E+02	8.845E+02
	Std. Dev.	7.243E+00	6.540E+00	8.070E−01	9.826E+00	9.433E+00	2.052E+00	1.348E+01	4.191E+00	1.985E+00	8.547E+00	7.554E+00
CEC-2014-F9	Best	**9.040E+02**	9.120E+02	1.006E+03	9.565E+02	9.162E+02	1.006E+03	9.534E+02	9.497E+02	9.701E+02	9.133E+02	9.537E+02
	Worst	**9.442E+02**	9.515E+02	1.011E+03	9.956E+02	9.632E+02	1.014E+03	9.914E+02	9.507E+02	9.748E+02	9.569E+02	9.883E+02
	Average	**9.231E+02**	9.418E+02	1.009E+03	9.815E+02	9.373E+02	1.010E+03	9.688E+02	9.507E+02	9.723E+02	9.370E+02	9.751E+02
	Std. Dev.	1.053E+01	9.079E+00	1.130E+00	8.165E+00	1.046E+01	1.897E+00	1.051E+01	2.702E−01	9.938E−01	1.114E+01	7.316E+00
CEC-2014-F10	Best	1.028E+03	**1.019E+03**	3.090E+03	2.087E+03	1.103E+03	3.055E+03	2.298E+03	2.250E+03	2.433E+03	1.103E+03	2.309E+03
	Worst	**1.610E+03**	1.680E+03	3.171E+03	2.779E+03	2.344E+03	3.241E+03	2.872E+03	2.448E+03	2.544E+03	2.190E+03	2.739E+03
	Average	**1.130E+03**	1.351E+03	3.141E+03	2.459E+03	1.579E+03	3.157E+03	2.583E+03	2.325E+03	2.499E+03	1.591E+03	2.577E+03
	Std. Dev.	1.172E+02	1.537E+02	1.969E+01	1.607E+02	2.664E+02	3.775E+01	1.481E+02	7.053E+01	2.645E+01	2.558E+02	1.005E+02
CEC-2014-F11	Best	**1.201E+03**	1.371E+03	3.665E+03	2.388E+03	1.367E+03	3.599E+03	2.561E+03	2.456E+03	2.883E+03	1.477E+03	2.459E+03
	Worst	2.783E+03	**2.456E+03**	3.747E+03	2.984E+03	2.925E+03	3.811E+03	3.399E+03	2.869E+03	2.963E+03	2.930E+03	3.246E+03
	Average	2.202E+03	**1.806E+03**	3.707E+03	2.777E+03	2.107E+03	3.723E+03	3.012E+03	2.821E+03	2.912E+03	2.140E+03	2.933E+03
	Std. Dev.	4.286E+02	2.569E+02	2.125E+01	1.454E+02	3.138E+02	4.890E+01	2.205E+02	5.931E+01	1.618E+01	3.094E+02	1.617E+02
CEC-2014-F12	Best	**1.200E+03**	**1.200E+03**	1.203E+03	1.201E+03	**1.200E+03**	1.203E+03	**1.200E+03**	**1.200E+03**	1.201E+03	**1.200E+03**	1.201E+03
	Worst	1.202E+03	**1.201E+03**	1.205E+03	1.202E+03	1.202E+03	1.205E+03	1.205E+03	1.202E+03	1.203E+03	1.202E+03	1.202E+03
	Average	1.201E+03	**1.200E+03**	1.204E+03	1.202E+03	1.201E+03	1.204E+03	1.202E+03	1.201E+03	1.202E+03	1.201E+03	1.202E+03
	Std. Dev.	4.314E−01	1.742E−01	4.051E−01	2.369E−01	3.491E−01	5.748E−01	9.153E−01	4.295E−01	5.017E−01	3.039E−01	1.469E−01
CEC-2014-F13	Best	**1.300E+03**	**1.300E+03**	1.308E+03	1.302E+03	**1.300E+03**	1.308E+03	1.302E+03	**1.300E+03**	1.307E+03	**1.300E+03**	1.302E+03
	Worst	**1.300E+03**	1.301E+03	1.308E+03	1.304E+03	1.301E+03	1.308E+03	1.306E+03	1.301E+03	1.307E+03	1.301E+03	1.305E+03
	Average	**1.300E+03**	**1.300E+03**	1.308E+03	1.303E+03	1.301E+03	1.308E+03	1.304E+03	**1.300E+03**	1.307E+03	1.301E+03	1.304E+03
	Std. Dev.	4.951E−02	1.264E−01	9.047E−03	4.653E−01	1.945E−01	2.142E−02	8.708E−01	1.361E−01	1.777E−02	2.079E−01	5.951E−01
CEC-2014-F14	Best	**1.400E+03**	**1.400E+03**	1.465E+03	1.412E+03	**1.400E+03**	1.464E+03	1.414E+03	**1.400E+03**	1.458E+03	**1.400E+03**	1.413E+03
	Worst	**1.401E+03**	**1.401E+03**	1.465E+03	1.439E+03	**1.401E+03**	1.465E+03	1.449E+03	**1.401E+03**	1.459E+03	**1.401E+03**	1.447E+03
	Average	**1.400E+03**	**1.400E+03**	1.465E+03	1.424E+03	**1.400E+03**	1.465E+03	1.433E+03	**1.400E+03**	1.459E+03	**1.400E+03**	1.432E+03
	Std. Dev.	8.361E−02	2.594E−01	1.071E−01	5.978E+00	2.640E−01	1.860E−01	7.915E+00	2.118E−01	1.612E−01	2.636E−01	6.700E+00
CEC-2014-F15	Best	1.502E+03	**1.501E+03**	9.355E+04	1.667E+03	1.502E+03	9.137E+04	1.518E+03	1.513E+03	4.469E+04	1.503E+03	1.741E+03
	Worst	**1.504E+03**	**1.504E+03**	9.804E+04	1.433E+04	1.521E+03	9.917E+04	5.154E+04	1.529E+03	5.016E+04	1.514E+03	1.445E+04
	Average	1.503E+03	**1.502E+03**	9.589E+04	5.992E+03	1.508E+03	9.663E+04	7.001E+03	1.519E+03	4.684E+04	1.508E+03	4.023E+03
	Std. Dev.	4.957E−01	7.737E−01	1.009E+03	3.347E+03	3.165E+00	1.986E+03	1.042E+04	4.041E+00	1.411E+03	2.567E+00	2.172E+03
CEC-2014-F16	Best	**1.602E+03**	**1.602E+03**	1.604E+03	1.604E+03	1.603E+03	1.604E+03	1.604E+03	1.604E+03	1.604E+03	1.603E+03	1.604E+03
	Worst	**1.604E+03**	**1.604E+03**	1.605E+03	1.604E+03	1.604E+03	1.605E+03	1.605E+03	1.604E+03	1.604E+03	1.604E+03	1.604E+03
	Average	**1.603E+03**	**1.603E+03**	1.605E+03	1.604E+03	1.603E+03	1.605E+03	1.604E+03	1.604E+03	1.604E+03	1.603E+03	1.604E+03
	Std. Dev.	3.132E−01	3.027E−01	1.687E−02	1.094E−01	2.514E−01	2.771E−02	2.297E−02	9.468E−03	6.240E−03	2.280E−01	1.206E−01

(*continued on next page*)

Table 16 (*continued*).

Benchmark	Metric	AHHO	HHO	CSA	CS	DE	FA	GWO	PSO	WDO	WOA	L-SHADE
CEC-2014-F17	Best	**1.701E+03**	2.548E+03	1.593E+07	3.629E+04	4.056E+03	1.548E+07	5.679E+05	2.653E+03	6.055E+05	7.636E+03	5.642E+04
	Worst	**2.188E+03**	1.757E+04	1.964E+07	9.398E+05	2.093E+05	2.189E+07	1.050E+06	4.124E+03	6.293E+05	3.617E+05	6.733E+05
	Average	**1.787E+03**	5.208E+03	1.790E+07	3.250E+05	6.924E+04	1.873E+07	6.713E+05	3.046E+03	6.151E+05	1.982E+05	5.049E+05
	Std. Dev.	1.022E+02	3.350E+03	7.109E+05	2.138E+05	5.944E+04	1.751E+06	1.269E+05	3.333E+02	5.588E+03	1.093E+05	1.255E+05
CEC-2014-F18	Best	**1.801E+03**	2.254E+03	1.617E+08	1.084E+04	2.152E+03	1.530E+08	8.239E+03	9.566E+03	5.748E+07	3.093E+03	3.269E+04
	Worst	**1.861E+03**	1.542E+04	1.668E+08	4.998E+06	2.543E+04	1.682E+08	6.667E+06	1.057E+04	7.375E+07	2.567E+04	6.639E+06
	Average	**1.805E+03**	1.015E+04	1.637E+08	9.095E+05	9.993E+03	1.613E+08	7.324E+05	9.907E+03	6.543E+07	1.055E+04	1.319E+06
	Std. Dev.	8.876E+00	2.686E+03	1.210E+06	1.066E+06	4.699E+03	3.489E+06	1.922E+06	1.930E+02	3.191E+06	5.497E+03	1.416E+06
CEC-2014-F19	Best	**1.901E+03**	**1.901E+03**	2.968E+03	1.907E+03	1.902E+03	2.951E+03	1.918E+03	1.917E+03	2.724E+03	1.902E+03	1.910E+03
	Worst	**1.905E+03**	**1.905E+03**	2.975E+03	1.918E+03	1.908E+03	2.974E+03	1.971E+03	1.999E+03	2.754E+03	1.907E+03	1.977E+03
	Average	**1.902E+03**	1.903E+03	2.971E+03	1.912E+03	1.905E+03	2.960E+03	1.963E+03	1.951E+03	2.737E+03	1.905E+03	1.936E+03
	Std. Dev.	1.037E+00	7.332E−01	1.324E+00	2.558E+00	1.375E+00	5.933E+00	1.524E+01	1.742E+01	7.426E+00	1.192E+00	1.283E+01
CEC-2014-F20	Best	**2.000E+03**	2.101E+03	6.750E+08	5.151E+03	2.063E+03	6.447E+08	1.356E+04	4.198E+03	2.462E+08	2.159E+03	7.103E+03
	Worst	**2.040E+03**	1.027E+04	6.925E+08	2.027E+05	1.680E+04	7.048E+08	2.471E+04	6.929E+03	2.899E+08	4.355E+04	4.169E+05
	Average	**2.004E+03**	5.304E+03	6.810E+08	3.740E+04	8.545E+03	6.686E+08	1.594E+04	5.642E+03	2.726E+08	1.097E+04	6.494E+04
	Std. Dev.	9.034E+00	1.959E+03	3.855E+06	3.713E+04	4.009E+03	1.410E+07	2.443E+03	5.419E+02	1.070E+07	9.320E+03	8.792E+04
CEC-2014-F21	Best	**2.100E+03**	2.523E+03	2.524E+09	6.299E+03	2.677E+03	2.498E+09	1.926E+05	4.812E+03	2.020E+09	3.502E+03	2.308E+04
	Worst	**2.280E+03**	3.199E+04	2.548E+09	3.162E+05	5.484E+05	2.563E+09	1.648E+07	2.121E+04	2.108E+09	1.106E+06	6.742E+06
	Average	**2.134E+03**	9.318E+03	2.536E+09	6.450E+04	5.815E+04	2.529E+09	2.978E+06	9.402E+03	2.064E+09	2.673E+05	1.928E+06
	Std. Dev.	4.936E+01	6.942E+03	6.098E+06	5.136E+04	1.188E+05	1.453E+07	5.521E+06	4.127E+03	1.861E+07	2.712E+05	1.436E+06
CEC-2014-F22	Best	**2.200E+03**	2.222E+03	1.012E+04	2.282E+03	2.226E+03	9.858E+03	2.423E+03	2.382E+03	6.398E+03	2.226E+03	2.402E+03
	Worst	**2.244E+03**	2.369E+03	1.032E+04	2.530E+03	2.479E+03	1.029E+04	3.234E+03	2.740E+03	6.875E+03	2.570E+03	2.740E+03
	Average	**2.211E+03**	2.305E+03	1.021E+04	2.425E+03	2.334E+03	1.002E+04	2.746E+03	2.556E+03	6.622E+03	2.344E+03	2.599E+03
	Std. Dev.	1.249E+01	6.091E+01	4.478E+01	6.391E+01	7.376E+01	1.029E+02	2.148E+02	6.006E+01	1.095E+02	8.437E+01	8.491E+01
CEC-2014-F23	Best	**2.500E+03**	**2.500E+03**	2.501E+03	2.514E+03	2.629E+03	**2.500E+03**	**2.500E+03**	**2.500E+03**	**2.500E+03**	**2.500E+03**	**2.500E+03**
	Worst	**2.500E+03**	**2.500E+03**	2.503E+03	2.525E+03	2.629E+03	2.502E+03	**2.500E+03**	2.501E+03	2.503E+03	**2.500E+03**	**2.500E+03**
	Average	**2.500E+03**	**2.500E+03**	2.502E+03	2.520E+03	2.629E+03	**2.500E+03**	**2.500E+03**	2.501E+03	2.501E+03	**2.500E+03**	**2.500E+03**
	Std. Dev.	0.000E+00	0.000E+00	3.744E−01	2.654E+00	9.780E−05	3.212E−01	1.155E−05	1.804E−01	1.154E+00	7.717E−13	0.000E+00
CEC-2014-F24	Best	**2.508E+03**	2.521E+03	2.600E+03	2.581E+03	2.534E+03	2.600E+03	2.600E+03	2.600E+03	2.600E+03	2.530E+03	2.598E+03
	Worst	**2.549E+03**	2.600E+03	2.600E+03	2.602E+03	2.600E+03	2.601E+03	2.601E+03	2.600E+03	2.600E+03	2.600E+03	2.600E+03
	Average	**2.523E+03**	2.551E+03	2.600E+03	2.598E+03	2.595E+03	2.601E+03	2.600E+03	2.600E+03	2.600E+03	2.591E+03	2.600E+03
	Std. Dev.	1.059E+01	2.960E+01	2.708E−02	5.414E+00	1.478E+01	1.761E−01	1.353E−01	2.585E−02	1.026E−01	1.907E+01	3.057E−01
CEC-2014-F25	Best	**2.618E+03**	2.630E+03	2.700E+03	2.683E+03	2.670E+03	2.700E+03	2.700E+03	2.700E+03	2.700E+03	2.626E+03	2.694E+03
	Worst	2.702E+03	**2.700E+03**	**2.700E+03**	**2.700E+03**	**2.700E+03**	**2.700E+03**	**2.700E+03**	**2.700E+03**	**2.700E+03**	**2.700E+03**	**2.700E+03**
	Average	**2.687E+03**	2.697E+03	2.700E+03	2.699E+03	2.698E+03	2.700E+03	2.700E+03	2.700E+03	2.700E+03	2.698E+03	2.700E+03
	Std. Dev.	2.938E+01	1.146E+01	1.759E−03	3.304E+00	5.851E+00	3.112E−03	2.602E−08	8.552E−04	5.828E−03	1.049E+01	8.638E−01
CEC-2014-F26	Best	**2.700E+03**	**2.700E+03**	2.800E+03	2.702E+03	**2.700E+03**	2.800E+03	2.800E+03	2.800E+03	2.800E+03	**2.700E+03**	2.702E+03
	Worst	**2.700E+03**	2.701E+03	2.800E+03	2.704E+03	2.800E+03	2.800E+03	2.800E+03	2.800E+03	2.800E+03	2.800E+03	2.708E+03
	Average	**2.700E+03**	2.700E+03	2.800E+03	2.703E+03	2.706E+03	2.800E+03	2.800E+03	2.800E+03	2.800E+03	2.706E+03	2.704E+03
	Std. Dev.	4.529E−02	1.131E−01	2.521E−05	4.276E−01	2.367E+01	1.817E−04	1.044E−04	1.751E−05	8.710E−05	2.368E+01	1.160E+00
CEC-2014-F27	Best	2.703E+03	**2.702E+03**	2.900E+03	2.849E+03	2.706E+03	2.900E+03	2.900E+03	2.900E+03	2.900E+03	2.710E+03	2.900E+03
	Worst	**2.900E+03**	3.111E+03	2.902E+03	2.993E+03	**2.900E+03**	2.903E+03	**2.900E+03**	**2.900E+03**	2.902E+03	**2.900E+03**	2.908E+03
	Average	2.881E+03	2.983E+03	2.901E+03	2.955E+03	2.896E+03	2.900E+03	2.900E+03	2.900E+03	2.900E+03	2.889E+03	2.900E+03
	Std. Dev.	5.844E+01	1.457E+02	2.724E−01	2.760E+01	2.711E+01	4.959E−01	8.049E−07	6.339E−02	6.607E−01	4.397E+01	1.082E+00
CEC-2014-F28	Best	**3.000E+03**	**3.000E+03**	3.002E+03	3.030E+03	3.157E+03	**3.000E+03**	**3.000E+03**	3.001E+03	**3.000E+03**	**3.000E+03**	**3.000E+03**
	Worst	**3.000E+03**	**3.000E+03**	3.004E+03	3.096E+03	3.350E+03	3.005E+03	**3.000E+03**	3.002E+03	3.005E+03	**3.000E+03**	**3.000E+03**
	Average	**3.000E+03**	**3.000E+03**	3.003E+03	3.064E+03	3.212E+03	**3.000E+03**	**3.000E+03**	3.001E+03	3.002E+03	**3.000E+03**	**3.000E+03**
	Std. Dev.	0.000E+00	0.000E+00	5.300E−01	1.477E+01	4.775E+01	1.000E+00	6.608E−06	2.588E−01	1.964E+00	1.009E−12	3.016E−13
CEC-2014-F29	Best	**3.100E+03**	**3.100E+03**	1.106E+06	1.460E+04	3.113E+03	**3.100E+03**	**3.100E+03**	3.004E+05	**3.100E+03**	3.175E+03	**3.100E+03**
	Worst	3.666E+06	3.666E+06	2.210E+06	8.196E+05	1.968E+06	1.903E+06	3.118E+03	8.227E+05	2.631E+06	2.104E+06	**3.100E+03**
	Average	1.478E+05	2.612E+05	1.808E+06	1.476E+05	1.431E+05	1.941E+05	3.103E+03	5.190E+05	7.725E+05	4.531E+04	**3.100E+03**
	Std. Dev.	7.179E+05	9.086E+05	2.760E+05	1.465E+05	4.854E+05	4.226E+05	4.382E+00	1.080E+05	1.011E+06	2.941E+05	3.226E−12
CEC-2014-F30	Best	**3.200E+03**	**3.200E+03**	1.765E+05	4.884E+03	3.465E+03	**3.200E+03**	**3.200E+03**	5.158E+04	**3.200E+03**	3.491E+03	**3.200E+03**
	Worst	**8.534E+03**	9.493E+03	4.262E+05	1.731E+04	3.988E+03	2.256E+05	3.204E+03	1.446E+05	4.500E+05	5.726E+03	2.485E+05
	Average	**6.212E+03**	6.229E+03	3.272E+05	9.257E+03	3.545E+03	2.767E+04	3.200E+03	9.922E+04	1.457E+05	4.031E+03	3.932E+04
	Std. Dev.	1.480E+03	1.161E+03	5.658E+04	2.704E+03	9.419E+01	5.805E+04	7.887E−01	2.343E+04	1.629E+05	5.231E+02	6.195E+04
Friedman average rank		2.43	2.77	10.23	6.40	4.03	9.70	7.23	5.00	8.40	3.70	6.10
Rank		1	2	11	7	4	10	8	5	9	3	6

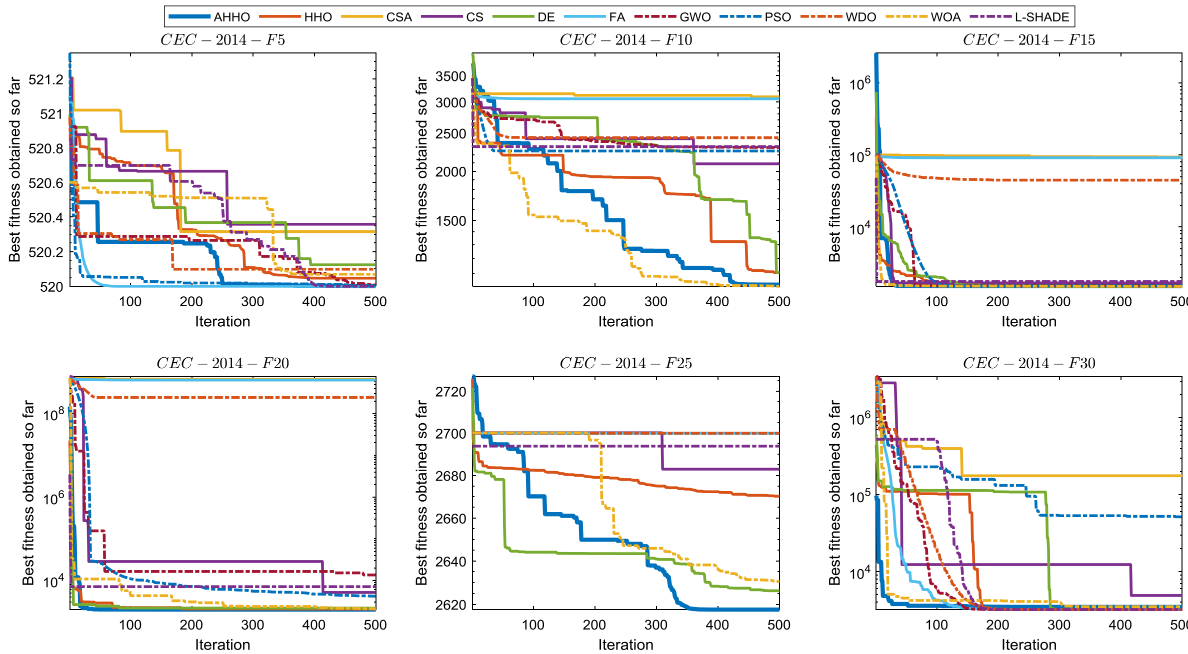

Fig. 8. The convergence curve of the six modern CEC 2014 test functions F5, F10, F15, F20, F25, and F30.

and

$$S_q^M(t,s) = \frac{1}{q-1}\left[1 - \sum_{i=t_{m-1}+1}^{L-1}\sum_{j=s_{m-1}+1}^{L-1}\left(\frac{p(i,j)}{P_{Dm}(t,s)}\right)^q\right].$$

Eq. (8) serves as a fitness function in a maximization problem for 2D Tsallis based multilevel thresholding. It is an exhaustive search process as the number of thresholds m increases leads to an optimization problem.

2.2. Harris hawks optimization (HHO) algorithm

The Harris hawks optimization (HHO) [59] is based on cooperative foraging behaviour of a well-known bird Harris hawks (Parabuteo unicinctus). The Harris hawks foraging behaviour based on the "leapfrog" motion and "surprise pounce". Using the leapfrog motion, the hawks perform rejoin and split several times to actively search for prey all over the target area. The surprise pounce is also known as the "seven kills" strategy, used for capturing the prey. In this strategy, several hawks cooperatively attack from diverse directions and converge to detected escaping prey. Based on the foraging behaviour, an exploratory, and exploitative phased HHO algorithm has been proposed [59] which depends on the equal perching chance and rabbit escape (prey) energy.

3. The proposed adaptive Harris hawks optimization (AHHO) algorithm

In this section, the author proposes an adaptive Harris hawks optimization (AHHO) keeping in view that no algorithm is perfect for all classes of problems as suggested by "no free lunch" (NFL) [81] and always there is a chance for improvement of search performance.

3.1. Mathematical formulation of AHHO

The development of the adaptive Harris hawks optimization (AHHO) algorithm is based on the underlying principle of escape energy of the prey and perching strategy of Harris hawk of HHO [59]. The AHHO algorithm broadly classified in three phases as exploration phases, transition phases and exploitation phases which can be mathematically modelled as follows.

Let us define $X(t)$ as the position vector of hawks, $X_{prey}(t)$ is the position of prey, $X_{rand}(t)$ is a randomly selected hawk within the current population at current iteration t (*i.e* $1 \le t \le t_{max}$), and t_{max} is the maximum number of iterations.

3.1.1. Exploration phase

Let the Harris hawk in HHO [59] perches randomly on the tall tree and wait for the prey with an equal perching chance u. If $u < 0.5$, they perch based on the neighbouring family members and perch on random tall trees when $u \ge 0.5$. Then the new position vector $X(t+1)$ can be defined as:

$$X(t+1) = \begin{cases} X_{rand}(t) - r_1\left|X_{rand}(t) - 2r_2X(t)\right| & u \ge 0.5 \\ \left(X_{prey}(t) - X_m(t)\right) - r_3\left(LB + r_4(UB - LB)\right) & u < 0.5 \end{cases} \tag{9}$$

where r_1, r_2, r_3 and r_4 are random numbers in the range [0, 1] updated in each iteration, UB is the upper boundary of search space, LB is the lower boundary of search space, $X_m(t)$ is the mean position vector of the current population of N hawks, and $X_{prey}(t)$ is the best location of the prey.

$$X_m(t) = \frac{1}{N}\sum_{i=1}^{N} X_i(t) \tag{10}$$

where $X_i(t)$ is the position of the ith hawk in the iteration t.

The exploration phase described by the Eq. (9) of HHO [59], the Harris hawks perch based on the equal chance of u, which is a random number. Let us consider two important cases as follow:

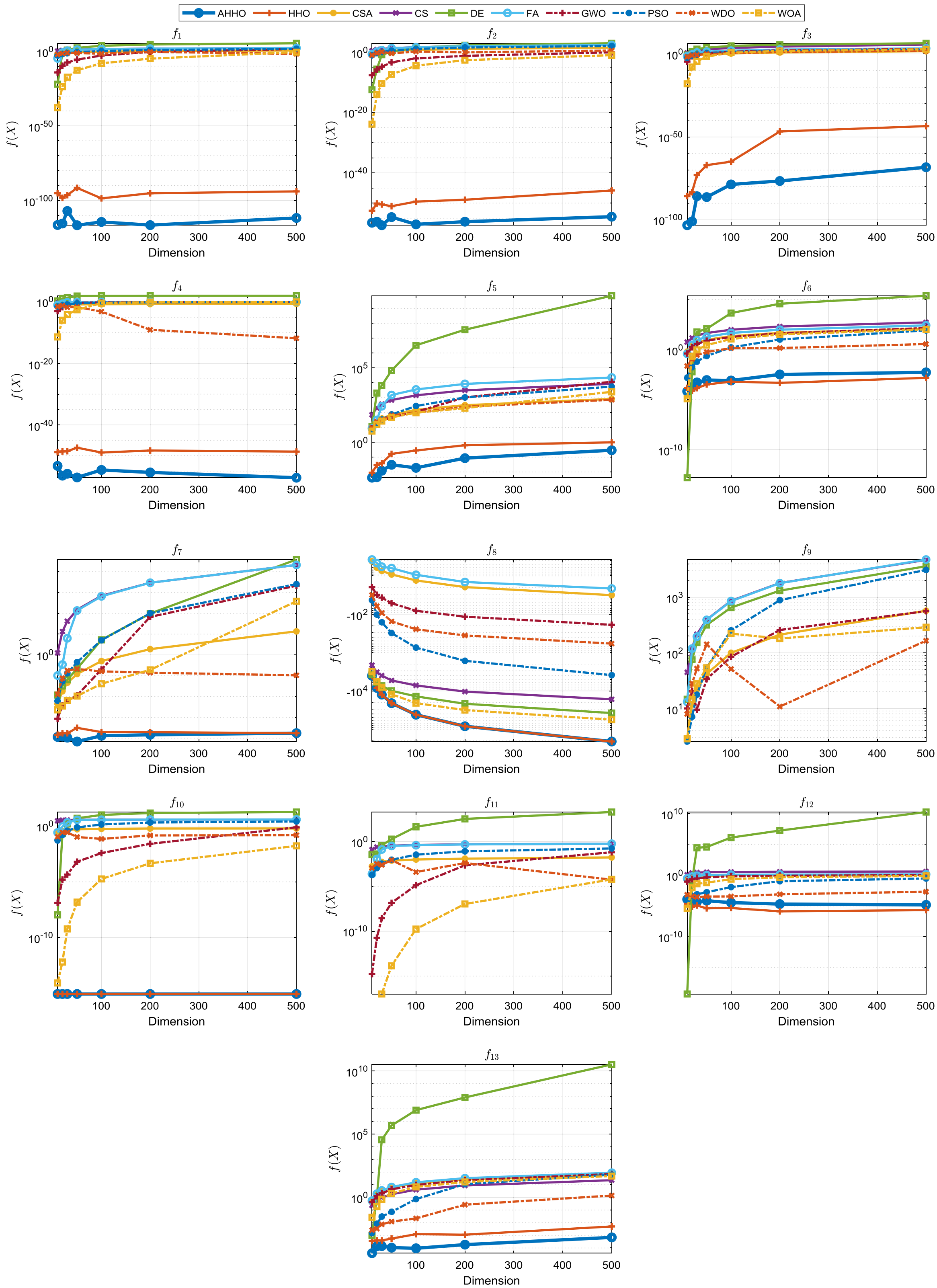

Fig. 9. Scalability results comparison of AHHO to other optimization algorithms of classical test functions $f_1 - f_{13}$.

Case 1: The perching chance is $(u \geq 0.5)$; and the Harris hawk is nearer to the prey $(f(X) > f_{opt})$

Case 2: The perching chance is $(u < 0.5)$; and the Harris hawk is far from the prey $(f(X) \gg f_{opt})$

For Case 1, the Harris hawk is nearer to the prey, it should continue to perch along with the other family members. However, due to a better perching chance$(u \geq 0.5)$, it moves to a random location, which is not desirable. In the other Case 2, Harris hawk is

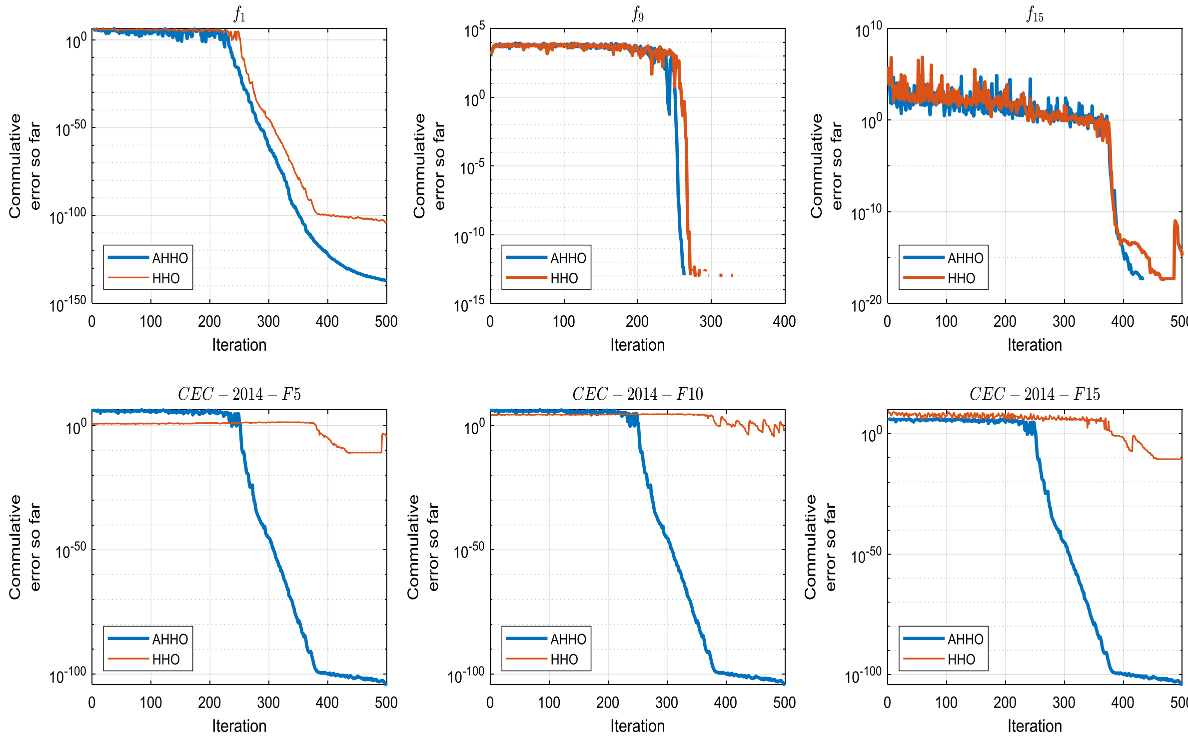

Fig. 10. Error curve of three classical test functions f_1, f_9, f_{15} and three modern test functions F5, F10, F15 from CEC 2014 test suite.

far from the prey, it should suddenly move to perch on a random tall tree. However, due to a lower perching chance ($u < 0.5$), it continues to perch along with the other family members. These cases lead to wastage of search agents (Harris hawk). Therefore, there is a strong need to investigate for an adaptive strategy. The algorithm can be supplemented by an adaptive method to decide when the Harris hawk would do perch along with the other family members or move to a random tall tree.

Let us define average fitness (f_{avg}) value of the Harris hawk search location ($X_i | i = 1, 2, \ldots, N$) as

$$f_{avg} = \frac{1}{N}\sum_{i=1}^{N} f\left(X_i\right) \tag{11}$$

where $f\left(X_i\right)$ denotes the fitness value of the individual Harris hawk.

The new search location $X_i\left(t+1\right)$ of Harris hawk in the exploration phase can be modelled as

$$X_i\left(t+1\right) = \begin{cases} X_{rand}\left(t\right) - r_1\left|X_{rand}\left(t\right) - 2r_2X_i\left(t\right)\right| & f\left(X_i\right) \geq f_{avg} \\ \left(X_{prey}\left(t\right) - X_m\left(t\right)\right) - r_3\left(LB + r_4\left(UB - LB\right)\right) & f\left(X_i\right) < f_{avg} \end{cases} \tag{12}$$

where r_1, r_2, r_3 and r_4 are random numbers in the range $[0, 1]$ updated in each iteration, UB is the upper bound of the search space, LB is the lower bound of the search space, $X_m\left(t\right)$ is the mean position vector of the current population of N hawks, and $X_{prey}\left(t\right)$ is the best location of the prey.

3.1.2. Transition phases

The foraging behaviour of Harris hawks depends on the exploratory phase, exploitative phase and the transition phase, which will be decided by escape energy E of the prey. The escaping energy E of HHO is modelled as:

$$E = 2E_0\left(1 - \frac{t}{t_{max}}\right) \tag{13}$$

where E_0 is the initial energy which changes its states in between $[-1, 1]$ at each iteration. When E_0 is decreasing 0 to -1, the prey is physically flagging, whereas E_0 is increasing the prey is strengthening. So, when $|E| \geq 1$, the hawks search different regions to explore the prey location, that HHO is in the exploration phase, and when $|E| < 1$, the HHO tries to exploit the neighbourhood of the solution for the period of the exploitation phase.

Let us consider the time-dependent behaviour of E of HHO, which is demonstrated in Fig. 2. The escape energy E of the prey helps to decide the movement of the Harris hawk. From Fig. 2, it is seen that the escape energy decreases, varies in the range of $[-2, 2]$. Sometime retains its states in the range $[0, 2]$ (for a while or more). As discussed in the literature [59], when the escape energy is equal to 0, the prey is completely exhausted. This is not desirable, because it is needed to further explore for improvising the results. This led us to modify the escape energy of HHO through investigations. In this work, an effort is made to adapt the escape energy by incorporating mutation. It is proposed that the escape energy should remain present mostly in the range $[0, 2]$; except for the mutation interval.

Let us define a random number r_5 in the range of $[0, 1]$, a maximum value of probability of mutation as p_{m_max}, a minimum value of probability of mutation as p_{m_min}, t as the current iteration and the maximum iteration as t_{max}. The mutation interval (MI) is adaptively calculated as

$$MI = mod\left(t, \left\lfloor \frac{1}{p_{m\_max} - \left(p_{m\_max} - p_{m\_min}\right)\left(\frac{t}{t_{max}}\right)} \right\rfloor\right) \quad (14)$$

where $mod(\bullet)$ represents the reminder.

The mutation energy (E_m) can be calculated using the following algorithm:

```
if (t == 1)
        Em = r5
else if (t ≠ 1)
        if (MI > 0)
                Em = r5
        else
                Em = −r5
        end
end
```

The escape energy of AHHO is modelled in Eq. (15) and the time-dependent behaviour of E_{AHHO} is demonstrated in Fig. 3.

$$E_{AHHO} = E_1 * E_m \quad (15)$$

where

$$E_1 = 2\left(1 - \frac{t}{t_{max}}\right). \quad (16)$$

The escape energy of the prey is varied from $(0, 2)$, except the mutation interval MI. The prey is physically flagging, when the escape energy is nearer to the zero (0) value. While the prey is strengthening, the escape energy is increasing from 0 to 2 value. The $|E_{AHHO}| \geq 1$ describes the exploration phase of the Harris hawk, which is required to explore the different regions for the prey. The $|E_{AHHO}| < 0$ pronounce the exploitation phase, where the hawk explores the neighbourhood for solution. More exploration is achieved in this way. To avoid the local minima, the mutation interval MI is introduced. The MI is important, on which the escape energy changes its polarity. This, in turn, helps to guide the AHHO to search for the global minima.

3.1.3. Exploitation phase

In the exploitation phase, the Harris hawk performs the surprise pounce by attacking the planned prey detected in the previous phase. However, the prey always tries to escape from the Harris hawk. Depending upon the escaping behaviours of the prey, the AHHO define successful escaping chance when $r < 0.5$, and unsuccessful escaping chance when $r \geq 0.5$, before surprise pounce. Based on the escaping energy E_{AHHO} of the prey, the Harris hawk attacking is modelled as soft besiege when $|E_{AHHO}| \geq 0.5$, and hard besiege when $|E_{AHHO}| < 0.5$. Henceforth, the AHHO exploitation phase can be modelled in four possible strategies as soft besiege, hard besiege, soft besiege with progressive rapid dives, and hard besiege with progressive rapid dives which depends on the random jump strength of the prey during escaping. The random jump strength J can be calculated as:

$$J = 2(1 - r_6) \quad (17)$$

where r_6 is a random number in the range $[0, 1]$.

- *Soft besiege* ($r \geq 0.5$ and $|E_{AHHO}| \geq 0.5$)
  The soft besiege is described as when the prey has enough energy to mislead the Harris hawk by taking random jumps. During this, the Harris hawk encircles the prey softly to make the prey exhausted and finally do the surprise pounce. This strategy can be modelled as:

$$X_i(t+1) = \Delta X_i(t) - E_{AHHO}\left|JX_{prey}(t) - X_i(t)\right| \quad (18)$$

where

$$\Delta X_i(t) = X_{prey}(t) - X_i(t) \quad (19)$$

- *Hard besiege* ($r \geq 0.5$ and $|E_{AHHO}| < 0.5$)
  The hard besiege is described as when the prey exhausted and low escaping energy, so the Harris hawk perform surprise pounce without encircling the prey. This strategy can be modelled as:

$$X_i(t+1) = X_{prey}(t) - E_{AHHO}\left|\Delta X_i(t)\right| \quad (20)$$

- *Soft besiege with progressive rapid dives* ($r < 0.5$ and $|E_{AHHO}| \geq 0.5$)
  In this strategy the Harris hawk encircles softly when the prey has enough energy to escape during the surprise pounce can be modelled as:

$$X_i(t+1) = \begin{cases} Y & \text{if } f(Y) < f(X_i(t)) \\ Z & \text{if } f(Z) < f(X_i(t)) \end{cases} \quad (21)$$

where

$$Y = X_{prey}(t) - E_{AHHO}\left|JX_{prey}(t) - X_i(t)\right| \quad (22)$$

$$Z = Y + S \times LF(d) \quad (23)$$

where d is the dimension of the problem, S is a random vector of size $1 \times d$, and LF is the levy flight [82] for the leapfrog movements experienced by the prey.

$$LF(x) = 0.01 \times \frac{u \times \sigma}{|v|^{\frac{1}{\beta}}}, \quad \sigma = \left(\frac{\Gamma(1+\beta) \times \sin\left(\frac{\pi\beta}{2}\right)}{\Gamma\left(\frac{1+\beta}{2}\right) \times \beta \times 2^{\left(\frac{\beta-1}{2}\right)}}\right)^{\frac{1}{\beta}}, \quad \beta = 1.5 \quad (24)$$

where u, v are random numbers in the range $(0, 1)$.

- *Hard besiege with progressive rapid dives* ($r < 0.5$ and $|E_{AHHO}| < 0.5$)
  In this strategy the Harris' hawk encircle hardly when the prey has not enough energy to escape during the surprise pounce can be modelled as

$$X_i(t+1) = \begin{cases} Y & \text{if } f(Y) < f(X_i(t)) \\ Z & \text{if } f(Z) < f(X_i(t)) \end{cases} \quad (25)$$

where

$$Y = X_{prey}(t) - E_{AHHO}\left|JX_{prey}(t) - X_m(t)\right| \quad (26)$$

$$Z = Y + S \times LF(D) \quad (27)$$

and LF is the levy flight which is evaluated using Eq. (24).

3.2. Pseudocode of AHHO

In the beginning, let us identify the dimension for the problem (d), number of Harris hawk (N), maximum number of iterations (t_{max}), maximum value of probability of mutation (p_{m_max}), minimum value of probability of mutation (p_{m_min}), fitness function ($f(\bullet)$) and range of search space as $[UB, LB]$.

→ Set the initial iteration $t = 1$.
→ Initialize the random search space $X_i = (x_i^1, x_i^2, \cdots x_i^d)$ for ith hawk of d dimensional problem within the search boundary $[UB, LB]$.

While $t \le t_{max}$
A. Evaluate the fitness value $f(X_i)$ of all N hawk for $i = 1,2,\cdots,N$.
B. Calculate the average fitness f_{avg} using the Eq. (11).
C. Calculate the mean position vector X_m using the Eq. (10).
D. Label the best prey location as X_{prey} based on the best fitness value $f(X)$.
E. Estimate the jump strength J using Eq. (17).
F. For $i = 1$: number of hawk *(N)*
  a. Update the escaping energy of prey E_{AHHO} using Eq. (15).
  b. If $(|E_{AHHO}| \ge 1)$
    → Randomly choose one hawk location as X_{rand} from the search space.
    → Update the new hawk location using Eq. (12).
  Elseif $(|E_{AHHO}| < 1)$
    → Generate a random escaping chance of prey r in the range [0,1].
    If $(r \ge 0.5\ and |E_{AHHO}| \ge 0.5)$
      Update the new hawk location using Eq. (18).
    Elseif $(r \ge 0.5\ and |E_{AHHO}| < 0.5)$
      Update the new hawk location using Eq. (20).
    Elseif $(r < 0.5\ and |E_{AHHO}| \ge 0.5)$
      Update the new hawk location using Eq. (21).
    Elseif $(r < 0.5\ and |E_{AHHO}| < 0.5)$
      Update the new hawk location using Eq. (25).
    End (If)
  End (If)
End (For)
G. Amend the search space X_i for $i = 1,2,\cdots,N$ based on the search boundary UB and LB.
H. $t = t + 1$;
End (While)
→ Return the best location X_{prey}.

3.3. Computational complexity of AHHO

The computational complexity of the AHHO mainly depends on the five processes: initialization, fitness evaluation, updating of escape energy and updating the position vector of the Harris hawk. The complexity is depending on number of Harris hawk (n), search dimensions (d), number of iterations (t), cost of fitness evaluation (c) and cost of escape energy evaluation (e). Then the complexity of the AHHO can be represented as

$$O\,(AHHO) = O\,(initialization) + O\,(fitness\ evaluation) + O\,(\ escape\ energy\ update) + O\,(position\ vector\ update) \tag{28}$$

The estimated computational complexity of AHHO is

$$O\,(AHHO) = O\,(n) + O\,(tndc) + O\,(tne) + O\,(tnd) \cong O\,(tnd\,(c+1) + tne) \tag{29}$$

3.4. Performance evaluation of the AHHO algorithm

3.4.1. Benchmark functions and compared algorithms

The performance of the proposed AHHO is investigated using a set of 23 diverse classical test functions from [60,83,84] and 30 test functions from the IEEE CEC 2014 competition [61]. The

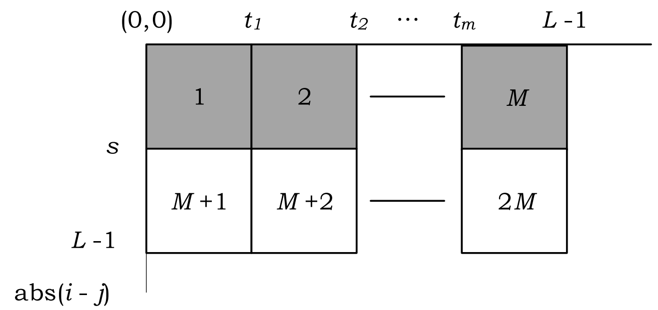

Fig. 11. 2D histogram plane based on the grey gradient for multilevel thresholding.

test functions are categorized into four groups: classical unimodal ($f_1 - f_7$), classical multimodal with varied dimension ($f_8 - f_{13}$), classical multimodal with fixed dimension ($f_{14} - f_{23}$) and modern CEC test functions (CEC-2014-F1 to CEC-2014-F30). The classical test functions also categorized as scalable test functions ($f_1 - f_{13}$) and non-scalable test functions ($f_{14} - f_{23}$) based on the scalability of dimension. The unimodal functions have a unique global optimum which can reveal the exploitative capability of the proposed optimization algorithm. The rate of convergence is the most important aspect. The multimodal functions have multiple optima. This can disclose the diversification together with the local optimum avoidance potentials of the proposed optimization algorithm. The details of the benchmark functions ($f_1 - f_{23}$) are presented in Appendix. The CEC 2014 test suite consists of unimodal, multimodal, hybrid and composite test functions for real parameter single-objective optimization. These test functions are used to expose the exploration and exploitation capability of the algorithm and how it escapes from the local optima.

To investigate the result and performance of AHHO is compared with other well recognized nature-inspired algorithm such as HHO [59], CSA [62,63], CS [64,65], DE [66–68], FA [69,70], GWO [72], WDO [73], WOA [74] and L-SHADE [75,76]. The quantitative analysis includes *best*, *worst*, *average*, and standard deviation (*std.dev.*), whereas qualitative analysis include the position of the prey, search history, trajectory, diversity history, average fitness history, error curve, box plot, and convergence curve. The non-parametric Wilcoxon signed-rank test at $\alpha = 0.05$ and Friedman mean rank test is performed to detect the substantial deference between various nature-inspired algorithms. The Wilcoxon signed ranked test are evaluated when AHHO was significantly better (+), significantly poorer (−−) and significantly equal (≈) then the other optimization algorithm using the p-value.

3.4.2. Experimental setup

To bring consistency among the optimization algorithm, the maximum iterations are set to 500, the maximum number of function evaluations is set to 5000 for a population size of 10, and the maximum number of function evaluations is set to 15000 for a population size of 30. The population size for various optimization algorithms are taken for the experiments as $N = 10$, and $N = 30$ for AHHO, HHO, CSA, CS, DE, FA, GWO, PSO, WDO, and WOA. As L-SHADE optimization algorithm population size depends on the dimension as Initial population size is $N_0 = 18d$ (d is the dimension of the problem) and the final population is $N_{min} = 4$. The AHHO parameter p_{m_max} and p_{m_min} are chosen as 0.3 and 0.1 after hit and trial methods based on test functions. The used parameter setting of various optimization algorithm are reported in Table 3. The result of the various optimization algorithm recorded over 50 independent runs implemented in MATLAB R2018b under WINDOWS 10 64-bit Home in Intel Core i3 (6th Gen.) with 8 GB RAM.

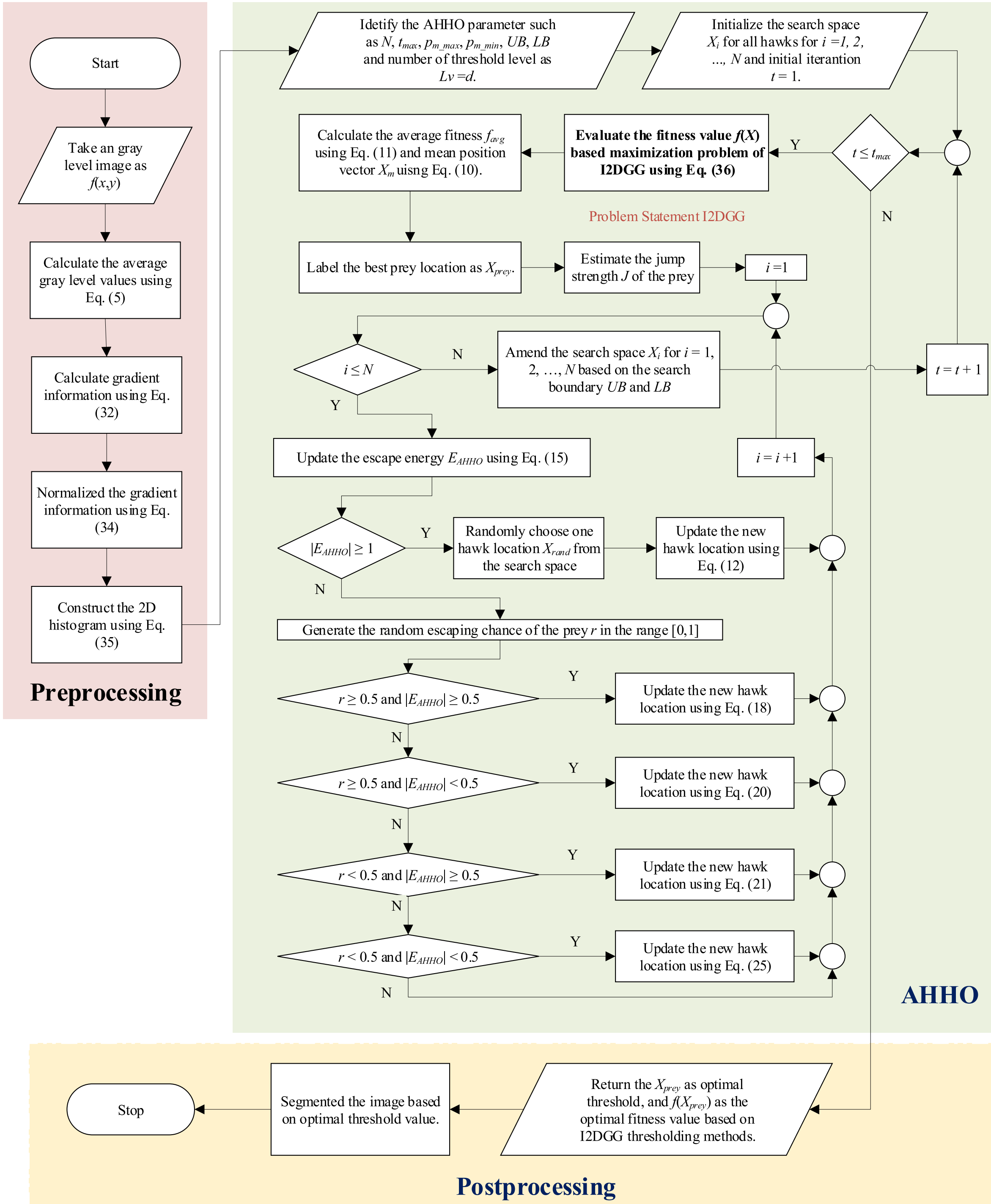

Fig. 12. Flowchart of AHHO-I2DGG based multilevel thresholding.

3.4.3. AHHO's qualitative results

The qualitative results of AHHO for three classical test functions are demonstrated in Fig. 3, and three modern test functions from CEC 2014 are demonstrated in Fig. 4. The qualitative performance is evaluated using the position of the prey, search history, trajectory, diversity history, and average fitness history to illustrate the clear pattern of search and in what way hawks contribute to find optimal solutions in AHHO.

The position of the prey diagram is described in Figs. 3–4, for the X_{prey} in search space during the 500 iterations, and it reveals that for f_1 and f_9, the search space converges to 0. The position of the prey for other functions shows that it tries to converge to the minimum value to attain the minima for specific test functions.

The search history diagram is presented here and is based on the first two-dimensional position as x and y variable for all N hawk during the 500 iterations. The search history from the Figs. 3–4, it can be visible that the position of hawks are more concentrated in the minima position on the contour plot for f_1, f_9, f_{14}, and CEC-2014-F15. For the CEC-2014-F5 and CEC-2014-F10 test function, the position of the hawks tries to reach nearer to minima.

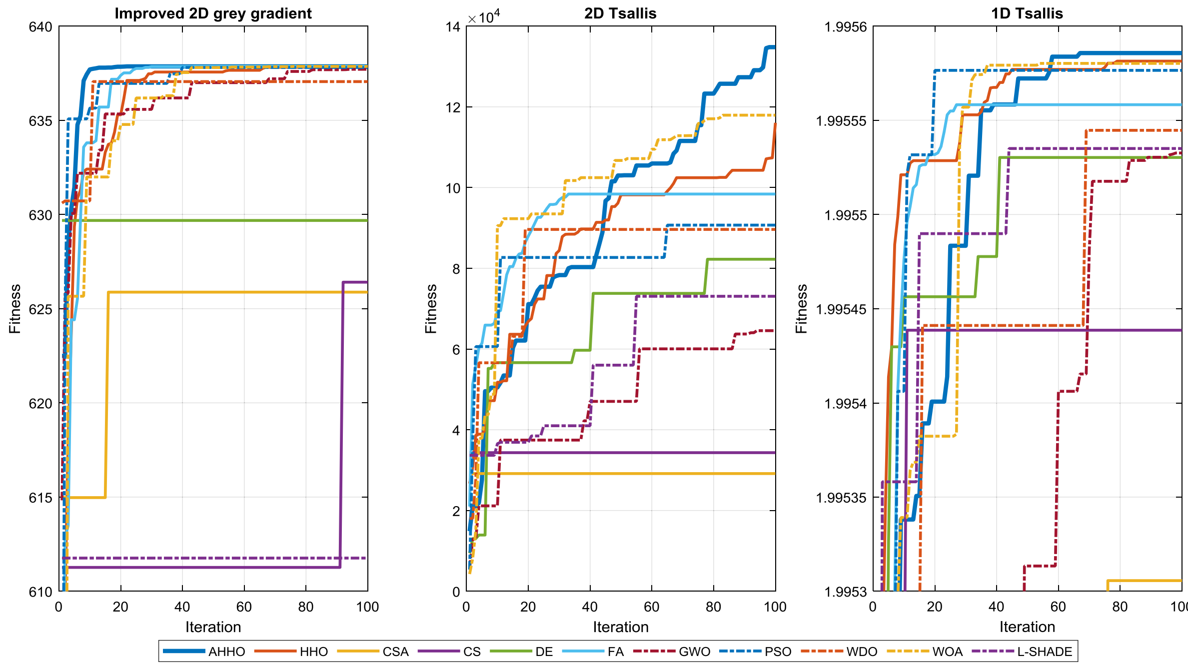

Fig. 13. Convergence plot of various optimization algorithms for identification number 3096 from BSDS 500 for $Lv = 5$.

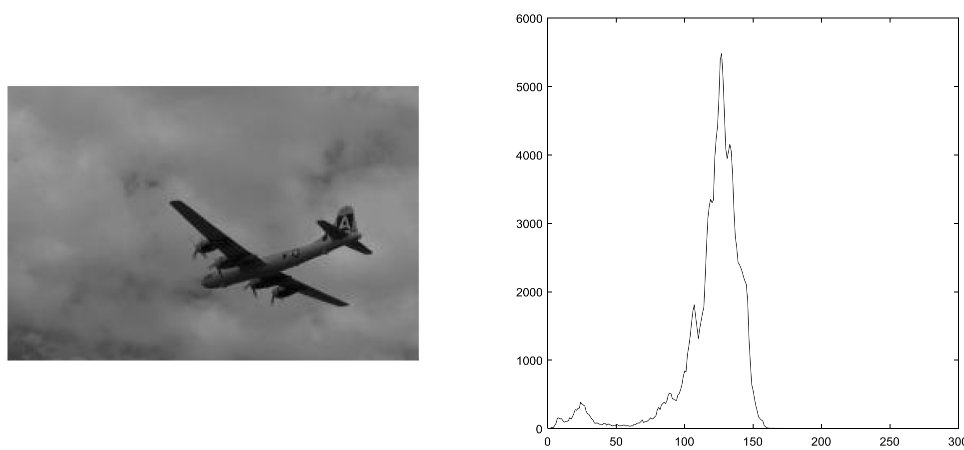

Fig. 14. Sample test image and the corresponding histogram of identification number 3096 from BSDS 500.

The trajectory diagram in Figs. 3–4, describe the position of 1st hawk in the 1st dimension during the 500 iterations. It can be visualized from Fig. 3 that in the initial iteration there is oscillatory behaviour of the curve due to exploration and after that, it converges to an optimal position in the 1st dimension. However, the trajectory diagram in Fig. 4 is from the CEC 2014 test functions, where the trajectory of 1st hawk in the 1st dimension also reaches the optimal position, which experience more fluctuation during the advancement of iteration count as they are complex.

The balance between exploration and exploitation is important for any optimization algorithm to obtain the optimal value. The feature diversity is an indirect approach to measure the exploration and exploitation capability of any optimization algorithm as described by [85]. The diversity is calculated based on the Euclidian distance between the position of N hawks. Let search space $X_i = \left(x_i^1, x_i^2, \ldots, x_i^d\right)$ for ith hawk of d dimensional problem, then at time t, the diversity can be calculated as:

$$divesity\,(t) = \sum_{i=1}^{N}\left(\sum_{j=1}^{N}\sqrt{\sum_{k=1}^{d}\left(x_j^k\,(t) - x_i^k\,(t)\right)^2}\right). \tag{30}$$

The diversity history of some functions is presented in the Figs. 3–4, from which we can visualize that during the initial stage of the optimization algorithm (iterations count are low) the diversity is more as compared to the later stage of the optimization algorithm (iterations count is high). The first observation is the AHHO performs more exploration in the initial stage and performs more exploitation in the later stage of the search process. The second observation can be noticed as the decreasing trend in the diversity value as iteration counts go increasing and reach to zero, that revels AHHO utilize the good balance between exploration and exploitation.

The collaborative behaviour of the hawk can be observed by the average fitness of all hawks' diagram, which are presented in Figs. 3–4. The decreasing trend of average fitness history shows the position of all hawks updated simultaneously to a better one as the generation goes on.

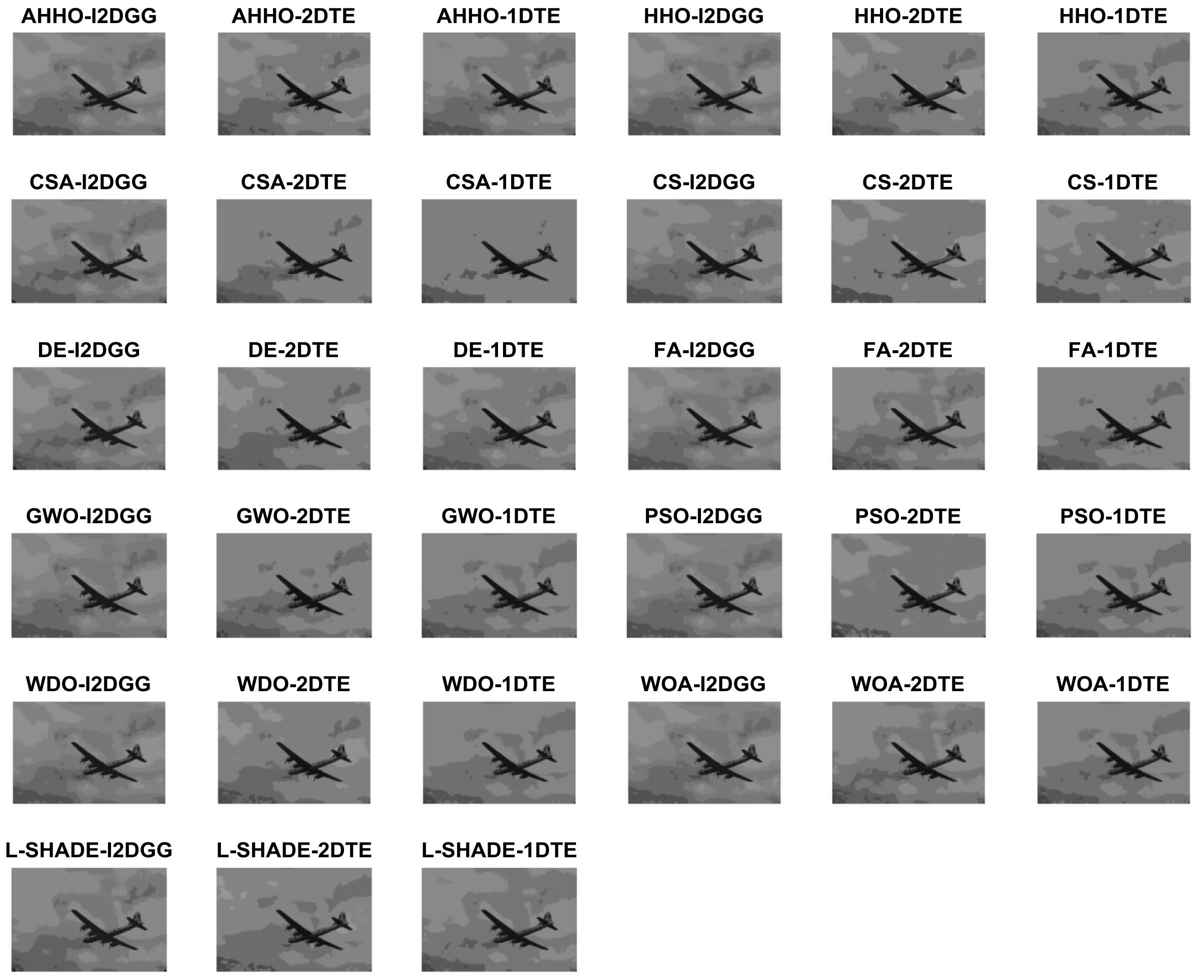

Fig. 15. Threshold image of subject with identification number 3096 from BSDS 500 for $Lv = 5$.

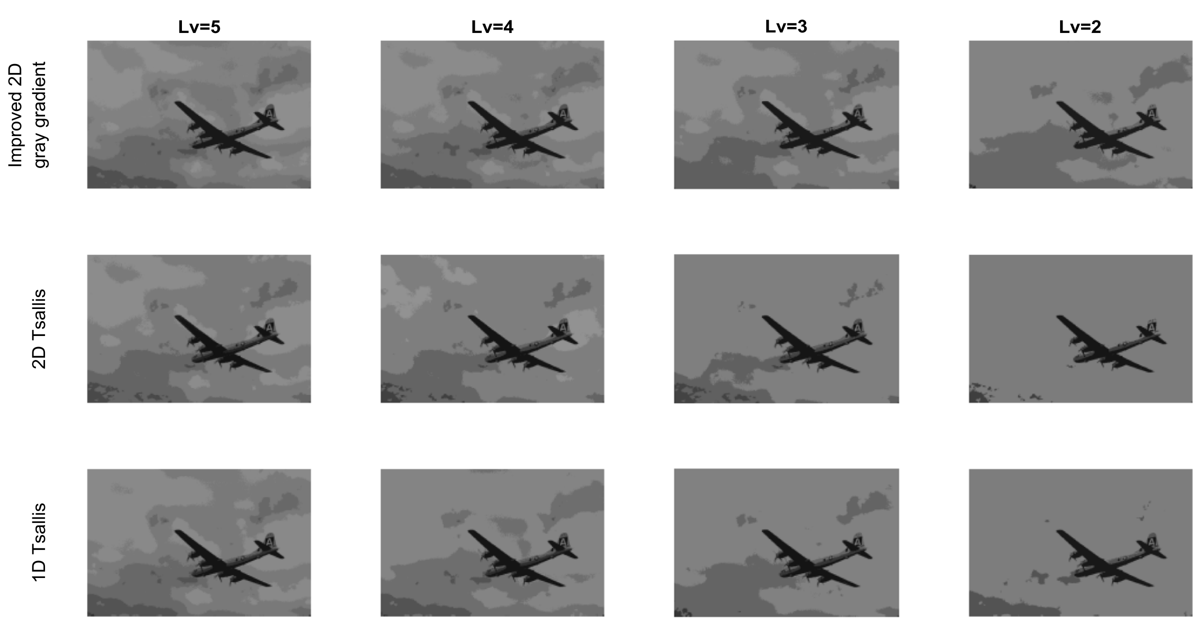

Fig. 16. Threshold image of subject with identification number 3096 from BSDS 500 using AHHO.

Table 17
p-value of the Wilcoxon rank-sum test with 5% significance of CEC-BC-2014 test functions (p-values ≥ 0.05 are shown in boldface). + means that AHHO is statistically significantly better at p-value at 0.05 than another algorithm; $\approx$ means that AHHO is statistically no significant at p-value at 0.05 than another algorithm; $-$ means that AHHO is statistically significant worse than another algorithm. Counts $+/\approx/-$ is the number of problems the AHHO is statistically better/equal/worse than other algorithms.

	HHO	CSA	CS	DE	FA	GWO	PSO	WDO	WOA	L-SHADE
CEC-2014-F1	2.416E−10	8.882E−16	8.882E−16	8.882E−16	8.882E−16	8.882E−16	8.882E−16	8.882E−16	1.179E−12	8.882E−16
CEC-2014-F2	3.389E−06	8.882E−16	8.882E−16	8.882E−16	8.882E−16	8.882E−16	8.882E−16	8.882E−16	8.882E−16	8.882E−16
CEC-2014-F3	8.882E−16	8.882E−16	8.882E−16	8.882E−16	8.882E−16	8.882E−16	8.882E−16	8.882E−16	8.882E−16	8.882E−16
CEC-2014-F4	1.769E−03	8.882E−16	8.882E−16	3.389E−06	8.882E−16	8.882E−16	6.867E−07	8.882E−16	1.769E−03	8.882E−16
CEC-2014-F5	4.887E−02	8.882E−16	8.882E−16	6.867E−07	**9.191E−02**	**5.758E−01**	8.882E−16	**7.798E−01**	4.601E−03	2.416E−10
CEC-2014-F6	6.867E−07	8.882E−16	8.882E−16	8.882E−16	8.882E−16	8.882E−16	8.882E−16	8.882E−16	8.882E−16	8.882E−16
CEC-2014-F7	8.882E−16	8.882E−16	8.882E−16	8.882E−16	8.882E−16	8.882E−16	8.882E−16	8.882E−16	8.882E−16	8.882E−16
CEC-2014-F8	**1.000E+00**	8.882E−16	8.882E−16	1.967E−11	8.882E−16	8.882E−16	8.882E−16	8.882E−16	2.416E−10	8.882E−16
CEC-2014-F9	1.967E−11	8.882E−16	8.882E−16	1.212E−07	8.882E−16	8.882E−16	8.882E−16	8.882E−16	5.704E−05	8.882E−16
CEC-2014-F10	1.832E−08	8.882E−16	8.882E−16	2.328E−09	8.882E−16	8.882E−16	8.882E−16	8.882E−16	1.179E−12	8.882E−16
CEC-2014-F11	1.474E−05	8.882E−16	1.967E−11	1.608E−01	8.882E−16	8.882E−16	4.619E−14	8.882E−16	**5.758E−01**	4.619E−14
CEC-2014-F12	2.328E−09	8.882E−16	2.328E−09	**1.608E−01**	8.882E−16	1.474E−05	1.097E−02	2.416E−10	1.097E−02	1.967E−11
CEC-2014-F13	8.882E−16	8.882E−16	8.882E−16	8.882E−16	8.882E−16	8.882E−16	3.389E−06	8.882E−16	4.619E−14	8.882E−16
CEC-2014-F14	1.769E−03	8.882E−16	8.882E−16	**1.000E+00**	8.882E−16	8.882E−16	**1.608E−01**	8.882E−16	**2.624E−01**	8.882E−16
CEC-2014-F15	2.409E−02	8.882E−16	8.882E−16	4.619E−14	8.882E−16	8.882E−16	8.882E−16	8.882E−16	8.882E−16	8.882E−16
CEC-2014-F16	**1.608E−01**	8.882E−16	8.882E−16	1.769E−03	8.882E−16	8.882E−16	8.882E−16	8.882E−16	3.389E−06	8.882E−16
CEC-2014-F17	8.882E−16	8.882E−16	8.882E−16	8.882E−16	8.882E−16	8.882E−16	8.882E−16	8.882E−16	8.882E−16	8.882E−16
CEC-2014-F18	8.882E−16	8.882E−16	8.882E−16	8.882E−16	8.882E−16	8.882E−16	8.882E−16	8.882E−16	8.882E−16	8.882E−16
CEC-2014-F19	5.704E−05	8.882E−16	8.882E−16	1.179E−12	8.882E−16	8.882E−16	8.882E−16	8.882E−16	1.179E−12	8.882E−16
CEC-2014-F20	8.882E−16	8.882E−16	8.882E−16	8.882E−16	8.882E−16	8.882E−16	8.882E−16	8.882E−16	8.882E−16	8.882E−16
CEC-2014-F21	8.882E−16	8.882E−16	8.882E−16	8.882E−16	8.882E−16	8.882E−16	8.882E−16	8.882E−16	8.882E−16	8.882E−16
CEC-2014-F22	1.967E−11	8.882E−16	8.882E−16	1.179E−12	8.882E−16	8.882E−16	8.882E−16	8.882E−16	4.619E−14	8.882E−16
CEC-2014-F23	**1.000E+00**	8.882E−16	8.882E−16	8.882E−16	8.882E−16	8.882E−16	8.882E−16	8.882E−16	8.882E−16	**1.000E+00**
CEC-2014-F24	6.867E−07	8.882E−16	8.882E−16	8.882E−16	8.882E−16	8.882E−16	8.882E−16	8.882E−16	8.882E−16	8.882E−16
CEC-2014-F25	1.769E−03	1.097E−02	1.769E−03	1.097E−02	1.097E−02	1.097E−02	1.097E−02	1.097E−02	1.097E−02	4.601E−03
CEC-2014-F26	2.416E−10	8.882E−16	8.882E−16	1.212E−07	8.882E−16	8.882E−16	8.882E−16	8.882E−16	3.389E−06	8.882E−16
CEC-2014-F27	1.474E−05	1.474E−05	1.474E−05	1.474E−05	1.474E−05	1.474E−05	1.474E−05	1.474E−05	1.474E−05	1.474E−05
CEC-2014-F28	**1.000E+00**	8.882E−16	8.882E−16	8.882E−16	8.882E−16	8.882E−16	8.882E−16	8.882E−16	8.882E−16	4.768E−07
CEC-2014-F29	**1.742E−01**	1.179E−12	1.179E−12	**1.608E−01**	4.887E−02	**2.624E−01**	1.179E−12	1.980E−04	4.887E−02	**2.624E−01**
CEC-2014-F30	**7.798E−01**	8.882E−16	1.832E−08	2.416E−10	4.601E−03	2.416E−10	8.882E−16	**1.608E−01**	1.832E−08	**2.624E−01**
Counts $+/\approx/-$	24/3/3	30/0/0	30/0/0	27/1/2	29/0/1	28/0/2	29/0/1	28/0/2	28/0/2	27/1/2

3.4.4. AHHO's performance on classical test functions

The statistical result of scalable functions (f_{1-13}) which consists of unimodal (f_{1-7}) and multimodal test functions with varied dimensions (f_{8-13}) are presented in Tables 4–7. The results are obtained with varied population and dimensions The statistical result of scalable functions (f_{1-13}) for N = 10 and d = 30 are presented in Table 4, for N = 30 and d = 30 are presented in Table 5, for N = 10 and d = 100 are presented in Table 6 and for N = 30 and d = 100 are presented in Table 7. Based on the Friedman average rank score the AHHO achieve first rank among all other optimization algorithms, although the HHO and L-SHADE are performing good in scalable test functions. The AHHO lags from L-SHADE in test function f_6, f_{12}, and f_{13}, and HHO in test functions f_6. The AHHO and HHO behave in the same way in statistical results for test functions f_{9-11}.

The statistical result of non-scalable functions (f_{14-23}) for $N = 10$ is presented in Table 8 and for $N = 30$ is presented in Table 9. Based on the Friedman average rank score the AHHO achieve the second rank for $N = 10$ followed by L-SHADE and third rank for $N = 30$ followed by DE and L-SHADE, however it has shown better than the its predecessors' algorithm HHO.

The data presented in Tables 4–9, describe the statistical result, for a better understanding of how 100 independents run to obtain the results are shown in a boxplot in Fig. 5 for the classical test functions. From boxplot, it can be seen AHHO and HHO consistently better than other optimization algorithms except the non-scalable functions. However, for the non-scalable functions, L-SHADE is shown more consistent as compared with the other algorithm. On an average AHHO shown comparable results with other optimization algorithm using the boxplot representation.

The p-value of the non-parametric Wilcoxon signed-rank test at $\alpha = 0.05$ for the classical test functions are presented in Tables 10–15. The AHHO is statistical significant than other optimization algorithm based on p-value are summarized as: HHO ('+' 37.5%, '≈' 22.2%, '−' 40.3%), CSA ('+' 100%), CS ('+' 100%), DE ('+' 95.8% , '−' 4.2%), FA ('+' 98.6% , '−' 1.4%), GWO ('+' 94.4% , '−' 5.6%), PSO ('+' 97.2% , '−' 2.8%), WDO ('+' 100%), WOA ('+' 93% , '−' 7%) and L-SHADE ('+' 98.6%, '≈' 1.4%). From the statistical value, it can be observed that AHHO shown improvement over the HHO and remarkable better than other optimization algorithms.

The convergence curve of six classical test functions are presented in Fig. 6, which is a curve of best fitness so far vs. iterations count. Based on the observation AHHO ranked 1st for f_1, f_5, f_9 and second for f_{12}. The AHHO converge curve behave the same way when compared to other optimization algorithms except CS on test functions f_{15}. For the test functions f_{23} AHHO behave the same as FA and HHO but outperform on other optimization algorithms. On an overall performance of AHHO on the classical test functions, which are the combination of unimodal and multimodal test functions, designed to test the ability of exploitation and exploration, it can be stated that AHHO can be used function optimization.

3.4.5. AHHO's performance on modern CEC 2014 test functions

In the recent days' modern test functions are designed by the researcher for a more complex problem such as CEC 2014 test suite [61], which includes rotated unimodal (CEC-2014-F1 to CEC-2014-F3), shifted and rotated multimodal (CEC-2014-F4 to CEC-2014-F16), hybrid (CEC-2014-F17 to CEC-2014- F22) and composite (CEC-2014-F23 to CEC-2014_F30) functions. The statistical result comparison of AHHO with other optimization algorithms presented in Table 16 is investigated for 51 independent runs with the number of search agents (population) $N = 30$, maximum number of iteration count as 500, the maximum number

Table 18
Performance comparison of various optimization algorithms (Computed over randomly chosen 500 images from BSDS 500) for $Lv = 2, 3, 4, 5$ using average fitness function value and standard deviation of fitness function.

Lv	Algorithm	Improved 2D Grey Gradient (I2DGG)		2D Tsallis Entropy (2DTE)		1D Tsallis Entropy (1DTE)	
		f_{avg}	Std	f_{avg}	Std	f_{avg}	Std
2	AHHO	**2.8271E+03**	**2.1055E+03**	**1.0654E+03**	**3.2983E+02**	**0.8886**	**0.0018**
	HHO	2.8270E+03	2.1563E+03	1.0653E+03	3.3049E+02	**0.8886**	**0.0018**
	CSA	2.8236E+03	2.1580E+03	1.0401E+03	3.4455E+02	**0.8886**	0.0020
	CS	2.8001E+03	2.1493E+03	1.0318E+03	3.3176E+02	**0.8886**	**0.0018**
	DE	2.6831E+03	2.1574E+03	1.0566E+03	3.3656E+02	**0.8886**	**0.0018**
	FA	2.8257E+03	2.1568E+03	1.0409E+03	3.3904E+02	**0.8886**	0.0019
	GWO	2.8239E+03	2.1574E+03	1.0309E+03	3.3909E+02	**0.8886**	0.0019
	PSO	2.8266E+03	2.1573E+03	1.0610E+03	3.3873E+02	**0.8886**	**0.0018**
	WDO	2.8267E+03	2.1573E+03	1.0614E+03	3.3872E+02	**0.8886**	0.0019
	WOA	2.8269E+03	2.1573E+03	1.0643E+03	3.3890E+02	**0.8886**	**0.0018**
	L-SHADE	2.7041E+03	2.1131E+03	1.0593E+03	3.3696E+02	**0.8886**	0.0018
3	AHHO	**2.9855E+03**	**2.1245E+03**	**1.2224E+04**	**4.2724E+03**	**1.2957**	**0.0031**
	HHO	2.9853E+03	2.1248E+03	1.2170E+04	4.7562E+03	**1.2957**	**0.0031**
	CSA	2.9741E+03	2.1776E+03	1.1526E+04	4.7941E+03	1.2956	0.0035
	CS	2.9271E+03	2.1762E+03	1.0202E+04	4.3180E+03	**1.2957**	0.0032
	DE	2.8038E+03	2.1364E+03	1.1588E+04	4.5799E+03	**1.2957**	0.0032
	FA	2.9720E+03	2.1674E+03	1.1108E+04	4.8042E+03	**1.2957**	**0.0031**
	GWO	2.9742E+03	2.1763E+03	1.0898E+04	4.3175E+03	**1.2957**	0.0032
	PSO	2.9832E+03	2.1768E+03	1.1972E+04	4.6846E+03	**1.2957**	**0.0031**
	WDO	2.9842E+03	2.1773E+03	1.1916E+04	4.7004E+03	**1.2957**	**0.0031**
	WOA	2.9852E+03	2.1776E+03	1.2125E+04	4.7392E+03	**1.2957**	**0.0031**
	L-SHADE	2.7786E+03	2.1101E+03	1.1653E+04	4.5883E+03	**1.2957**	0.0031
4	AHHO	**3.0562E+03**	**2.1245E+03**	**1.2988E+05**	**4.3743E+04**	**1.6536**	**0.0038**
	HHO	3.0561E+03	2.1856E+03	1.2948E+05	4.5768E+04	**1.6536**	**0.0038**
	CSA	3.0397E+03	2.1879E+03	1.1772E+05	5.9881E+04	1.6534	0.0044
	CS	2.9739E+03	2.1776E+03	8.9688E+04	5.9659E+04	1.6535	0.0040
	DE	2.8374E+03	2.1854E+03	1.1308E+05	5.2874E+04	**1.6536**	0.0039
	FA	3.0282E+03	2.1692E+03	1.0183E+05	5.8581E+04	**1.6536**	**0.0038**
	GWO	3.0391E+03	2.1783E+03	1.0600E+05	5.1267E+04	**1.6536**	0.0039
	PSO	3.0501E+03	2.1838E+03	1.2458E+05	5.7290E+04	**1.6536**	0.0039
	WDO	3.0529E+03	2.1852E+03	1.1891E+05	5.4306E+04	1.6535	0.0039
	WOA	3.0551E+03	2.1858E+03	1.2597E+05	5.6858E+04	**1.6536**	**0.0038**
	L-SHADE	2.8462E+03	2.1216E+03	1.1304E+05	5.3897E+04	**1.6536**	0.0039
5	AHHO	**3.0947E+03**	**2.1442E+03**	**1.2420E+06**	**3.7248E+05**	**1.9950**	**0.0042**
	HHO	3.0945E+03	2.1720E+03	1.2353E+06	3.8879E+05	**1.9950**	**0.0042**
	CSA	3.0714E+03	2.1900E+03	1.0816E+06	6.3521E+05	1.9947	0.0051
	CS	3.0070E+03	2.1838E+03	6.3244E+05	4.2015E+05	1.9949	0.0044
	DE	2.9072E+03	2.1889E+03	9.4057E+05	5.0518E+05	1.9949	0.0044
	FA	3.0640E+03	2.1888E+03	7.7529E+05	5.6541E+05	**1.9950**	**0.0042**
	GWO	3.0785E+03	2.1861E+03	9.1635E+05	4.9650E+05	**1.9950**	0.0043
	PSO	3.0879E+03	2.1874E+03	1.1511E+06	5.9379E+05	**1.9950**	0.0043
	WDO	3.0902E+03	2.1884E+03	1.0694E+06	6.3994E+05	1.9949	0.0043
	WOA	3.0931E+03	2.1887E+03	1.1725E+06	6.0522E+05	**1.9950**	**0.0042**
	L-SHADE	2.8953E+03	2.1384E+03	9.4292E+05	5.1511E+05	**1.9950**	0.0044

of function evaluation as 15000, search dimension of the problem $d = 10$, and the search boundary for all functions are used as $[-100, 100]$. Based on Friedman mean rank AHHO score will be first but although a very close encounter with HHO, WOA, and DE.

More details on how the 51 independent runs achieve the optimal value can be demonstrated on the boxplot of six test function in Fig. 7, which demonstrated that AHHO has consistent and optimal value as compare to other optimization algorithms. Also, the p-value of non-parametric Wilcoxon signed-rank test at $\alpha = 0.05$ for the CEC 2014 test functions are presented in Table 17, which demonstrate that AHHO statistically reject the null hypothesis. The convergence curve of the six test functions are presented in Fig. 8, from which AHHO have shown quite good consistent response concerning iteration count. Based on these analyses, the AHHO can be used for function optimization in complex problem.

3.4.6. Scalability analysis

This section presents the robustness of AHHO on scalability tests related to low to high dimensional test cases and it demonstrated in Fig. 9. The scalability test is conducted for dimension $d = 10, 20, 30, 50, 100, 200, 500$ for search agents $N = 30$ with maximum iteration is equal to 500. Here AHHO is compared with HHO, CSA, CS, DE, GWO, PSO, WDO and WOA, but due to the search agent's requirement $N = 18 \times d$ of L-SHADE, L-SHADE is excluded from scalability analysis. The AHHO outperforms other optimization algorithms for the 8 scalable classical test function $f_1 - f_5, f_7$ and f_{13}. However, the AHHO perform the same way for the scalable classical test function $f_8 - f_{11}$, and lag very closely from HHO in f_6 and f_{12}. This reveals that the AHHO provides a consistent result in low high dimension without degrading the performance.

3.4.7. Performance of adaptiveness in AHHO when compared to HHO

The AHHO is based on the adaptive decision making on the exploration behaviour of the Harris hawks. The adaptive decision making is based on the average fitness f_{avg} and current fitness $f(X_i)$ of ith hawks, that can be evaluated as Eq. (11). To investigate the behaviour of the adaptiveness in AHHO we formulate an error 'err' that related to deviation of individual hawk fitness to average fitness. Then error can be calculated as:

$$err(t) = \sum_{i=1}^{N} \left| f_{avg}(t) - f(X_i(t)) \right| \tag{31}$$

Table 19
Performance comparison of various optimization algorithms (Computed over randomly chosen 500 images from BSDS 500) for $Lv = 2, 3, 4, 5$ using average PSNR, average SSIM, and average FSIM.

Lv	Algorithm	Improved 2D Grey Gradient (I2DGG)			2D Tsallis Entropy (2DTE)			1D Tsallis Entropy (1DTE)		
		$PSNR_{avg}$	$SSIM_{avg}$	$FSIM_{avg}$	$PSNR_{avg}$	$SSIM_{avg}$	$FSIM_{avg}$	$PSNR_{avg}$	$SSIM_{avg}$	$FSIM_{avg}$
2	AHHO	**23.0611**	**0.7181**	**0.7218**	**21.7601**	**0.6850**	0.7019	**20.5867**	**0.6556**	**0.6758**
	HHO	23.0608	0.7180	0.7214	21.7271	0.6838	0.7011	20.5480	0.6546	0.6756
	CSA	23.0167	0.7171	0.7205	21.6803	0.6797	0.6977	20.3863	0.6484	0.6700
	CS	22.7823	0.7113	0.7150	20.8647	0.6423	0.6600	20.4147	0.6495	0.6712
	DE	21.8864	0.6858	0.6939	21.6568	0.6836	0.7008	20.4042	0.6489	0.6708
	FA	23.0479	0.7177	0.7203	21.4924	0.6803	0.6958	20.3906	0.6483	0.6701
	GWO	23.0431	0.7163	0.7202	21.5112	0.6811	0.6981	20.4080	0.6510	0.6717
	PSO	23.0611	0.7175	0.7214	21.6937	0.6825	0.6968	20.4206	0.6491	0.6707
	WDO	23.0594	0.7176	0.7215	21.6856	0.6848	**0.7020**	20.5277	0.6518	0.6743
	WOA	23.0601	0.7176	0.7216	21.6722	0.6846	0.7017	20.4309	0.6496	0.6713
	L-SHADE	22.0106	0.6908	0.6989	21.6789	0.6826	0.7001	20.3873	0.6483	0.6699
3	AHHO	**25.5607**	**0.7871**	**0.7911**	**24.2951**	**0.7521**	**0.7678**	**22.7091**	**0.7302**	**0.7452**
	HHO	25.5602	0.7869	0.7910	24.0670	0.7507	0.7677	22.5677	0.7264	0.7434
	CSA	25.3434	0.7802	0.7853	24.0111	0.7518	0.7690	22.5171	0.7257	0.7439
	CS	24.4762	0.7631	0.7667	22.2917	0.6953	0.7139	22.4894	0.7245	0.7427
	DE	23.0944	0.7317	0.7344	23.8365	0.7446	0.7616	22.4534	0.7237	0.7420
	FA	25.3122	0.7828	0.7876	23.3140	0.7447	0.7593	22.3180	0.7228	0.7402
	GWO	25.4582	0.7839	0.7893	23.7269	0.7461	0.7613	22.3365	0.7199	0.7384
	PSO	25.5440	0.7856	0.7899	23.7968	0.7501	0.7635	22.4568	0.7246	0.7424
	WDO	25.5379	0.7862	0.7907	23.9779	0.7501	0.7665	22.5151	0.7262	0.7441
	WOA	25.5592	0.7867	0.7908	23.9580	0.7503	0.7670	22.4894	0.7242	0.7423
	L-SHADE	22.7973	0.7261	0.7310	24.0391	0.7527	0.7682	22.5078	0.7252	0.7436
4	AHHO	**27.4371**	**0.8301**	**0.8367**	**26.1247**	**0.8042**	**0.8199**	**24.6361**	**0.7799**	**0.7937**
	HHO	27.4349	0.8299	0.8363	25.9972	0.8008	0.8176	24.2715	0.7764	0.7909
	CSA	26.9779	0.8194	0.8285	25.9692	0.7960	0.8110	24.1755	0.7731	0.7894
	CS	25.4665	0.7890	0.7964	23.3988	0.7308	0.7453	24.1635	0.7727	0.7888
	DE	23.7327	0.7527	0.7591	25.6125	0.7913	0.8087	24.1900	0.7735	0.7894
	FA	26.6777	0.8194	0.8250	24.3374	0.7800	0.7925	23.5287	0.7622	0.7764
	GWO	27.0498	0.8243	0.8293	25.2845	0.7887	0.8023	24.1215	0.7749	0.7913
	PSO	27.3313	0.8263	0.8341	25.8900	0.7988	0.8131	24.1606	0.7726	0.7892
	WDO	27.3518	0.8288	0.8355	25.8404	0.7978	0.8120	24.0665	0.7713	0.7868
	WOA	27.4294	0.8294	0.8364	25.9551	0.7978	0.8143	24.2199	0.7737	0.7898
	L-SHADE	23.6917	0.7580	0.7609	25.7925	0.7941	0.8112	24.1584	0.7730	0.7898
5	AHHO	**28.9495**	**0.8597**	**0.8688**	**27.6313**	**0.8347**	**0.8521**	**26.1181**	**0.8156**	**0.8322**
	HHO	28.9450	0.8593	0.8687	27.5620	0.8343	0.8515	25.6185	0.8066	0.8230
	CSA	28.2188	0.8442	0.8549	27.5628	0.8309	0.8482	25.5757	0.8077	0.8236
	CS	26.2996	0.8102	0.8172	24.6702	0.7636	0.7771	25.5016	0.8045	0.8209
	DE	24.5666	0.7811	0.7829	27.1116	0.8244	0.8400	25.5749	0.8063	0.8223
	FA	27.9596	0.8492	0.8534	24.9774	0.8013	0.8127	24.3562	0.7919	0.8060
	GWO	28.4500	0.8509	0.8601	26.8733	0.8267	0.8412	25.6927	0.8122	0.8260
	PSO	28.7773	0.8560	0.8667	27.1409	0.8268	0.8409	25.5721	0.8071	0.8228
	WDO	28.7817	0.8581	0.8666	27.3311	0.8311	0.8474	25.2328	0.8021	0.8176
	WOA	28.9363	0.8591	0.8687	27.5326	0.8342	0.8510	25.5306	0.8068	0.8233
	L-SHADE	24.4422	0.7778	0.7794	27.1804	0.8281	0.8432	25.5776	0.8060	0.8230

where N is the number of hawks, f is fitness functions and t is the current iterations.

The error curve of three classical test functions f_1, f_9, f_{15} and three modern test functions F5, F10, F15 from CEC 2014 test suite are presented in Fig. 10. The error curve shows that error is low in AHHO than HHO, so it indicates the adaptiveness of AHHO enhancing the performance.

3.5. Discussion on results of AHHO

Based on the Friedman average rank the AHHO shown first rank for scalability classical test functions $f_1 - f_{13}$, second rank for fixed dimension classical test functions $f_{14} - f_{23}$ (a marginal difference from L-SHADE algorithm), and first-rank for 30 modern test function CEC-2014-F1 to CEC-2014-F30 of CEC 2014 test suite compared to well established nature-inspired algorithms HHO, CSA, CS, FA, PSO, DE, GWO, WDO, WOA, and L-SHADE. The AHHO perform well in test functions except f_6, f_{12} and f_{13} out of all 23 classical test function and 30 modern test functions from the CEC 2014 test suite. The performance is also comparable to its predecessors HHO, which can be visualized in Friedman average rank, Wilcoxon rank-sum test, scalability test, error curve, and convergence curve along with the statistical results. The error curve in Fig. 10, shows that the effect of the cumulative error between average fitness and current fitness due to adaptive in the exploration stage. The modification of escaping energy also helps the transition of exploration and exploitation stage effectively. The AHHO inherits the searching property like diversification mechanism based on the average location of the hawk, Levy flight pattern in exploitation and progressive search mechanism, along with its mechanism average fitness-based adaptive perching strategy and modified escape energy helps it to be more efficient to search optimal value, maintain a good balance between exploration and exploitation.

4. Problem formulation on grey level image thresholding

The grey gradient-based approach [20] generally uses the gradient information. Let $f(x, y)$ is a grey level value of an image and $a(x, y)$ be the average grey level value of the image as described by the Eq. (5), then gradient information $g(x, y)$ can

Table 20
Optimal threshold value of subject with identification number 3096 from BSDS 500.

Lv	Method	Optimization Algorithm										
		AHHO	HHO	CSA	CS	DE	FA	GWO	PSO	WDO	WOA	L-SHADE
2	Improved 2D Grey Gradient	65, 117	65, 117	67, 119	64, 118	66,116	66, 118	65, 117	65, 117	65,118	65, 117	68,120
	2D Tsallis	37, 79	37, 78	37, 75	58, 255	37, 80	38, 78	39, 73	38, 70	37, 76	37, 80	37, 80
	1D Tsallis	54, 97	53, 96	33, 77	53, 97	53, 96	53, 97	53, 96	52, 96	59, 96	52, 96	52, 97
3	Improved 2D Grey Gradient	61, 108, 129	61, 108, 129	48, 108, 126	75, 108,129	70, 90,122	62, 108, 129	62, 108, 129	61,108, 129	61, 108, 129	61, 108, 129	80,110, 128
	2D Tsallis	37, 83, 105	29, 64, 100	33, 58, 79	42, 62, 238	31,81, 104	35, 68, 100	26, 57, 93	26, 57, 93	32, 62, 102	26, 51, 68	27, 67, 103
	1D Tsallis	40, 76, 120	35, 72, 113	34, 72, 113	33, 71, 114	35, 72, 113	35, 70, 113	35,70, 113	35, 71, 113	39, 62, 96	35, 72, 112	35, 66, 96
4	Improved 2D Grey Gradient	55, 97,116, 132	54, 96, 116, 131	61, 93, 108, 127	65, 114, 126, 136	70, 108, 116, 129	55, 97,117, 131	53, 96, 117, 131	54, 95.115, 131	56, 95, 116, 131	54, 96, 116, 131	63, 94, 114, 122
	2D Tsallis	36, 67,108, 139	38, 76, 99, 119	35, 61, 94, 147	16,62, 107, 211	29, 70, 108, 136	24, 46, 67, 98	25, 55, 92, 111	26, 52, 116, 136	35, 81, 110, 141	47, 76, 99, 119	26, 47, 81, 94
	1D Tsallis	34, 64, 94, 120	35, 63, 94, 119	40, 60, 96, 115	35, 59, 91, 119	38, 66, 94, 120	34, 63, 92, 114	34, 66, 96, 118	34, 65, 95, 119	39, 66, 99, 129	35, 64, 94, 120	35, 63, 95, 118
5	Improved 2D Grey Gradient	53, 92, 111, 126, 136	52, 92, 111, 124, 135	65, 102, 121, 132, 167	57, 94, 114, 130, 251	66,82, 102, 119, 135	53, 92, 111, 124, 138	53, 93, 112, 126, 136	52, 91, 111, 123, 136	52, 93,109, 124, 137	53, 93, 112, 125, 135	65, 69, 77, 108, 126
	2D Tsallis	28, 52, 83, 110, 132	32, 76, 96, 112, 138	47, 64, 77, 96, 110	1, 32, 95, 136, 236	34, 57, 78, 111, 138	45, 66, 88, 106, 126	25, 39, 71,100, 117	27, 38, 75, 89, 134	25, 51, 87, 111, 140	28, 56, 82, 104, 126	28, 52, 86, 120, 146
	1D Tsallis	35, 67, 92, 113, 132	34, 65, 93, 112, 128	26, 56, 75, 99, 161	33, 62, 101, 132, 160	31, 56, 77, 96, 121	35, 58, 77, 96, 114	31, 55, 75, 96, 121	32, 51, 76, 95, 120	32, 56, 75, 92, 121	31, 53, 77, 96, 121	32, 62, 78, 99, 128

be formulated as:

$$g(x,y) = abs\left(f(x,y) - a(x,y)\right) \tag{32}$$

The 2D histogram based on the grey gradient can be constructed using the grey level values $f(x,y)$ and gradient information $g(x,y)$ as:

$$p_{GG}(i,j) = \frac{1}{M \bullet N}\left\{r_{ij} | f(x,y) = i, g(x,y) = j; i,j \in (0, L-1)\right\} \tag{33}$$

where the r_{ij} represents the number of pixels with grey level values with i and gradient information with j.

However, the analysis of the 2D histogram plot exhibits non-uniformity in the distribution of edge magnitudes. Some of the peak values are very large, which causes edge magnitude limiting issues. Hence, there is a strong need to normalize these peaks while construction of the 2D histogram. In this context, here an attempt is made to take care of the existing issue. Here, we propose a new improved 2D grey gradient (I2DGG) algorithm used for the experiment.

This edge magnitude is normalized to eliminate the edge magnitude peaks. The normalized edge magnitude is

$$g_n(x,y) = \frac{(g(x,y) - g_{min}) \times K}{g_{max} - g_{min}} \tag{34}$$

where g_{max} and g_{min} are the maximum and minimum values of the edge magnitudes, respectively. Note that K is a constant and is chosen as $L-1 = 255$ for the experiment. Then, the 2D histogram based on normalized grey gradient can be constructed as

$$p_{iGG}(i,j) = \frac{1}{M \bullet N}\left\{r_{ij} | f(x,y) = i, g_n(x,y) = j; i,j \in (0, L-1)\right\} \tag{35}$$

The multilevel thresholding grey gradient approach, and the corresponding 2D histogram plane is presented in Fig. 11. The 2D histogram plane of grey gradient-based approach is subdivided by a set of m thresholds $t = [t_1, t_2, \ldots, t_m]$ of grey-level image; a threshold value s of gradient information, which resulted in a $2M$ quadrants, where $M = m + 1$. As the 2D histogram plane of bi-level based on grey gradient, the first-row wise quadrants consists of grey level information that can be used for thresholding, and the second-row wise quadrants consist of edge and noise information that can be ignored. Based on the m number of thresholds, the image is divided into M number of regions as $\{R1, R2, \ldots, RM\}$.

The optimal multilevel thresholding of a M class problem with m thresholds $[t_1, t_2, \ldots, t_m]$ for a given image is a maximization problem as:

$$\begin{aligned}&\{(t_1,s),(t_2,s),\ldots,(t_m,s)\}_{opt}\\ &\quad = \arg\max\left\{\sigma_b^2\left[(t_1,s),(t_2,s),\ldots,(t_m,s)\right]\right\}\end{aligned} \tag{36}$$

where the between-class variance σ_b^2 is

$$\begin{aligned}\sigma_b^2 &= P_{R1}\left[(\mu_{C11} - \mu_1)^2 + (\mu_{C12} - \mu_2)^2\right]\\ &\quad + P_{R2}\left[(\mu_{C21} - \mu_1)^2 + (\mu_{C22} - \mu_2)^2\right] + \cdots\\ &\quad + P_{RM}\left[(\mu_{CM1} - \mu_1)^2 + (\mu_{CM2} - \mu_2)^2\right].\end{aligned} \tag{37}$$

The probability distributions $\{P_{R1}, P_{R2}, \ldots, P_{RM}\}$ are defined as:

$$P_{R1} = \sum_{i=0}^{t_1}\sum_{j=0}^{s} p_{iGG}(i,j),$$

$$P_{R2} = \sum_{i=t_1+1}^{t_2}\sum_{j=0}^{s} p_{iGG}(i,j),$$

and

$$P_{RM} = \sum_{i=t_m+1}^{L-1}\sum_{j=0}^{s} p_{iGG}(i,j). \tag{38}$$

The overall mean vector μ is defined as

$$\mu = \left[\sum_{i=0}^{L-1}\sum_{j=0}^{L-1} i p_{GG}(i,j), \sum_{i=0}^{L-1}\sum_{j=0}^{L-1} j p_{GG}(i,j)\right]^T \tag{39}$$

and the mean vectors for multilevel thresholding are $\{\mu_{R1}, \mu_{R2}, \ldots, \mu_{RM}\}$ and are defined as:

$$\mu_{R1} = (\mu_{R11}, \mu_{R12})^T = \left[\sum_{i=0}^{t_1}\sum_{j=0}^{s}\frac{i p_{iGG}(i,j)}{P_{R1}}, \sum_{i=0}^{t_1}\sum_{j=0}^{s}\frac{j p_{iGG}(i,j)}{P_{R1}}\right]^T$$

$$\mu_{R1} = (\mu_{R11}, \mu_{R12})^T = \left[\sum_{i=0}^{t_1}\sum_{j=0}^{s}\frac{i p_{iGG}(i,j)}{P_{R1}}, \sum_{i=0}^{t_1}\sum_{j=0}^{s}\frac{j p_{iGG}(i,j)}{P_{R1}}\right]^T$$

$$\vdots$$

$$\begin{aligned}\mu_{RM} &= (\mu_{RM1}, \mu_{RM2})^T\\ &= \left[\sum_{i=t_m+1}^{L-1}\sum_{j=0}^{s}\frac{i p_{iGG}(i,j)}{P_{RM}}, \sum_{i=t_m+1}^{L-1}\sum_{j=0}^{s}\frac{j p_{iGG}(i,j)}{P_{RM}}\right]^T\end{aligned} \tag{40}$$

Note that the Eq. (36) is the fitness function. It is an exhaustive search process as the number of thresholds m increases, leads to an optimization problem

5. Results and discussions

The proposed AHHO algorithm is applied for the multilevel thresholding using the benchmark images from the Berkeley Segmentation Data set (BSDS 500) [77]. To evaluate the performance of our proposed AHHO based multilevel thresholding, we implement and compare the result of AHHO with several well-known soft computing optimization techniques based multilevel thresholding using — differential evolution (DE) [9,67], particle swarm optimization (PSO) [17,71], Cuckoo search (CS) [7,8,65], firefly algorithm (FA) [10,70], wind driven optimization (WDO) [8,73] and recently developed Harris hawks optimization (HHO) [59], crow search algorithm (CSA) [6,63], grey wolf optimizer (GWO) [13,72], whale optimization algorithm (WOA) [16,74] and successful history-based adaptive DE variants with linear population size reduction (L-SHADE) [75,76] . To validate our technique, we use three well-known performance metrics peak signal to noise ratio (PSNR) [7], feature similarity (FSIM) [86] and structured similarity (SSIM) [87]. The experimental parameter setup for various soft computing optimization algorithms is shown in Table 3, with the number of search agents $N = 30$ and maximum number of iteration counts is $t_{max} = 100$, where as the number of search agents of L-SHADE depends on the dimension of the problem as $N = 18 \times d$ at the initialization $N = 4$ at the termination. As the search agents in requirement various algorithm varies, special L-SHADE, so to make consistency among the multilevel thresholding using optimization algorithm we fixed the maximum function evaluation as 3000. So, if any algorithm requires a greater number of functions to converge, it must break when it reaches 3000 function evaluation.

All the 500 images from BSDS 500 are used for the performance in multilevel thresholding using three different fitness

Table 21
p-value of the Wilcoxon rank-sum test with 5% significance of for 500 images form the BSDS 500 dataset (p-values ≥ 0.05 are shown in boldface). + means that AHHO is statistically significantly better at p-value at 0.05 than another algorithm; $\approx$ means that AHHO is statistically no significant at p-value at 0.05 than another algorithm; $-$ means that AHHO is statistically significant worse than another algorithm. Counts $+/\approx/-$ is the number of problems the AHHO is statistically better/equal/worse than other algorithms.

Lv	Method	HHO	CSA	CS	DE	FA	GWO	PSO	WDO	WOA	L-SHADE
2	Improved 2D Grey Gradient	2.06E−03	2.59E−110	2.59E−110	2.59E−110	3.30E−56	9.72E−76	3.30E−56	6.64E−93	3.75E−25	2.59E−110
	2D Tsallis	**1.57E−01**	8.42E−102	8.42E−102	1.23E−93	2.34E−76	2.59E−110	8.42E−102	1.23E−93	1.89E−36	2.41E−78
	1D Tsallis	**1.00E+00**	8.72E−104	4.42E−95	1.07E−53	1.07E−53	5.69E−45	1.86E−09	3.88E−108	1.95E−03	1.78E−15
3	Improved 2D Grey Gradient	1.00E−07	2.59E−110	2.59E−110	2.59E−110	6.85E−70	8.42E−102	3.01E−77	1.25E−99	2.01E−42	2.59E−110
	2D Tsallis	4.11E−04	2.59E−110	2.59E−110	8.42E−102	8.13E−86	2.59E−110	8.42E−102	1.23E−93	5.28E−58	1.23E−93
	1D Tsallis	**2.82E−01**	2.59E−110	2.59E−110	2.59E−110	1.44E−73	1.96E−99	4.36E−21	2.59E−110	2.06E−03	1.31E−101
4	Improved 2D Grey Gradient	**1.00E+00**	2.59E−110	2.59E−110	2.59E−110	5.81E−106	2.59E−110	1.13E−83	2.59E−110	7.04E−17	2.59E−110
	2D Tsallis	1.15E−12	8.42E−102	2.59E−110	2.59E−110	8.42E−102	2.59E−110	3.23E−71	8.42E−102	3.23E−71	2.59E−110
	1D Tsallis	1.01E−15	2.59E−110	2.59E−110	2.59E−110	9.08E−89	1.25E−99	3.76E−87	2.59E−110	1.03E−15	2.59E−110
5	Improved 2D Grey Gradient	4.96E−07	2.59E−110	2.59E−110	2.59E−110	1.57E−81	8.42E−102	2.59E−110	2.59E−110	5.02E−48	2.59E−110
	2D Tsallis	**3.95E−01**	1.23E−93	2.59E−110	2.59E−110	2.59E−110	2.59E−110	8.42E−102	1.23E−93	5.28E−58	8.42E−102
	1D Tsallis	1.18E−11	2.59E−110	2.59E−110	2.59E−110	1.25E−99	2.59E−110	8.42E−102	2.59E−110	1.46E−03	2.59E−110
Counts $+/\approx/-$		7/2/3	12/0/0	12/0/0	12/0/0	12/0/0	12/0/0	12/0/0	12/0/0	12/0/0	12/0/0

functions: improved 2D grey gradient (I2DGG), 2D Tsallis entropy (2DTE), and 1D Tsallis entropy (1DTE). The initial solutions are chosen randomly for each optimization algorithms. To measure the stability, each optimization algorithms is repeated for 50 independent runs. The AHHO-I2DGG based multilevel image thresholding is presented in Fig. 12.

Table 18 shows the performance of various optimization algorithms considering their average fitness values (f_{avg}) and standard deviation (Std) among 50 independent runs for the threshold levels of $Lv = 2, 3, 4, 5$. The higher the fitness value with a lower standard deviation, results in a better thresholding performance. It can be observed that almost all the optimization algorithms are doing well in 1DTE based multilevel thresholding, when we consider the average fitness value. However, the standard deviation value is comparatively less in AHHO, HHO, FA, and WOA optimization algorithms, which is desirable. Therefore, the performance of the AHHO algorithm is recommendable. When we compare the multilevel thresholding performance using I2DGG and 2DTE, then the AHHO performs better concerning the average fitness value and standard deviation. This shows the potential of our proposed algorithm for image thresholding.

Similarly, Table 19 shows the comparison results of various optimization algorithms using average PSNR, average SSIM, and average FSIM. These measures are mostly used to quantity the multilevel thresholding performance. The higher value indicates the better thresholding approach. It is observed that the AHHO performs better than other optimization algorithms in all three methods, i.e. I2DGG, 2DTE and 1DTE.

The convergence plots of the various optimization algorithms for threshold level 5 of an image from BSDS 500 with identification number 3096 are displayed in Fig. 13. The figure present three convergence curve related to I2DGG (left side), 2DTE (middle) and 1DTE (right side). The convergence curve from Fig. 13, it is observed that the AHHO converges faster than any other optimization algorithm concerning the iteration count, because the movement depends on the adaptiveness of AHHO depends on average fitness in the exploration phases, which is not depends on a random value 'q' as discussed in HHO [59]. It is reiterated that the 'q' value was set at 0.5 in HHO [59].

In these experiments, all the 500 images from the BSDS 500 are considered to evaluate. For an in-depth analysis, a sample image from the BSDS 500 with identification number 3096 is considered, which is displayed along with its histogram is displayed in Fig. 14. The corresponding optimal threshold value of subject 3096 are presented in Table 20. The careful study on the threshold value it can be observed that all the state-of-art algorithm perform in the same way for threshold level 2 on all three thresholding methods, however when the threshold level increases, AHHO threshold levels are closely related to HHO, FA, GWO, PSO, WDO and WOA, and divergent from the CSA, CS, DE, and L-SHADE. If we relate the optimal threshold value with the convergence curve, the AHHO convergence curve related to the other optimization algorithm in the same way.

The qualitative result based on the threshold value of subject 3096 from BSDS 500, threshold image for threshold level 5 for various optimization algorithms on I2DGG, 2DTE, and 1DTE are presented in Fig. 15. From Fig. 15, it can be visualized that, the AHHO-I2DGG shown the best threshold image when compared combinedly with other algorithms and methods.

Recently, Heidari et al. [59] proposed a new metaheuristic algorithm called Harris Hawks Optimization (HHO) taking inspiration from the cooperative perching strategy of Harris' hawk. The HHO gives quite an impressive result when compared with some well-known optimization algorithms. This has motivated us to analyse the HHO algorithm, where we found that the transition from explorations to exploitations or vice-versa, has depends on a random value. This warrants us to modify the perching strategy control parameter of the exploration and exploitation are made adaptive fitness value of Harris' hawk. The Harris's hawk chasing strategy mostly depends on the rabbit (prey) energy, which is in the range of -2 to 2. The rabbit energy less than 0 means the rabbit has no energy to flagging, that motivates us to do some modification to rabbit energy in the proposed work. The modification of rabbit energy and introducing the adaptive fitness-based control parameter, the proposed algorithm is coined as adaptive Harris hawks optimization (AHHO). The performance of the AHHO is evaluated using the 23 well known classical benchmark test function [55,60] and modern CEC 2014 test functions [61]. A comparison of AHHO with state-of-art algorithm such as Harris hawks optimization (HHO) [59], crow search algorithm (CSA) [62,63], Cuckoo search (CS) [64,65], differential evolution (DE) [66–68], firefly algorithm (FA) [69,70], grey wolf optimizer (GWO) [72], wind driven optimization (WDO) [73], whale optimization algorithm (WOA) [74] and successful history-based adaptive DE with linear population size reduction (L-SHADE) [75,76]. As a result, AHHO shows better convergence along with superior results when compare statistical with Wilcoxon's test and Friedman test.

The qualitative result performance of AHHO on three thresholding methods such as I2DGG, 2DTE, and 1DTE is presented in Fig. 16, which shows that I2DGG outperforms other methods on threshold level equal to 2,3,4 and 5. Specifically, from Fig. 16, it is observed that the proposed I2DGG yields better threshold images even with the lower levels of thresholding, i.e. when $Lv =$

Table A.1
Unimodal benchmark functions.

Function	d	Range	f_{min}
$f_1(X) = \sum_{i=1}^{d} x_i^2$	30, 100	$[-100,\ 100]^d$	0
$f_2(X) = \sum_{i=1}^{d} \lvert x_i \rvert + \prod_{i=1}^{d} \lvert x_i \rvert$	30, 100	$[-10,\ 10]^d$	0
$f_3(X) = \sum_{i=1}^{d} \left(\sum_{j=1}^{i} x_j \right)^2$	30, 100	$[-100,\ 100]^d$	0
$f_4(X) = \max_i \{\lvert x_i \rvert,\ 1 \le i \le d\}$	30, 100	$[-100,\ 100]^d$	0
$f_5(X) = \sum_{i=1}^{d-1} \left[100\left(x_{i+1} - x_i^2\right)^2 + (x_i - 1)^2 \right]$	30, 100	$[-30,\ 30]^d$	0
$f_6(X) = \sum_{i=1}^{d} \left(\lfloor x_i + 0.5 \rfloor\right)^2$	30, 100	$[-100,\ 100]^d$	0
$f_7(X) = \sum_{i=1}^{d} i x_i^4 + random[0,\ 1)$	30, 100	$[-1.28,\ 1.28]^d$	0

Table A.2
Multimodal benchmark functions.

Function	d	Range	f_{min}
$f_8(X) = \sum_{i=1}^{d} -x_i \sin\left(\sqrt{\lvert x_i \rvert}\right)$	30, 100	$[-500, 500]^d$	$-418.9829 \times d$
$f_9(X) = \sum_{i=1}^{d} \left[x_i^2 - 10\cos(2\pi x_i) + 10 \right]$	30, 100	$[-5.12,\ 5.12]^d$	0
$f_{10}(X) = -20\exp\left(-0.2\sqrt{\frac{1}{d}\sum_{i=1}^{d} x_i^2}\right) - \exp\left(\frac{1}{d}\sum_{i=1}^{d}\cos(2\pi x_i)\right) + 20 + e$	30, 100	$[-32,\ 32]^d$	0
$f_{11}(X) = \frac{1}{4000}\sum_{i=1}^{d} x_i^2 - \prod_{i=1}^{d}\cos\left(\frac{x_i}{\sqrt{i}}\right) + 1$	30, 100	$[-600,\ 600]^d$	0
$f_{12}(X) = \frac{\pi}{d}\left\{ 10\sin(\pi y_1) + \sum_{i=1}^{d-1}(y_i - 1)^2\left[1 + 10\sin^2(\pi y_{i+1})\right] + (y_d - 1)^2 \right\}$	30, 100	$[-50,\ 50]^d$	0
$+ \sum_{i=1}^{d} u(x_i, 10,\ 100,\ 4)$			
$y_i = 1 + \frac{x_i+1}{4} u(x_i, a, k, m) = \begin{cases} k(x_i - a)^m & x_i > a \\ 0 & -a < x_i < a \\ k(-x_i - a)^m & x_i < -a \end{cases}$			
$f_{13}(X) = 0.1\left\{ \sin^2(3\pi x_1) + \sum_{i=1}^{d}(x_i - 1)^2\left[1 + \sin^2(3\pi x_i + 1)\right] + (x_d - 1)^2\left[1 + \sin^2(2\pi x_d)\right] \right\}$	30, 100	$[-50,\ 50]^d$	0
$+ \sum_{i=1}^{d} u(x_i, 5,\ 100,\ 4)$			
$y_i = 1 + \frac{x_i+1}{4} u(x_i, a, k, m) = \begin{cases} k(x_i - a)^m & x_i > a \\ 0 & -a < x_i < a \\ k(-x_i - a)^m & x_i < -a \end{cases}$			

Table A.3
Multimodal benchmark functions with fixed dimension.

Function	Range	f_{min}
$f_{14}(X) = \left(\frac{1}{500} + \sum_{j=1}^{25} \frac{1}{j + \sum_{i=1}^{2}(x_i - a_{ij})^6} \right)^{-1}$	$\begin{bmatrix} -65.536, \\ 65.536 \end{bmatrix}^2$	1
$a_{ij} = \begin{pmatrix} -32 & -16 & 0 & 16 & 32 & -32 & \cdots & 0 & 16 & 32 \\ -32 & -32 & -32 & -32 & -32 & -16 & \cdots & 32 & 32 & 32 \end{pmatrix}$		
$f_{15}(X) = \sum_{i=1}^{11}\left[a_i - \frac{x_1\left(b_i^2 + b_i x_2\right)}{b_i^2 + b_i x_3 + x_4} \right]^2$ The coefficients are displayed in Table A.4.	$[-5,\ 5]^4$	0.0003075
$f_{16}(X) = 4x_1^2 - 2.1x_1^4 + \frac{1}{3}x_1^6 + x_1 x_2 - 4x_2^2 + 4x_2^4$	$[-5,\ 5]^2$	-1.0316285
$f_{17}(X) = \left(x_2 - \frac{5.1}{4\pi^2}x_1^2 + \frac{5}{\pi}x_1 - 6 \right)^2 + 10\left(1 - \frac{1}{8\pi}\right)\cos x_1 + 10$	$[-5, 10] \times [0, 15]$	0.398
$f_{18}(X) = \left[1 + (x_1 + x_2 + 1)^2 \times \left(19 - 14x_1 + 3x_1^2 - 14x_2 + 6x_1x_2 + 3x_2^2\right)\right]$ $\times \left[30 + (2x_1 - 3x_2)^2 \times \left(18 - 32x_1 + 12x_1^2 + 48x_2 - 36x_1x_2 + 27x_2^2\right)\right]$	$[-2,\ 2]^2$	3
$f_{19}(X) = -\sum_{i=1}^{4} c_i \exp\left(-\sum_{j=1}^{3} a_{ij}\left(x_j - p_{ij}\right)^2 \right)$ The coefficients are displayed in Table A.5.	$[0,\ 1]^3$	-3.86
$f_{20}(X) = -\sum_{i=1}^{4} c_i \exp\left(-\sum_{j=1}^{6} a_{ij}\left(x_j - p_{ij}\right)^2 \right)$ The coefficients are displayed in Table A.6.	$[0,\ 1]^6$	-3.32
$f_{21}(X) = -\sum_{i=1}^{5}\left[(X - a_i)(X - a_i)^T + c_i\right]^{-1}$ The coefficients are displayed in Table A.7.	$[0,\ 10]^4$	-10.1532
$f_{22}(X) = -\sum_{i=1}^{7}\left[(X - a_i)(X - a_i)^T + c_i\right]^{-1}$ The coefficients are displayed in Table A.7.	$[0,\ 10]^4$	-10.4028
$f_{23}(X) = -\sum_{i=1}^{10}\left[(X - a_i)(X - a_i)^T + c_i\right]^{-1}$ The coefficients are displayed in Table A.7.	$[0,\ 10]^4$	-10.5363

2 *and* $Lv = 3$, whereas 2D Tsallis and 1D Tsallis methods do not perform well with the lower levels of image thresholding.

To understand how the AHHO results are statistically significantly better than other optimization techniques and methods,

Table A.4
Coefficients related to benchmark function f_{15}.

i	a_i	b_i^{-1}
1	0.1957	0.25
2	0.1947	0.5
3	0.1735	1
4	0.1600	2
5	0.0844	4
6	0.0627	6
7	0.0456	8
8	0.0342	10
9	0.0323	12
10	0.0235	14
11	0.0246	16

Table A.7
Coefficients related to benchmark function f_{21-23}.

i	a_{i1}	a_{i2}	a_{i3}	a_{i4}	c_i
1	4	4	4	4	0.1
2	1	1	1	1	0.2
3	8	8	8	8	0.2
4	6	6	6	6	0.4
5	3	7	3	7	0.4
6	2	9	2	9	0.6
7	5	5	3	3	0.3
8	8	1	8	1	0.7
9	6	2	6	2	0.5
10	7	3.6	7	3.6	0.5

Table A.5
Coefficients related to benchmark function f_{19}.

i	a_{i1}	a_{i2}	a_{i3}	c_i	p_{i1}	p_{i2}	p_{i3}
1	3	10	30	1	0.3689	0.1170	0.2673
2	0.1	10	35	2	0.4699	0.4387	0.7470
3	3	10	30	3	0.1091	0.8732	0.5547
4	0.1	10	35	4	0.03815	0.5743	0.8828

a Wilcoxon rank-sum test with 5% significance based on the best fitness value among 50 independent runs are presented in Table 21. Based on the observation AHHO shows statistically 58% better, 17% similar, and 25% worse than HHO, however, AHHO shows statistically 100% better than CSA, CS, DE, FA, GWO, PSO, WDO, WOA, and L-SHADE.

I2DGG seems to be computationally efficient because it computes intra-class variance using row-wise blocks only and the reason behind this improvement is due to the preservation of more edge information in our method. It is seen that AHHO based I2DGG thresholding technique sounds better for multilevel image thresholding applications in the future.

6. Conclusion

This paper proposes an adaptive Harris hawks optimization (AHHO) algorithm based on the variation of escape energy and including the adaptiveness in the perching strategy of Harris hawk. The idea of adaptive mechanism in the perching strategy provides us a computationally efficient technique, the reason is that the wastage of the search agents (Harris hawk) could be avoided. Due to the adaptiveness in the perching strategy, which is based on the averaging of fitness value, the AHHO performance shows significant improvement than HHO. Although, the computational complexity of AHHO marginally increases than HHO, based on the iteration counts and function evaluations, the AHHO converge faster than HHO. The qualitative and quantitative results of AHHO compared with well-established optimization algorithms HHO, CSA, CS, DE, FA, PSO, GWO, WDO, WOA and L-SHADE on the test functions, which shows AHHO outperforms other optimization algorithms. The AHHO algorithm has potential and can be used to find an optimal solution in various applications in engineering. The AHHO can be extended to the multi-objective problem, as this study only focused on single-objective problem.

Here, the effectiveness and superiority of the AHHO algorithm is applied to the multilevel image thresholding. The paper also proposes an improved 2D grey gradient (I2DGG) multilevel image thresholding method, a normalized gradient to avoid the large peaks and relatively less sensitive to high edge values, which is an optimization problem to find the optimal threshold values. To study the effectiveness of our proposed I2DGG multilevel thresholding methods, the 2D Tsallis entropy (2DTE) and Tsallis entropy (1DTE) are used for comparisons. The proposed evolutionary multilevel image thresholding method, AHHO using I2DGG yields superior results as compared to other methods based on 2DTE and 1DTE, because it extracts the both spatial and edge information together efficiently. The proposed method could extract parts that have low-contrast inhomogeneous visual features. The method is suitable for solving complex segmentation problems, as we need to compute row-wise regions, not the diagonal regions. The adaptive perching approach implemented in AHHO helps in more localization, therefore true optimal threshold values are achieved. A comparison of threshold segmented image along with statistical results using average fitness, PSNR, SSIM, and FSIM are shown in this article. The state-of-the-art optimization algorithms are compared with AHHO for convincing the readers. The future scope of the work include colour image thresholding and breast cancer thermal image thresholding. Finally, we believe that the suggested method can also be employed for the computational intelligence-based image segmentation for smart health care applications.

CRediT authorship contribution statement

Aneesh Wunnava: Methodology, Software, Validation, Visualization, Witing - orignal Draft. **Manoj Kumar Naik:** Methodology, Validation, Visualization, Writing - review & Editing, Conceptualization. **Rutuparna Panda:** Methodology, Writing - review & Editing, Conceptualization. **Bibekananda Jena:** Methodology, Software, Validation. **Ajith Abraham:** Conceptualization, Methodology, Supervision.

Declaration of competing interest

The authors declare that they have no known competing financial interests or personal relationships that could have appeared to influencethe work reported in this paper.

Appendix

See Tables A.1–A.7.

Table A.6
Coefficients related to benchmark function f_{20}.

i	a_{i1}	a_{i2}	a_{i3}	a_{i4}	a_{i5}	a_{i6}	c_i	p_{i1}	p_{i2}	p_{i3}	p_{i4}	p_{i5}	p_{i6}
1	10	3	17	3.5	1.7	8	1	0.1312	0.1696	0.5569	0.0124	0.8283	0.5886
2	0.05	10	17	0.1	8	14	1.2	0.2329	0.4135	0.8307	0.3736	0.1004	0.9991
3	3	3.5	1.7	10	17	8	3	0.2348	0.1415	0.3522	0.2883	0.3047	0.6650
4	17	8	0.05	10	0.1	14	3.2	0.4047	0.8828	0.8732	0.5743	0.1091	0.0381

References

[1] Y. Zhiwei, Z. Zhaobao, Y. Xin, N. Xiaogang, Automatic threshold selection based on ant colony optimization algorithm, in: 2005 Int. Conf. Neural Networks Brain, 2005, pp. 728–732, http://dx.doi.org/10.1109/ICNNB.2005.1614730.

[2] M.-H. Horng, Multilevel thresholding selection based on the artificial bee colony algorithm for image segmentation, Expert Syst. Appl. 38 (2011) 13785–13791, http://dx.doi.org/10.1016/j.eswa.2011.04.180.

[3] Y. Zhang, L. Wu, Optimal multi-level thresholding based on maximum tsallis entropy via an artificial bee colony approach, 13 (2011) 841–859. https://www.mdpi.com/1099-4300/13/4/841.

[4] S. Agrawal, R. Panda, A. Abraham, A novel diagonal class entropy-based multilevel image thresholding using coral reef optimization, IEEE Trans. Syst. Man Cybern. Syst. (2018) 1–9, http://dx.doi.org/10.1109/TSMC.2018.2859429.

[5] F. Shahabi, F. Pourahangarian, H. Beheshti, A multilevel image thresholding approach based on crow search algorithm and Otsu method, J. Decis. Oper. Res. 4 (2019) 33–41, http://dx.doi.org/10.22105/dmor.2019.88580.

[6] P. Upadhyay, J.K. Chhabra, Kapur's entropy based optimal multilevel image segmentation using Crow Search Algorithm, Appl. Soft Comput. (2019) 105522, http://dx.doi.org/10.1016/j.asoc.2019.105522.

[7] S. Agrawal, R. Panda, S. Bhuyan, B.K. Panigrahi, Tsallis entropy based optimal multilevel thresholding using cuckoo search algorithm, Swarm Evol. Comput. 11 (2013) 16–30, http://dx.doi.org/10.1016/j.swevo.2013.02.001.

[8] A.K. Bhandari, V.K. Singh, A. Kumar, G.K. Singh, Cuckoo search algorithm and wind driven optimization based study of satellite image segmentation for multilevel thresholding using Kapur's entropy, Expert Syst. Appl. 41 (2014) 3538–3560, http://dx.doi.org/10.1016/j.eswa.2013.10.059.

[9] S. Sarkar, S. Das, Multilevel image thresholding based on 2d histogram and maximum Tsallis entropy—A differential evolution approach, IEEE Trans. Image Process. 22 (2013) 4788–4797, http://dx.doi.org/10.1109/TIP.2013.2277832.

[10] N. Sri Madhava Raja, V. Rajinikanth, K. Latha, Otsu based optimal multilevel image thresholding using firefly algorithm, J. Model. Simul. Eng. 2014 (2014) 17, http://dx.doi.org/10.1155/2014/794574.

[11] M.-H. Horng, R.-J. Liou, Multilevel minimum cross entropy threshold selection based on the firefly algorithm, Expert Syst. Appl. 38 (2011) 14805–14811, http://dx.doi.org/10.1016/j.eswa.2011.05.069.

[12] K. Hammouche, M. Diaf, P. Siarry, A multilevel automatic thresholding method based on a genetic algorithm for a fast image segmentation, Comput. Vis. Image Understand. 109 (2008) 163–175, http://dx.doi.org/10.1016/j.cviu.2007.09.001.

[13] A.K.M. Khairuzzaman, S. Chaudhury, Multilevel thresholding using grey wolf optimizer for image segmentation, Expert Syst. Appl. 86 (2017) 64–76, http://dx.doi.org/10.1016/j.eswa.2017.04.029.

[14] M.-H. Horng, Multilevel minimum cross entropy threshold selection based on the honey bee mating optimization, Expert Syst. Appl. 37 (2010) 4580–4592, http://dx.doi.org/10.1016/j.eswa.2009.12.050.

[15] K.P. Baby Resma, M.S. Nair, Multilevel thresholding for image segmentation using krill herd optimization algorithm, J. King Saud Univ., Comput. Inf. Sci. (2018) http://dx.doi.org/10.1016/j.jksuci.2018.04.007.

[16] M.A. El Aziz, A.A. Ewees, A.E. Hassanien, Whale optimization algorithm and moth-flame optimization for multilevel thresholding image segmentation, Expert Syst. Appl. 83 (2017) 242–256, http://dx.doi.org/10.1016/j.eswa.2017.04.023.

[17] W. Chen, K. Fang, Multilevel thresholding algorithm based on particle swarm optimization for image segmentation, in: 2008 27th Chinese Control Conf., 2008, pp. 348–351, http://dx.doi.org/10.1109/CHICC.2008.4605745.

[18] P.-Y. Yin, Multilevel minimum cross entropy threshold selection based on particle swarm optimization, Appl. Math. Comput. 184 (2007) 503–513, http://dx.doi.org/10.1016/j.amc.2006.06.057.

[19] B. Küçükuğurlu, E. Gedikli, Symbiotic organisms search algorithm for multilevel thresholding of images, Expert Syst. Appl. 147 (2020) 113210, http://dx.doi.org/10.1016/j.eswa.2020.113210.

[20] R. Panda, S. Agrawal, L. Samantaray, A. Abraham, An evolutionary gray gradient algorithm for multilevel thresholding of brain MR images using soft computing techniques, Appl. Soft Comput. 50 (2017) 94–108, http://dx.doi.org/10.1016/j.asoc.2016.11.011.

[21] E. Zahara, S.-K.S. Fan, D.-M. Tsai, Optimal multi-thresholding using a hybrid optimization approach, Pattern Recognit. Lett. 26 (2005) 1082–1095, http://dx.doi.org/10.1016/j.patrec.2004.10.003.

[22] M. Maitra, A. Chatterjee, A hybrid cooperative–comprehensive learning based PSO algorithm for image segmentation using multilevel thresholding, Expert Syst. Appl. 34 (2008) 1341–1350, http://dx.doi.org/10.1016/j.eswa.2007.01.002.

[23] P.D. Sathya, R. Kayalvizhi, Modified bacterial foraging algorithm based multilevel thresholding for image segmentation, Eng. Appl. Artif. Intell. 24 (2011) 595–615, http://dx.doi.org/10.1016/j.engappai.2010.12.001.

[24] U. Mlakar, B. Potočnik, J. Brest, A hybrid differential evolution for optimal multilevel image thresholding, Expert Syst. Appl. 65 (2016) 221–232, http://dx.doi.org/10.1016/j.eswa.2016.08.046.

[25] A. Alihodzic, M. Tuba, Improved bat algorithm applied to multilevel image thresholding, J. Sci. World J. 2014 (2014) 16, http://dx.doi.org/10.1155/2014/176718.

[26] L. He, S. Huang, Modified firefly algorithm based multilevel thresholding for color image segmentation, Neurocomputing 240 (2017) 152–174, http://dx.doi.org/10.1016/j.neucom.2017.02.040.

[27] G. Sun, A. Zhang, Y. Yao, Z. Wang, A novel hybrid algorithm of gravitational search algorithm with genetic algorithm for multi-level thresholding, Appl. Soft Comput. 46 (2016) 703–730, http://dx.doi.org/10.1016/j.asoc.2016.01.054.

[28] H.V.H. Ayala, F.M. dos Santos, V.C. Mariani, L. dos S. Coelho, Image thresholding segmentation based on a novel beta differential evolution approach, Expert Syst. Appl. 42 (2015) 2136–2142, http://dx.doi.org/10.1016/j.eswa.2014.09.043.

[29] K.S. Fu, J.K. Mui, A survey on image segmentation, Pattern Recognit. 13 (1981) 3–16, http://dx.doi.org/10.1016/0031-3203(81)90028-5.

[30] P.K. Sahoo, S. Soltani, A.K.C. Wong, A survey of thresholding techniques, Comput. Vis. Graph. Image Process. 41 (1988) 233–260, http://dx.doi.org/10.1016/0734-189X(88)90022-9.

[31] N.R. Pal, S.K. Pal, A review on image segmentation techniques, Pattern Recognit. 26 (1993) 1277–1294, http://dx.doi.org/10.1016/0031-3203(93)90135-J.

[32] J. Freixenet, X. Muñoz, D. Raba, J. Martí, X. Cufí, A. Heyden, G. Sparr, M. Nielsen, P. Johansen, Yet Another Survey on Image Segmentation: Region and Boundary Information Integration, Springer Berlin Heidelberg, Berlin, Heidelberg, 2002, pp. 408–422.

[33] M. Sezgin, B. Sankur, Survey over image thresholding techniques and quantitative performance evaluation, J. Electron. Imaging. 13 (2004) 146–168, http://dx.doi.org/10.1117/1.1631315.

[34] H. Zhang, J.E. Fritts, S.A. Goldman, Image segmentation evaluation: A survey of unsupervised methods, Comput. Vis. Image Understand. 110 (2008) 260–280, http://dx.doi.org/10.1016/j.cviu.2007.08.003.

[35] N.M. Zaitoun, M.J. Aqel, Survey on image segmentation techniques, Procedia Comput. Sci. 65 (2015) 797–806, http://dx.doi.org/10.1016/j.procs.2015.09.027.

[36] B. Sankur, M. Sezgin, Image thresholding techniques: A survey over categories, Pattern Recognit. 34 (2001) 1573–1583.

[37] N. Otsu, A threshold selection method from gray-level histograms, IEEE Trans. Syst. Man. Cybern. 9 (1979) 62–66, http://dx.doi.org/10.1109/TSMC.1979.4310076.

[38] J.N. Kapur, P.K. Sahoo, A.K.C. Wong, A new method for gray-level picture thresholding using the entropy of the histogram, Comput. Vis. Graph. Image Process. 29 (1985) 273–285, http://dx.doi.org/10.1016/0734-189X(85)90125-2.

[39] C. Tsallis, Nonextensive statistical mechanics and its applications, Lecture Notes in Phys. 560 (2001) 3–98.

[40] C. Tsallis, Possible generalization of Boltzmann–Gibbs statistics, 52 (1988) 479–487, http://dx.doi.org/10.1007/bf01016429.

[41] N. Pavesic, S. Ribaric, Gray level thresholding using the havrda and charvat entropy, in: 2000 10th Mediterr. Electrotech. Conf. Inf. Technol. Electrotechnol. Mediterr. Countries. Proceedings. MeleCon 2000 (Cat. No.00CH37099), vol. 2, 2000, pp. 631–634, http://dx.doi.org/10.1109/MELCON.2000.880013.

[42] M. Portes de Albuquerque, I.A. Esquef, A.R. Gesualdi Mello, M. Portes de Albuquerque, Image thresholding using tsallis entropy, Pattern Recognit. Lett. 25 (2004) 1059–1065, http://dx.doi.org/10.1016/j.patrec.2004.03.003.

[43] A. Renyi, On measures of entropy and information, in: Proc. Fourth Berkeley Symp. Math. Stat. Probab, in: Contrib. to Theory Stat., vol. 1, University of California Press, Berkeley, Calif, 1961, pp. 547–561, https://projecteuclid.org/euclid.bsmsp/1200512181.

[44] M. Masi, A step beyond Tsallis and Renyi entropies, Phys. Lett. A. 338 (2005) 217–224, http://dx.doi.org/10.1016/j.physleta.2005.01.094.

[45] A.S. Abutaleb, Automatic thresholding of gray-level pictures using two-dimensional entropy, Comput. Vis. Graph. Image Process. 47 (1989) 22–32, http://dx.doi.org/10.1016/0734-189X(89)90051-0.

[46] A.D. Brink, Thresholding of digital images using two-dimensional entropies, Pattern Recognit. 25 (1992) 803–808, http://dx.doi.org/10.1016/0031-3203(92)90034-G.

[47] J. Liu, W. Li, Y. Tian, Automatic thresholding of gray-level pictures using two-dimension otsu method, in: China. 1991 Int. Conf. Circuits Syst., vol. 1, 1991, pp. 325–327, http://dx.doi.org/10.1109/CICCAS.1991.184351.

[48] P.K. Sahoo, G. Arora, Image thresholding using two-dimensional Tsallis–Havrda–Charvát entropy, Pattern Recognit. Lett. 27 (2006) 520–528, http://dx.doi.org/10.1016/j.patrec.2005.09.017.

[49] P.K. Sahoo, G. Arora, A thresholding method based on two-dimensional Renyi's entropy, Pattern Recognit. 37 (2004) 1149–1161, http://dx.doi.org/10.1016/j.patcog.2003.10.008.

[50] A. Bhandari, Tsallis entropy based multilevel thresholding for colored satellite image segmentation using evolutionary algorithms, Expert Syst. Appl. (2015) http://dx.doi.org/10.1016/j.eswa.2015.07.025.
[51] P.-S. Liao, T.-S. Chen, P.-C. Chung, A fast algorithm for multilevel thresholding, J. Inf. Sci. Eng. 17 (2001) 713–727.
[52] Y. Peng-Yeng, C. Ling-Hwei, A new method for multilevel thresholding using symmetry and duality of the histogram, in: Proc. ICSIPNN '94. Int. Conf. Speech, Image Process. Neural Networks, vol. 1, 1994, pp. 45–48, http://dx.doi.org/10.1109/SIPNN.1994.344969.
[53] P.-Y. Yin, L.-H. Chen, A fast iterative scheme for multilevel thresholding methods, Signal Process. 60 (1997) 305–313, http://dx.doi.org/10.1016/S0165-1684(97)00080-7.
[54] J.H. Song, W. Cong, J. Li, A fuzzy C-means clustering algorithm for image segmentation using nonlinear weighted local information, J. Inf. Hiding Multimed. Signal Process. 8 (2017) 578–588.
[55] M.K. Naik, R. Panda, A novel adaptive cuckoo search algorithm for intrinsic discriminant analysis based face recognition, Appl. Soft Comput. 38 (2016) 661–675, http://dx.doi.org/10.1016/j.asoc.2015.10.039.
[56] B. Farnad, A. Jafarian, D. Baleanu, A new hybrid algorithm for continuous optimization problem, Appl. Math. Model. 55 (2018) 652–673, http://dx.doi.org/10.1016/j.apm.2017.10.001.
[57] M.K. Naik, L. Samantaray, R. Panda, A hybrid CS–GSA algorithm for optimization, in: S. Bhattacharyya, P. Dutta, S. Chakraborty (Eds.), Hybrid Soft Comput. Approaches, Springer, India, 2016, pp. 3–35, http://dx.doi.org/10.1007/978-81-322-2544-7_1.
[58] R. Panda, M.K. Naik, A novel adaptive crossover bacterial foraging optimization algorithm for linear discriminant analysis based face recognition, Appl. Soft Comput. J. (2015) http://dx.doi.org/10.1016/j.asoc.2015.02.021.
[59] A.A. Heidari, S. Mirjalili, H. Faris, I. Aljarah, M. Mafarja, H. Chen, Harris hawks optimization: Algorithm and applications, Future Gener. Comput. Syst. 97 (2019) 849–872, http://dx.doi.org/10.1016/j.future.2019.02.028.
[60] X. Yao, L. Yong, L. Guangming, Evolutionary programming made faster, Evol. Comput. IEEE Trans. 3 (1999) 82–102, http://dx.doi.org/10.1109/4235.771163.
[61] J.J. Liang, B.Y. Qu, P.N. Suganthan, Problem Definitions and Evaluation Criteria for the CEC 2014 Special Session and Competition on Single Objective Real-Parameter Numerical Optimization, 2013.
[62] B. Zolghadr-Asli, O. Bozorg-Haddad, X. Chu, Crow search algorithm (CSA), in: O. Bozorg-Haddad (Ed.), Adv. Optim. By Nature-Inspired Algorithms, Springer Singapore, Singapore, 2018, pp. 143–149, http://dx.doi.org/10.1007/978-981-10-5221-7_14.
[63] A. Askarzadeh, A novel metaheuristic method for solving constrained engineering optimization problems: Crow search algorithm, Comput. Struct. 169 (2016) 1–12, http://dx.doi.org/10.1016/j.compstruc.2016.03.001.
[64] X.-S. Yang, S. Deb, Cuckoo search: recent advances and applications, Neural Comput. Appl. 24 (2014) 169–174, http://dx.doi.org/10.1007/s00521-013-1367-1.
[65] X.-S. Yang, S. Deb, Cuckoo search via lavy flights, in: Nat. Biol. Inspired Comput. 2009. NaBIC 2009. World Congr., 2009, pp. 210–214, http://dx.doi.org/10.1109/NABIC.2009.5393690.
[66] V. Feoktistov, Differential Evolution, Springer, 2006.
[67] R. Storn, K. Price, Differential evolution – A simple and efficient heuristic for global optimization over continuous spaces, J. Global Optim. 11 (1997) 341–359, http://dx.doi.org/10.1023/A:1008202821328.
[68] K. Price, R.M. Storn, J.A. Lampinen, Differential Evolution, Springer, 2005.
[69] X.-S. Yang, Cuckoo search and firefly algorithm: Overview and analysis, in: X.-S. Yang (Ed.), Cuckoo Search and Firefly Algorithm, Springer International Publishing, 2014, pp. 1–26, http://dx.doi.org/10.1007/978-3-319-02141-6_1.
[70] X.-S. Yang, Firefly algorithms for multimodal optimization, in: O. Watanabe, T. Zeugmann (Eds.), Stoch. Algorithms Found. Appl., Springer, Berlin Heidelberg, 2009, pp. 169–178, http://dx.doi.org/10.1007/978-3-642-04944-6_14.
[71] J. Kennedy, R. Eberhart, Particle swarm optimization, in: Neural Networks, 1995. Proceedings. IEEE Int. Conf., vol. 4, 1995, pp. 1942–1948, http://dx.doi.org/10.1109/ICNN.1995.488968.
[72] S. Mirjalili, S.M. Mirjalili, A. Lewis, Grey wolf optimizer, Adv. Eng. Softw. 69 (2014) 46–61, http://dx.doi.org/10.1016/j.advengsoft.2013.12.007.
[73] Z. Bayraktar, M. Komurcu, J.A. Bossard, D.H. Werner, The wind driven optimization technique and its application in electromagnetics, IEEE Trans. Antennas Propag. 61 (2013) 2745–2757, http://dx.doi.org/10.1109/TAP.2013.2238654.
[74] S. Mirjalili, A. Lewis, The whale optimization algorithm, Adv. Eng. Softw. 95 (2016) 51–67, http://dx.doi.org/10.1016/j.advengsoft.2016.01.008.
[75] R. Tanabe, A.S. Fukunaga, Improving the search performance of SHADE using linear population size reduction, in: 2014 IEEE Congr. Evol. Comput., 2014, pp. 1658–1665, http://dx.doi.org/10.1109/CEC.2014.6900380.
[76] A.P. Piotrowski, L-SHADE optimization algorithms with population-wide inertia, Inf. Sci. (Ny) 468 (2018) 117–141, http://dx.doi.org/10.1016/j.ins.2018.08.030.
[77] D. Martin, C. Fowlkes, D. Tal, J. Malik, A database of human segmented natural images and its application to evaluating segmentation algorithms and measuring ecological statistics, in: Proc. Eighth IEEE Int. Conf. Comput. Vision. ICCV 2001, vol. 2, 2001, pp. 416–423, http://dx.doi.org/10.1109/ICCV.2001.937655.
[78] M.-H. Horng, T.-W. Jiang, F.L. Wang, H. Deng, Y. Gao, J. Lei, Multilevel Image Thresholding Selection using the Artificial Bee Colony Algorithm, Springer Berlin Heidelberg, Berlin, Heidelberg, 2010, pp. 318–325.
[79] D. Xu, X. Tang, Multi-threshold image segmentation based on two-dimensional tsallis, in: 2010 3rd Int. Conf. Comput. Sci. Inf. Technol., 2010, pp. 1–5, http://dx.doi.org/10.1109/ICCSIT.2010.5563584.
[80] H.D. Cheng, Y.H. Chen, X.H. Jiang, Thresholding using two-dimensional histogram and fuzzy entropy principle, IEEE Trans. Image Process. 9 (2000) 732–735, http://dx.doi.org/10.1109/83.841949.
[81] D.H. Wolpert, W.G. Macready, No free lunch theorems for optimization, Evol. Comput. IEEE Trans. 1 (1997) 67–82, http://dx.doi.org/10.1109/4235.585893.
[82] X.-S. Yang, Nature-Inspired Metaheuristic Algorithms, second ed., Luniver press, UK, 2010.
[83] M. Jamil, X.-S. Yang, A literature survey of benchmark functions for global optimization problems, Int. J. Math. Model. Numer. Optim. 4 (2013) 150–194, http://dx.doi.org/10.1504/IJMMNO.2013.055204.
[84] M.K. Naik, R. Panda, A novel adaptive cuckoo search algorithm for intrinsic discriminant analysis based face recognition, Appl. Soft Comput. J. 38 (2016) 661–675, http://dx.doi.org/10.1016/j.asoc.2015.10.039.
[85] M. Črepinšek, S. Liu, M. Mernik, Exploration and exploitation in evolutionary algorithms: A survey, ACM Comput. Surv. 45 (2013) 35, http://dx.doi.org/10.1145/2480741.2480752.
[86] L. Zhang, L. Zhang, X. Mou, D. Zhang, FSIM: A feature similarity index for image quality assessment, IEEE Trans. Image Process. 20 (2011) 2378–2386, http://dx.doi.org/10.1109/TIP.2011.2109730.
[87] W. Zhou, A.C. Bovik, H.R. Sheikh, E.P. Simoncelli, Image quality assessment: from error visibility to structural similarity, IEEE Trans. Image Process. 13 (2004) 600–612, http://dx.doi.org/10.1109/TIP.2003.819861.